

Epidemic Mitigation via Awareness Propagation in Multi-layer Networks

Chuyi CHEN

Technische Universiteit Delft

EPIDEMIC MITIGATION VIA AWARENESS PROPAGATION IN MULTI-LAYER NETWORKS

by

Chuyi CHEN

in partial fulfillment of the requirements for the degree of

Master of Science

in Electrical Engineering, Telecommunication Track

at Faculty of Electrical Engineering, Mathematics and Computer Science (EWI),
Delft University of Technology,

to be defended publicly on Friday September 11, 2015 at 10:00 AM.

Student number:	4274431	
Supervisor:	Dr. H. Wang	
	B. Qu	
Thesis committee:	Prof. Dr. A. Hanjalic,	TU Delft
	Dr. H. Wang,	TU Delft
	Dr. W. Ruszel,	TU Delft
	B. Qu,	TU Delft

This thesis is confidential and cannot be made public until September 11, 2015.

An electronic version of this thesis is available at <http://repository.tudelft.nl/>.

ABSTRACT

The pervasiveness of the Internet and smartphones enables individuals to participate in online social networks such as Twitter and Facebook, besides the classic physical contact network. Such multi-layer network allows for feedback between networks / layers. For instance, the spread of a biological disease such as Ebola in a physical contact network may trigger the spreading of the information related to this disease in online social networks. The information propagated online may increase the alertness of some individuals resulting in avoidance of the physical contact with infected members in the physical contact network, which possibly protects the population from the infection [1, 2].

In this thesis, we propose two models for studying not only epidemic spreading and information propagation, but also the interactions between the epidemic and information. We explore two key factors that may influence the performance of such epidemic mitigation via awareness propagation: (i) the time scale of the epidemic information propagation in online social networks relative to that of the epidemic spreading in the physical contact network, or equivalently, the information update frequency in the social network, and (ii) the structure of the multi-layer networks. Contrary to our intuition, we find that very frequent information updates in an online social network sometimes reduce the mitigation effect when using awareness information. Such mitigation tends to perform better when the physical contact network and the online social network overlap more. We explain these findings analytically, with the help of our original Individual-Based Mean Field Approximation IBMFA. Moreover, we derive the analytical approach Microscopic Markov Chain Approach MMCA [1, 2] according to our models. We show that IBMFA is a better approximation than the MMCA in some scenarios, especially around the epidemic threshold. Our results indicate that the optimum effect of epidemic mitigation does not require very frequent information updates in an online social network which dilute the alertness information and therefore reduce the effect of mitigation, whereas encouraging individuals to keep in touch with their physical contacts as well online is beneficial for the mitigation.

Key words: Epidemic mitigation, Awareness propagation, Interactions, Multi-layer networks, Time scale, Overlap, Individual-Based Mean-Field Approximation (IBMFA), Microscopic Markov Chain Approach (MMCA)

CONTENTS

1	Introduction	1
1.1	Motivation	1
1.2	Related Researches	2
1.3	Thesis Outline	3
2	Basic Concepts and Methods	5
2.1	Network Properties	5
2.1.1	Relations between nodes.	5
2.1.2	Degree	6
2.2	Network Models.	6
2.2.1	Erdős-Rényi Random Network.	6
2.2.2	Scale-free Network.	7
2.3	Multi-layer Networks	8
3	SIS model on a single network	9
3.1	SIS model description.	9
3.2	Mean-field Approximation for the SIS model	10
3.3	N-Intertwined Mean field Approximation (NIMFA)	11

4	Epidemic and Awareness Interaction Processes model I	13
4.1	Definition of processes in the EAIP model I	13
4.2	Monte-Carol Simulation	15
4.3	Individual-Based Mean Field Approximation	17
4.3.1	Individual-Based Mean Field Approximation equations	17
4.3.2	Method of solving IBMFA equations	19
4.4	Microscopic Markov Chain Approach	20
4.4.1	Derivation of MMCA equations	20
4.4.2	Solving MMCA equations	21
4.5	Accuracy of IBMFA and MMCA	22
4.6	The influence of time scale γ on epidemic mitigation	22
4.6.1	The relative time scale γ VS Epidemic spreading	23
4.6.2	Accuracy of sampled-time Markov processes in simulations	26
4.6.3	Upper bound and lower bound of ρ_2	28
4.7	Influence of overlap ϕ	30
5	Epidemic and Awareness Interaction Processes model II	33
5.1	Definition of processes in the EAIP model II	33
5.2	Monte-Carol Simulations	35
5.3	Individual-Based Mean Field Approximation I	36
5.3.1	Individual-Based Mean Field Approximation equations	36
5.3.2	Method of solving IBMFA equations	39

5.4	Individual-Based Mean Field Approximation II.	39
5.5	Microscopic Markov Chain Approach	40
5.6	Accuracy of IBMFA and MMCA	41
5.7	The influence of time scale γ on epidemic mitigation.	44
5.7.1	The relative time scale γ VS Epidemic spreading	44
5.7.2	Upper bound and lower bound of ρ_2	46
5.7.3	Optimum epidemic mitigation.	47
5.8	Influence of overlap ϕ	50
6	Conclusion and Future work	53
6.1	Conclusion of our works	53
6.2	Future works	54
A	Appendix for the Epidemic and Awareness Interaction Processes model I	55
A.1	Derivation of Individual-Based Mean Field Approximation in Epidemic and Awareness Interaction Processes model I	55
A.2	Derivation of the epidemic threshold τ_c in the MMCA	57
A.3	Comparison of the accuracy of the IBMFA and the MMCA	58
A.4	Investigate the influence of time scale γ in the IBMFA and the MMCA	58
B	Appendix for the Epidemic and Awareness Interaction Processes model II	61
B.1	Derivation of Individual-Based Mean Field Approximation I in Epidemic and Awareness Interaction Processes model II	61
B.2	Derivation of the epidemic threshold τ_c in the MMCA	64
B.3	Investigate the influence of time scale γ with IBMFA and MMCA	65

B.4	Influence of the time scale γ in two-layer Erdős-Rényi (ER) random networks	65
B.5	Influence of overlap ϕ in two-layer Erdős-Rényi (ER) random networks	65
	Bibliography	73

1

INTRODUCTION

1.1. MOTIVATION

Epidemic spreading in complex networks has been extensively studied in recent years. While a large number of researches aimed at epidemic processes on a single network, in reality, networks are interdependent on each other [3–11]. Function and behavior of nodes not only depend on the network they locate in, but also rely on other networks. For example, computer networks rely on power networks for electricity supply, while power stations are controlled by computer networks [3]. When nodes of all the networks that depend on each other represent the same set of entities, such an interdependent network is also called a multi-layer network, representing different types of relations among the same set of nodes [12–14]. An example of multi-layer network is that individuals could participate in a physical contact network with friends, families and coworkers, while they may also join an online social network such as Facebook or Twitter [15]. The multi-layer network allows interactions or feedbacks between the processes in different network layers. Study of multi-layer networks could provide us a strong tool to characterize processes and properties in real world.

Besides epidemic spreading, information diffusion is also an important dynamic process in complex networks [16–20]. The outbreak of a disease in a population would also lead to the spread of information about this disease. Information could get individuals aware of the disease, which allows people to take protective actions against the disease, e.g. wearing face masks and decreasing physical contact with others [21]. Therefore, the awareness about epidemics propagated in the online social network could possibly mitigate epidemics spreading in the physical contact network. An example is the severe acute respiratory syndrome (SARS) that widely spread in China in 2003, where people's behavior responded to received information contributed to the control of the SARS [20, 22]. The possible mitigation effect the awareness could have on the outbreak of epidemics was recently noticed by Granell *et al.* in 2013 [2].

In the interesting novel discovery which is of great practical significance, one key question is how to achieve the optimum mitigation performance by using the awareness information. We find out two essential factors that could affect the epidemics spreading when using awareness information propagated in an online social network in this thesis. One is the relative time scale of awareness propagation, or equivalently, the relative frequency of information updates in online social networks compared to the time scale of epidemic spreading in the physical contact network. If a person checks his social network account more frequently, he could likely share the awareness information more timely, possibly influencing the epidemic spreading. Besides the time scale of awareness information propagation relative to that of the epidemic spreading, the multi-

layer network structure affects the spread of an epidemic as well.

Our thesis aims to understand the effect of the relative time scale of the awareness propagation, as well as the structure of multi-layer networks, on preventing the spread of epidemics. We consider two-layer networks, which are consisted of a virtual social network (e.g. Facebook or Twitter) in which the awareness of an epidemic propagates, and a physical contact network in which the epidemic spreads. We propose two models that describe two scenarios of the interaction between epidemic spreading and awareness propagation. These two models allow us to unveil the role of the relative time scale of the awareness propagation and the multi-layer network topology in epidemic spreading. We carry out both simulations and theoretical analysis to answer crucial questions such as: Is fast information propagation always beneficial for the mitigation of an epidemic? Which multi-layer topology best facilitates the epidemic mitigation?

1.2. RELATED RESEARCHES

Graph theory, which was born in 1736, has been used to simplify real-world complex systems into a network or graph that describes the relations or interactions between entities. Entities are mapped as nodes in a network, and relations between entities are shown by links in the network.

The Susceptible-Infected-Susceptible (SIS) model [23–26] is one of the simplest and widely used epidemic spreading model. In the SIS model, each node in the network has only two possible states: either healthy but susceptible, or infected by the disease. Susceptible nodes does not have the disease, but they could catch the disease from its infected neighbors. Infected nodes are disease disseminators because of the infectivity of the disease, meanwhile they could recover from the disease and become healthy but susceptible. The infection process only happens from an infected node to a susceptible node, where the time for the susceptible node to infect is determined by an infection rate β . A large infection rate β leads to a short time to infect. Similarly, the time for an infected node to recover from the disease is determined by a recovery rate δ . Another popular model for diseases spreading is the Susceptible-Infected-Recovered (SIR) model[27, 28]. In the SIR model, besides the healthy but susceptible state and the infected state, there is a recovered state. A node reaches the recovered state instead of the susceptible state after it is recovered from the infected state, and it could not get infected again by the same epidemic.

In epidemiology, we are interested in exploring the fraction of individuals that get infected by an epidemic in the network. In a single network, the fraction of infected individuals (which we denote as ρ) highly depends on the network topology[24]. In a complete graph where each node is connected to all the other nodes in the graph, an epidemic could spread out easily due to the large number of links for epidemic spreading. However, a very sparse network leads to the difficult epidemic spreading. Researches showed that the degree distribution of a network significantly influences epidemic spreading[28] where the degree of a node is the number of neighbors it has. A network with a broad degree distribution, such as scale-free networks where most of nodes have a small degree while few "hub" nodes possess a large degree, requires a smaller infection rate for an epidemic to outbreak in the network [29]. The smallest effective infection rate $\tau = \beta/\delta$ for an epidemic to outbreak in a network is also called as "epidemic threshold", below which the epidemic would die out exponentially fast in the network[28, 30–33]. A classic mathematical analysis, N-Intertwined Mean-Field Approximation (NIMFA) was proposed by Van Mieghem *et al.* [23, 24] for theoretically studying the transition between the infected state and the susceptible state, and calculating the fraction of infection as well as the epidemic threshold in a single network. Since an exact mathematical solution for the fraction of infection and the epidemic threshold in any network has not been found yet, the NIMFA is currently the most accurate approximation for a single network.

The two-layer network with an online social network where the awareness about an epidemic propagates, and a physical contact network where the epidemic itself spreads, was noticed [2]. When a node gets in-

ected by the epidemic, it immediately gets aware of the epidemic. We define this mechanism as "injection of information" from the physical network to the social network. Awareness gives a node protection from the epidemic. Information injection and the protection from awareness shows the interaction between two network layers. The fraction of infection in this two-layer network indicates the fraction of infected nodes in the physical network, while the fraction of awareness is the fraction of aware nodes in the online social network. The mitigation possibility via awareness propagation was firstly studied by Granell *et al.* They proposed microscopic Markov chain approach (MMCA) as an mathematical approximation to calculate the fraction of infection and the epidemic threshold in two-layer networks [2]. They showed that the rate of information dissemination has to be large enough to influence the epidemic propagation processes. The impact of the mass media on the epidemic propagation, and the minimum information spreading rate where the onset of an epidemic starts depending on the awareness propagation, were also studied in [1] under a special two-layer network where the physical contact layer is a scale-free network, and the information layer is the same scale-free network with some extra randomly connected links.

A similar two-layer network, where injection of information happens with a probability, was studied in [20] with the H7N9 outbreak data. Discussions about H7N9 in Weibo (an online social network that is similar to Twitter) was regarded as the awareness in the online social network. They found that because of the fast loss of alertness about H7N9 after the epidemic was under controlled, the H7N9 virus had a second outbreak. The influence of degree correlation between the physical contact network and the online social network was explored in [16] with the SIR (Susceptible-Infected-Recovered) model. A special case of two-layer interacting network, where aware individuals are temporary immunized of the epidemic, was investigated in [34].

On top of these existing researches, this thesis concentrates on the two-layer network with a social network layer and a physical network layer that interacts with each other. We propose two models to approximate the real-life interaction between epidemic spreading and information propagation. In one model the immediately information injection is considered in accordance with [2], while in the other model we propose an "delayed information injection" mechanism. Our aim is to achieve the optimum epidemic mitigation effect by using awareness propagated in the social network. We find that the fast time scale of information propagation, which has not been studied in two-layer networks, could sometimes be harmful for the epidemic mitigation. We also investigate the robust network structure against viruses, which could provide us a guidance in the network design. For both models, we not only develop Monte Carol simulations, but also develop our original mathematical analysis method, Individual-Based Mean-Field Approximation (IBMFA), as well as the MMCA to discover the average fraction of infected nodes in relation to the time scale and the two-layered network topology.

1.3. THESIS OUTLINE

Chapter 1 addresses real-life problems that motivate us to study how the time scale in the social network and the two-layered network topology influence epidemic spreading in two-layer interacting networks, as well as state-of-the-art researches in the complex network field.

Basic concepts such as network properties, network models, and multi-layer networks are introduced in Chapter 2.

Chapter 3 introduces the classic epidemics spreading model on a single network, the SIS model. The basis of our mathematical analysis method, the mean-field approximation which has been extensively used to simplify theoretical analysis of epidemics spreading in single networks, is presented. The N-Intertwined Mean-Field Approximation that could be applied to calculate the fraction of infection and the epidemic threshold in a single network is discusses.

The first two-layer network process model we propose is explained in Chapter 4. In this model, when an individual is infected by an epidemic, he or she immediately gets aware of the epidemic. Aware individuals are less likely to get infected by the epidemic. Our aim is to explore the epidemic spreading, specifically, the average fraction of infection in the meta-stable state in the physical network layer under different time scales in the social network and different two-layer network structures. Since epidemic mitigation aims at a low fraction of infected individuals, we would like to find out a scheme that leads to the lowest fraction of infected individuals. We tackle the problem by three methods: (i) We develop Monte-Carol simulations to simulate dynamic stochastic processes of information and epidemic propagation in two-layer networks. (ii) We develop our original theoretical analysis method: Individual-Based Mean Field Approximation (IBMFA) for analyzing the fraction of infected individuals and the fraction of aware individuals in two-layer networks. (iii) According to Microscopic Markov Chain Approach (MMCA) which was proposed by Granell *et al.*, we develop MMCA equations according to our model as a second theoretical analysis method for the awareness propagation and epidemics spreading. We demonstrate that our original IBMFA is a more accurate approximation compared to the MMCA, especially at small epidemic spreading rates where the epidemic only infects a small fraction of people. We find that awareness propagation indeed reduces the fraction of infection. But surprisingly, very frequent update of information in the online social network is unfavorable for the epidemic mitigation effect. In addition, a large extent of overlap between the two network layers tends to facilitate the mitigation.

Chapter 5 present the second two-layer network process model where an infected individual does not get aware immediately in the social network but with a certain rate depending on the time scale of the social network, i.e. the frequency of information update in the social network. If people are not enthusiastic about online social networks, they tend not to immediately start propagating awareness in social networks about the epidemic once they get infected. We would like to find an optimum time scale in the social network and an optimum two-layer network topology for epidemic mitigation under this circumstance. We solve this problem by developing Monte-Carol simulations as well as IBMFA and MMCA approximations. We find that by controlling the frequency of information updates in the online social network to a certain extent, the best mitigation effect could be achieved. Meanwhile, a large extent of overlap between two network layers is still beneficial for restricting the spread of the epidemic.

Chapter 6 summarizes our conclusions and possible future work.

2

BASIC CONCEPTS AND METHODS

In this chapter, we review some basic concepts and methods related to network properties and network models. Based on network models for a single network, we propose a method to construct two-layer networks, where both layers follow a same network model, with a controllable overlap extent between two layers.

2.1. NETWORK PROPERTIES

A graph $G = (N,L)$, where N stands for the number of nodes, and L represents the number of links in this graph, specifies how nodes in a network are interconnected or related to other nodes by links. Each node indicates an individual in the network, and each link connects two nodes to represent a particular relationship between these two nodes. A network is as usual distinguished from other networks by its network properties. In order to understand characterizations of different graphs, we would like to firstly introduce fundamental properties in a graph $G = (N,L)$.

2.1.1. RELATIONS BETWEEN NODES

Given the number of nodes N in a network, the adjacency matrix A is a $N * N$ binary matrix that indicates all links in this network. For example, the structure of an adjacency matrix for a network with six nodes is:

$$A = \begin{bmatrix} a_{11} & a_{12} & a_{13} & a_{14} & a_{15} & a_{16} \\ a_{21} & a_{22} & a_{23} & a_{24} & a_{25} & a_{26} \\ a_{31} & a_{32} & a_{33} & a_{34} & a_{35} & a_{36} \\ a_{41} & a_{42} & a_{43} & a_{44} & a_{45} & a_{46} \\ a_{51} & a_{52} & a_{53} & a_{54} & a_{55} & a_{56} \\ a_{61} & a_{62} & a_{63} & a_{64} & a_{65} & a_{66} \end{bmatrix} \quad (2.1)$$

Element a_{ij} represents the existence of a link between node i and node j . $a_{ij} = 1$ if a link exists between node i and node j , otherwise $a_{ij} = 0$. In this thesis, a_{ii} in adjacency matrices is always 0 because we don't consider self-links. If a network is undirected, the adjacency matrix is symmetric, i.e. $a_{ij} = a_{ji}$.

2.1.2. DEGREE

The degree d_i shows the number of neighbors node i possesses. Given the adjacency matrix A of a network, we could calculate the degree of node i in this network by

$$d_i = \sum_{k=1}^N a_{ik} \quad (2.2)$$

The average degree $E[D]$ shows the density of links in a network. In a graph $G = (N,L)$, the average degree is calculated from

$$E[D] = \frac{2 * L}{N} \quad (2.3)$$

In addition, the degree distribution $Pr[D = k]$ provides information about the fraction of nodes with degree k in a network. We could derive the average degree of a network from the degree distribution by

$$E[D] = \sum_{k=K_{min}}^{K_{max}} k Pr[D = k] \quad (2.4)$$

2.2. NETWORK MODELS

In order to study single layer networks, a number of random graph models have been proposed to model the complex real-world networks with particular properties. We would briefly introduce two representative random graph models, Erdős-Rényi random networks, and scale-free networks.

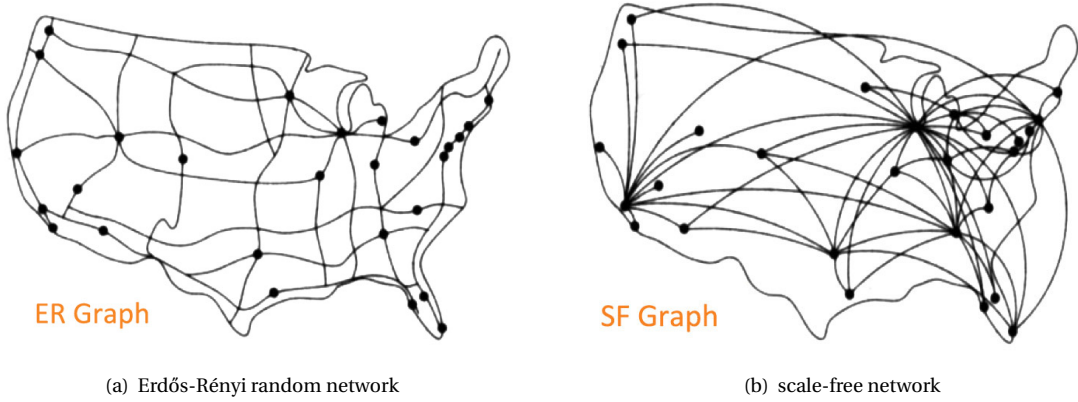


Figure 2.1: An example of (a) an Erdős-Rényi random network, and (b) a scale-free network [35].

2.2.1. ERDŐS-RÉNYI RANDOM NETWORK

The Erdős-Rényi (ER) random network is one of the most studied random network models that allows many problems analytically traceable [36, 37]. Assume an Erdős-Rényi random network is composed of N nodes and L links, which we denote as $G(N,L)$. The characteristic of Erdős-Rényi random networks is that all links are placed uniformly at random. The probability that any two nodes in the network are connected is p . On average there are $E[L] = \frac{N(N-1)}{2} p$ links connected in an Erdős-Rényi random network $G(N,L)$, while at most $\frac{N(N-1)}{2}$ links could exist in a network with N nodes. The degree distribution in Erdős-Rényi random networks follows a binomial distribution,

$$Pr[D = k] = \binom{N-1}{k} p^k (1-p)^{N-1-k} \quad (2.5)$$

When the number of nodes N is large, the degree distribution of Erdős-Rényi random networks approaches a Poisson distribution,

$$Pr[D = k] = \frac{(pN)^k}{k!} e^{-Np} \quad (2.6)$$

Erdős-Rényi random networks have the advantage of easy construction and analysis without losing generality.

2.2.2. SCALE-FREE NETWORK

We introduce in this section scale-free networks whose power-law degree distribution $Pr[D = k] \sim k^{-\lambda}$ has been observed in many real-world networks [38–41]. A positive number λ means that the degree distribution in scale-free networks has a heavy tail. Most of nodes in a scale-free network have a small degree, while a small portion of nodes possess many more connections than other nodes. These high-degree nodes are called "hubs" in networks. In real life, Internet has been observed to possess a power-law degree distribution. Most of websites have few number of links that point at them, while a small fraction of websites are so popular that many links point at them [41]. Social networks like facebook and twitter also follow power-law degree distributions, where most people have a small number of friends in online social networks, while a few popular stars have a dominantly large number of followers.

With a determined exponent λ , the power-law degree distribution in a scale-free network could be expressed as

$$Pr[D = k] = ck^{-\lambda}, D \in [K_{min}, K_{max}] \quad (2.7)$$

Given the minimal degree K_{min} and the maximum degree K_{max} in a scale-free network, and the normalization condition for the degree distribution of a network

$$\left(\sum_{k=K_{min}}^{K_{max}} Pr[D = k] \right) = 1 \quad (2.8)$$

We could calculate the parameter c in Equ.2.7 by

$$c = \frac{1}{\left(\sum_{k=K_{min}}^{K_{max}} k^{-\lambda} \right)} \quad (2.9)$$

To generate a scale-free network, we could use the configuration model. The configuration model is a model to generate a random graph with a given degree sequence. Steps of implementing the configuration model to generate a scale-free network are as followed:

1. Calculate the cumulative distribution function (cdf) $F(x) = Pr[D \leq x] = \left(\sum_{k=K_{min}}^x Pr[D = k] \right)$ according to the power-law degree distribution.
2. Generate the degree sequence for N nodes according to the cumulative distribution function. For each node, we generate a uniformly distributed random number n_{rad} in the range $n_{rad} \in [0, 1)$. The degree k of a node is determined by

$$k = \begin{cases} K_{min}, & 0 \leq n_{rad} < F(K_{min}) \\ x, & x > K_{min} \cap F(x-1) \leq n_{rad} < F(x) \end{cases} \quad (2.10)$$

3. Assign each node as many "stubs" as its degree.
4. Each time we randomly choose two spare stubs from two different nodes which are not already connected, and connect these two spare stubs with a link. We continue connecting spare stubs by links until all stubs are connected. Then the scale-free network is constructed.

2.3. MULTI-LAYER NETWORKS

Multi-layer networks, also called as multiplex networks, are composite of several interdependent network layers. The same set of nodes with different types of relations between nodes exist in different network layers [12–14]. In other words, links in one layer might be different from other layers. In this thesis, we consider two-layer networks that are consist of a bottom network layer of physical contact where an epidemic spreads, and a top network layer of an online social network like Facebook or Twitter where information (or awareness) propagates. Intuitively, an individual could have some friends that they meet face to face everyday, such as classmates, coworkers and families, while he or she could also possesses an social account in Facebook. When an individual meets face to face with a friend, there is a chance that an infectious virus spreads from one to the other. In the meantime, interesting news are shared between friends in Facebook. Epidemic spreading and information propagation interacts with each other. For example, an epidemic outbreak could stimulate the propagation of awareness about this epidemic, while the awareness urges people to take precautions against the epidemic.

The two network layers (or component networks) are assumed to have the same degree distribution in this thesis, but the overlap extent between two network layers can be tuned. Two layers in a two-layer network could be both Erdős-Rényi random networks (ER-ER), or both scale-free networks (SF-SF).

We propose here the method we use to generate a two-layer network with a certain overlap extent ϕ . We define the overlap extent ϕ between layers in a two-layer network as the fraction of links that exist in both layers. $\phi = 1$ indicates that friends of an individual on Facebook are completely the same as his or her friends in real life. On the other hand, $\phi = 0$ means that people do not socialize with their real life friends on Facebook.

In order to further understand how the overlap extent ϕ between the two layers of a two-layer network affects the epidemic spreading, we control the overlap extent when generating two-layer networks. Controlling the overlap extent ϕ in a two layer Erdős-Rényi random network ER-ER is feasible. To generate a two-layer ER-ER network $G = (N, L)$ with a fraction ϕ of overlapped links, we firstly generate $\phi * L$ random links that exist on both network layers, then randomly generate the rest of $(1 - \phi) * L$ links in the two layers separately under the constraint that links exist in one layer do not show up in the other layer.

Controlling the overlap extent ϕ in two-layer scale-free networks SF-SF is more difficult than in two-layer Erdős-Rényi random networks ER-ER. A two-layer scale-free network SF-SF with an overlap $\phi = 1$ can be constructed by generating a single scale-free network with the configuration model as one layer in the two-layer network, and copying all links to the other layer. Moreover, a SF-SF network with an overlap $\phi = 0$ can be obtained by generating degree sequences for the two network layers independently, and constructing the two layers independently with the configuration model according to their particular degree sequences. In our setting, parameters $\lambda = 2.5$ and $N = 1000$ in a single scale-free network bring about 2000 links, while the maximal possible number of links in a network with $N = 1000$ nodes is around 500000. Hence, these two independently generated network layers hardly overlap, which leads to a SF-SF network with $\phi = 0$. For SF-SF networks, we only consider overlap extents $\phi = 1$ and $\phi = 0$.

3

SIS MODEL ON A SINGLE NETWORK

In this chapter we introduce dynamic processes of epidemic spreading and information propagation. Classical Susceptible-Infected-Susceptible (SIS) model, which has been widely used to model the virus spreading in networks, is explained. Since the way information propagates is similar to the way the epidemic spreads, information propagation is also modeled by the SIS model in this thesis. The mean field approximation, which is used to simplify theoretical analysis of epidemic spreading in the SIS model, is introduced. The currently most advanced mathematical analysis method NIMFA that has been used for calculating the fraction of infection and the epidemic threshold in a single network is presented in differential equations form.

3.1. SIS MODEL DESCRIPTION

The Susceptible-Infected-Susceptible (SIS) model [23–26] is a simple continuous-time model that has been extensively used to describe a broad range of processes, such as epidemic/virus spreading, information propagation, and power supply [3]. Epidemics spreading is a representative spreading process in complex networks, therefore we use epidemics as an example to illustrate the famous SIS model in a single network.

In the SIS model, a node only has two possible states, healthy but susceptible to the disease state (S), or infected state (I). The viral state of a node i at any time t is specified by a Bernoulli random variable $X_i(t) \in \{0, 1\}$. $X_i(t) = 0$ represents that node i is healthy at time t , and $X_i(t) = 1$ means node i is infected at time t . Infected individuals could recover from the epidemic and become healthy and susceptible. The recovery (curing) process of each infected node is assumed to be an independent Poisson process with a recover rate δ . Infected individuals are epidemic disseminators that could infect their healthy neighbors. Each infected agent could spread the epidemic via links that are connected to susceptible neighbors with an infection rate β in each link. Each infection spreading over a link is an independent Poisson process [29]. The interarrival times of a Poisson process are independent and identically distributed exponential random variables. Due to the memoryless property of exponential random variables $Pr(T > s + t | T > t) = Pr(T > s)$, the SIS model has in nature Markov property. In other words, the conditional probability distribution of future states of a node depends upon the present states, not on the past states.

The ratio $\tau \triangleq \beta/\delta$ is defined as the effective infection rate. A phase transition phenomenon has been observed around a critical point τ_c in single networks. When the effective infection rate $\tau > \tau_c$, a non-zero fraction of agents will be infected in the steady state, whereas if $\tau < \tau_c$, infection rapidly kidnappers [30, 32]. The SIS

process possesses an absorbing state that all nodes are healthy, and no epidemic would spread in the network anymore. When $\tau \leq \tau_c$, the absorbing state is reached at least exponentially fast [20]. For $\tau > \tau_c$, the epidemic processes require extremely long time to reach the absorbing state [29]. For a large τ , the network is observed to reside in a state with many infected nodes for a long time. This regime is called the metastable state to which the epidemic rapidly converges, but very slowly leaves [29]. In this thesis, we are only interested in the meta-stable state in networks. In the following thesis, the steady state denotes the metastable state without further announcement.

3.2. MEAN-FIELD APPROXIMATION FOR THE SIS MODEL

In the SIS model, since the curing and infected processes are Poisson processes, the whole epidemic processes are Markov processes. A figure that shows the state transition of a node i , which could be regarded as a two state Markov chain, is plotted in Fig.3.1.

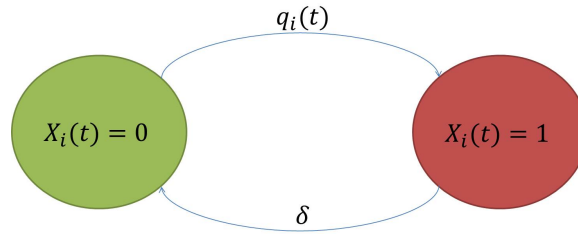


Figure 3.1: The state transition for a node i in the SIS model. $X_i(t) = 0$ is the healthy but susceptible state, and $X_i(t) = 1$ is the infected state.

According to the Markov theory, this two state continuous-time Markov chain is characterized by its infinitesimal generator $Q_i(t)$ as

$$Q_i(t) = \begin{bmatrix} -q_i(t) & q_i(t) \\ \delta & -\delta \end{bmatrix} \quad (3.1)$$

Given the adjacency matrix A for a network with N nodes, as well as the infection rate on each link β and the recover rate for each node δ , the total infection rate of a susceptible node i at time t is [23]:

$$q_i(t) = \beta \sum_{j=1}^N a_{ji} \mathbf{1}_{\{X_j(t)=1\}} \quad (3.2)$$

which is the summation of infection rates β on each link of node i that connects to an infected neighbor $X_j(t) = 1$. Networks we consider in this thesis are undirected, therefore $a_{ji} = a_{ij}$. Equ.3.2 shows the coupling of node i to the rest of the network by the infection rate q_i [24]. The rate q_i is a random variable due to the randomness of states in neighbors of node i $X_j(t)$. Markov theory requires that all elements in the infinitesimal generator $Q_i(t)$ are not random variables. In order to apply Markov theory, the randomness in the rate $q_i(t)$ needs to be removed. One way of removing the randomness in $q_i(t)$ is to consider all possible state combinations of N nodes in a network, which leads to the exact Markov chain with 2^N possible states in the network. Obviously, this exact 2^N states Markov chain is difficult to compute since the number of states increases exponentially with the number of nodes N .

To theoretically analyze the evolution of epidemic spreading in a network, we apply the mean-field approximation [23, 24, 29, 42, 43]. Instead of considering all possible combinations of states in the infection rate $q_i(t)$, the mean-field approximation replaces $q_i(t)$ by the average infection rate

$$E[q_i(t)] = E \left[\beta \sum_{j=1}^N a_{ji} \mathbf{1}_{\{X_j(t)=1\}} \right] \quad (3.3)$$

We denote $v_i(t) = Pr[X_i(t) = 1]$ as the probability that node i is infected at time t , and $Pr[X_i(t) = 0] = 1 - v_i(t)$ as the probability that node i is healthy at time t . Replacing the term $E[1_x] = Pr[x]$ in Equ.3.3, we get

$$E[q_i(t)] = \beta \sum_{j=1}^N a_{ij} v_j(t) \quad (3.4)$$

The random nature of the infection rate $q_i(t)$ is removed in Equ.3.4. Now the infinitesimal generator in Equ.3.1 becomes

$$Q_i(t) = \begin{bmatrix} -E[q_i(t)] & E[q_i(t)] \\ \delta & -\delta \end{bmatrix} \quad (3.5)$$

By applying the mean-field approximation, instead of computing the exact 2^N states Markov process, only N random variables $v_i(t)$ need to be considered in the Markov process.

The limitation of the mean-field approximation is, we lose some accuracy by ignoring the dependency of states between nodes in Equ.3.4. The mean field approximation simply uses the average probability of node i being infected at time t $v_i(t)$ to replace the summation of dependent indicators $\sum_{j=1}^N 1_{\{X_j(t)\}}$. Even so, the mean field approximation has been proved accurate in a lot of situations, and has been widely used as an effective tool to theoretically analyze the epidemic spread in the SIS model.

3.3. N-INTERTWINED MEAN FIELD APPROXIMATION (NIMFA)

By applying the mean field approximation in the infinitesimal generator $Q_i(t)$, each node obeys a differential equation [44, pp. 182]

$$\begin{cases} \frac{dv_1(t)}{dt} = (1 - v_1(t)) \beta \sum_{j=1}^N a_{1j} v_j(t) - v_1(t) \delta \\ \frac{dv_2(t)}{dt} = (1 - v_2(t)) \beta \sum_{j=1}^N a_{2j} v_j(t) - v_2(t) \delta \\ \vdots \\ \frac{dv_N(t)}{dt} = (1 - v_N(t)) \beta \sum_{j=1}^N a_{Nj} v_j(t) - v_N(t) \delta \end{cases} \quad (3.6)$$

Written in the matrix form [24],

$$\frac{dV(t)}{dt} = \beta AV(t) - \text{diag}(v_i(t)) (\beta AV(t) + \delta u) \quad (3.7)$$

where the vector $V(t) = [v_1(t) \ v_2(t) \ \dots \ v_N(t)]^T$, and u is the all-one vector[24]. The NIMFA Equ.3.6 for node i has the following physical interpretation: when node i is healthy with the probability $1 - v_i(t)$, each infected neighbor of node i tries to infect node i with a rate β . The total infection rate for node i is $\beta \sum_{j=1}^N a_{ij} v_j(t)$. When a node is infected with the probability $v_i(t)$, the node is recovered with a rate δ .

By solving differential equations 3.6 for all nodes in a single network, we could calculate the steady state fraction of infection ρ with

$$\rho = \frac{\sum_{i=1}^N v_i}{N} \quad (3.8)$$

where v_i is the steady state infection probability of node i . In the mean time, for the N-intertwined approximation, the largest eigenvalue λ_1 of the graph's adjacency matrix rigorously defines the epidemic threshold $\tau_c = \frac{1}{\lambda_1}$ [24, 45].

According to the differential equations [Equ.3.6](#), the N-intertwined approximation gives the upper bound of the SIS epidemics [\[23\]](#).

In this section we laid the foundation of interacting processes between two network layers. Specific interactions between network layers will be introduced in each of our two-layer network models in the following parts of the thesis.

4

EPIDEMIC AND AWARENESS INTERACTION PROCESSES MODEL I

In this chapter, we introduce the first epidemic and awareness interaction processes (EAIP) model that describes the scenario where individuals get immediately aware when they get infected by an epidemic. We develop Monte-Carlo (MC) simulations in C++ to obtain the meta-stable state fraction of infected nodes and the fraction of nodes that are aware of the epidemic. As for the theoretical analysis of this model I, we develop our original individual-based mean field approximation (IBMFA) for two-layer networks. In addition, we further develop microscopic Markov chain approach (MMCA) that was proposed by Granell *et al.* [2] according to our model I.

With a variety of tools we propose for studying the EAIP model I in two-layer networks, we focus on discovering the influence of two factors that influence the effectiveness of epidemic mitigation via awareness propagation. The two factors are the relatively time scale of the awareness propagation compared to the epidemic spreading, and the extent of overlap between two network layers.

4.1. DEFINITION OF PROCESSES IN THE EAIP MODEL I

In order to study the dynamic interactions between epidemic spreading and awareness propagation, we propose this epidemic and awareness interaction processes (EAIP) model I in two-layer networks. A two-layer network in this thesis consists of a physical contact network where an epidemic spreads, and an online social network where awareness about the epidemic propagates. We use the SIS model to specify the epidemic spreading process in the physical contact network. There are two possible states for a node in the physical contact network, healthy but susceptible (S) and infected (I). The infection rate on each link and the recover rate for each node are represented by β_2 and δ_2 , respectively. Meanwhile, the upper layer is the online social network, in which the awareness propagates in the same way as the SIS model. There are two possible states for a node in the online social network, aware (A) and unaware (U). An aware node informs each of its unaware neighbors with an awareness spreading rate β_1 , whereas an aware node recovers from the awareness to become unaware with an awareness recovering rate δ_1 . We call this model for awareness propagation the Unaware-Aware-Unaware (UAU) model, although it is the same model as the SIS model in nature. We use a parameter γ to specify the relative time scale of awareness propagation compared to epidemic spreading. Taking the time scale γ into consideration, the awareness spreading rate and the awareness recovering rate

in the social network becomes $\gamma\beta_1$ and $\gamma\delta_1$, respectively.

In our EAIP model I, the epidemic spreading and awareness propagation interacts with each other. In reality, if an individual is infected by e.g. flu, he or she would immediately know the existence of this flu, in other words, become aware. Consequently, in this EAIP model I, we define that when an individual gets infected, he or she gets immediately aware of the epidemic in the social network. This mechanism that individuals get aware of an epidemic due to being infected by the epidemic is regarded as the "injection of information" from the physical network layer to the social network layer. The injection happens only at the moment when an individual gets newly infected in this EAIP model. After the injection, the aware node could lose awareness and become unaware even if this node still remains infected in the physical layer, since an individual may lose (or forget about) the alertness about the epidemic and stop informing others in the social network after some time. In other words, the recovery of awareness in the social network layer is independent with epidemic spreading.

The injection of information represents how epidemic spreading influences awareness propagation. The other way around, people who see the information about the flu in the social network might pay attention to this information and start using protection safeguards, such as wearing masks and staying at home to reduce contact with other people, to reduce the probability that they get infected by the flu. This is how awareness propagation impacts epidemic spreading. Taking precautions because of getting aware of an epidemic possibly mitigates the epidemic spreading. We model the effect of safeguard methods with a parameter α . When a node is aware, the rate that this node gets infected in the physical contact network is reduced by a factor of α . The recovery of infection in the physical network layer is independent with awareness propagation.

On top of the interactions between epidemic spreading and awareness propagation, here we define some symbols for further analysis of the EAIP model I. The viral state of a node i at any time t is specified by a Bernoulli random variable $X_i(t) \in \{0, 1\}$. $X_i(t) = 0$ represents that node i is healthy at time t in the physical network, and $X_i(t) = 1$ means node i is infected at time t in the physical network. Similarly, a Bernoulli random variable $Y_i(t) \in \{0, 1\}$ specifies the state of node i at any time t in the social network. $Y_i(t) = 0$ means that node i is unaware of the epidemic at time t in the social network, and $Y_i(t) = 1$ indicates node i is aware of the epidemic at time t . Furthermore, we denote the probability that a node i is aware in the online social network at time t by $u_i(t) = Pr[Y_i(t) = 1]$, therefore $Pr[Y_i(t) = 0] = 1 - u_i(t)$ is the probability that node i is unaware. Similarly, we denote the probability that a node i is infected in the physical contact network at time t by $v_i(t) = Pr[X_i(t) = 1]$, and the probability that node i is susceptible at time t by $Pr[X_i(t) = 0] = 1 - v_i(t)$.

We denote the adjacency matrix of the social network as A , where the element $a_{ij} = 1$ means there is a link that connects node i and node j , and $a_{ij} = 0$ otherwise. Similarly, the adjacency matrix of the physical contact network is B , where the element $b_{ij} = 1$ represents there is a link between node i and node j , and $b_{ij} = 0$ otherwise. Links in our networks are undirected, hence $a_{ij} = a_{ji}$, and $b_{ij} = b_{ji}$. a_{ii} and b_{ii} are always 0, since there is no self-loop in our networks.

Since there are 2 possible states for each node in the social network layer (unaware and aware), and 2 possible states for each node in the physical network layer (susceptible and infected), we combine them and get 4 possible states for each node in our two-layer networks. These 4 possible states are:

* **US:** Unaware and Susceptible

* **UI:** Unaware and Infected

* **AS:** Aware and Susceptible

* **AI:** Aware and Infected

Since we model the dynamic processes in this EAIP model I with the continuous-time Markov process, the chance that two events occur in one node at the same time is infinitesimal. We define that only one of two states in two network layers could change for a node at a time (unless an US node is infected and the injection happens at the moment). The state transition processes are illustrated in detail as followed:

Unaware and Susceptible (US) state. A node i could leave the US_i state with 2 possibilities. One possibility is that node i gets informed by its aware neighbors to become aware and susceptible (AS). The other possibility is node i gets infected by its infected neighbors in the physical network, and at the same time the injection of information happens. Thus node i becomes aware and infected (AI).

Unaware and Infected (UI) state. A node i in the UI state could be informed in the social network and become aware and infected (AI). In the meantime, the infection of node i in the physical layer could be recovered to the unaware and susceptible (US) state.

Aware and Susceptible (AS) state. An AS node i who is aware of the epidemic could lose alertness about the epidemic to become US. Furthermore, even if an individual is aware of the epidemic, and protective methods are taken like wearing masks, he or she could still get infected anyway. As a consequent, a node i in the AS state could be infected and become Aware and Infected (AI).

Aware and Infected (AI) state. An AI node could either lose the alertness and become Unaware and Infected (UI), or recover from the epidemic in the physical layer and become Aware and Susceptible (AS).

The idea of injection comes from [2], but our dynamic processes is different from processes used in [2] in the recovery of awareness. In their work, when an individual is infected in the physical layer, he or she stays aware until the recovery of the disease for this individual in the physical layer. However, we consider that when people get sick, they may inform their friends about this virus in the online social network, but they would not keep bothering friends with their illness status everyday. Hence, in our processes, after the injection, the recovery of awareness is independent with the recovery of the infection. Furthermore, in our work, in each time step processes on both layers are performed simultaneously, while in [1, 2] inside each time step awareness propagation is performed before epidemic spreading.

4.2. MONTE-CAROL SIMULATION

To simulate dynamic processes in our model, we developed Monte-Carol (MC) simulations in the C++ language. Here we would introduce how we implemented simulations.

Node is a class that we define with several variables indicating different states of a node. An object of Node class locates in either the physical network layer or the social network layer, and is connected to a node object in the other layer with an inter-layer link. Each node in our two-layer networks owns one and only one inter-layer link. Two nodes linked by an inter-layer link are actually the same node. Each node would be in either the healthy state or the infected state at any time t , which signifies unaware and aware states respectively if this node is in the social network layer, and susceptible and infected states respectively if this node is in the physical network layer. Furthermore, each node possesses a vector of neighbors which specifies intra-layer links that are connected to this node. We define a graph class that integrates a vector of node objects to represent a network layer.

We use the sample time $\Delta t = 0.01$ to sample continuous-time Markov processes in our model. As proofed in [29], when the sample rate $(\Delta t)^{-1}$ is larger than the fastest possible transition rate $\max_i q_i$ in the Markov process $\left(\Delta t \leq \frac{1}{\max_i q_i}\right)$, the steady state (or the long-run behavior) of the sampled-time Markov chain exactly equals to the steady state of the continuous-time Markov chain [29, Chapter 10.4].

In our MC simulations, each time we generate two graph objects as the two layers in a two-layer network. Each network owns $N = 1000$ nodes, and all nodes have one-one inter-layer links representing the same set of nodes in different network layers. Both layers are the same type of networks, either Erdős-Rényi (ER) random networks with the Poisson degree distributions ER-ER, or scale-free (SF) networks with the power-law degree distributions SF-SF. For an ER random network, we set the average degree $E[D] = 4$, which leads to in total $L = \frac{E[D]*N}{2} = 2000$ links in an ER random network. To generate such an ER random network, we randomly connect two nodes that are not already connected each time until 2000 links are established. For a SF network, the degree sequence follows a power law degree distribution $Pr[D = k] = ck^{-\lambda}$ with exponent $\lambda = 2.5$ for $N = 1000$ nodes. We set the minimum degree $K_{min} = 2$, and the maximum degree $K_{max} = 100$ for scale-free networks. The exponent $\lambda = 2.5$ results in $E[D] \approx 4$ in scale-free networks. Scale-free networks are constructed by the configuration model which has been introduced in Chapter.2.2.2.

We would like to further understand how the overlap extent between the two network layers of a two-layer network affects the spread of an epidemic. Hence, we control the overlap extent when generating two-layer networks. In order to generate a two-layer ER-ER network with a fraction ϕ of overlapping links, we first generate $\phi * L$ random links that exist on both layers, then randomly generate the rest of links in the two layers separately under the constraint that links exist in one layer do not show up in the other layer. A two-layer SF-SF network with the overlap $\phi = 1$ can be constructed by generating one layer scale-free network with the configuration model, and copying all the links to the other layer. A two-layer SF-SF network with overlap $\phi = 0$ can be obtained by generating the degree sequences for the two layers independently and constructing the two layers independently. In our setting, $\lambda = 2.5$ and $N = 1000$ in scale-free networks bring about 2000 links, while the maximal possible number of links in a network with $N = 1000$ nodes is about 500000. Hence, these two independently generated layers hardly overlap, leading to $\phi = 0$.

Since we sample the continuous-time Markov processes, we need to run enough time steps for processes in the two-layer network to reach the steady state in simulations. Some constant parameters that we chose for all simulations are: the basic awareness spreading rate on each link (without considering the time scale γ) $\beta_1 = 0.3$, the basic awareness recovery rate on each node $\delta_1 = 0.6$, the epidemic recovery rate on each node $\delta_2 = 1.0$. When a susceptible node is aware of the epidemic, the infection rate for this node is reduced by a factor of $\alpha = 0.5$. The epidemic spreading rate on each link β_2 , the time scale γ and the overlap extent between two layers ϕ are controllable parameters, and manipulated in our simulations to understand the influence of these parameters. At the beginning of a simulation, 10% of randomly chosen nodes are set to be aware and infected (AI). The rest of nodes in the network are unaware and susceptible (US). For each set of parameters $\beta_1, \delta_1, \beta_2, \delta_2, \gamma, \phi$ and the degree distribution etc, 200 realizations are implemented. The results of the simulation are the average steady state fraction of awareness and the average steady state fraction of infection over 200 realizations.

In the discrete-time simulations in [1, 2], sub sequential processes are performed in each time step. In their simulations, the infection processes were always performed after the awareness processes in each time step. In our simulations, we improve the simulation method by performing the processes in both layers simultaneously, which better approximates the continuous-time situation. We simulate processes in both layers simultaneously by recording states of all nodes at the end of each time step. In the time step $t+1$, all processes are run according to states of nodes at the end of time step t . In the social network layer, at each time step aware nodes would inform each of its unaware neighbors with the probability $\Delta t * \gamma * \beta_1$, and disregard awareness to become unaware with a probability $\Delta t * \gamma * \delta_1$. In the physical network layer, at each time step susceptible nodes could be infected by each of its infected neighbors with a probability $\Delta t * \beta_2$ or $\Delta t * \alpha * \beta_2$, according to the state of its counterpart in the social network layer at the end of last time step. For a newly infected node in this time step, if its counterpart in the social network was unaware at the end of last time step, the injection of information would occur and make its counterpart in the social network aware at the end of this time step. Infected nodes could recover from the epidemic with a probability $\Delta t * \delta_2$ in one time step.

We find the steady state for each two-layer network, and sum up steady states from 200 realizations to get

average to reduce the influence of the strong randomness in Monte-Carlo simulations. Besides the random numbers generated for each infection process and each recovery process, networks are also generated randomly, therefore the fluctuation of results happens between realizations. 200 times realizations with a certain set of parameters provide us a more stable result. Both the steady state fraction of awareness in the social network layer and the fraction of infection in the physical network layer are recorded as the primary outcome of simulations. In addition, the time evolution of the spread of an epidemic and the propagation of awareness are recorded for us to check whether the steady state in this simulation is actually reached.

4.3. INDIVIDUAL-BASED MEAN FIELD APPROXIMATION

The Individual-Based Mean Field Approximation, abbreviated as IBMFA, is a theoretical tool that we propose to analyze the dynamic processes in our EAIP model I. The IBMFA is our original method to tackle the steady state probability that each node is infected and the probability that each node is aware in the this model I with two-layer networks. This IBMFA is inspired by NIMFA (N-Intertwined Mean Field Approximation) for single networks [23, 24, 29].

4.3.1. INDIVIDUAL-BASED MEAN FIELD APPROXIMATION EQUATIONS

First of all, we would like to present the IBMFA equations we derive for each node in our EAIP model I:

$$\frac{du_i(t)}{dt} = -\gamma\delta_1 u_i(t) + (1 - u_i(t)) \left(\sum_{j=1}^N a_{ji} \gamma \beta_1 u_j(t) + (1 - v_i(t)) \sum_{j=1}^N b_{ij} \beta_2 v_j(t) \right) \quad (4.1a)$$

$$\frac{dv_i(t)}{dt} = -\delta_2 v_i(t) + (1 - v_i(t)) \left(\sum_{j=1}^N b_{ji} (u_i(t) \alpha + (1 - u_i(t))) \beta_2 v_j(t) \right) \quad (4.1b)$$

To clearly display the transition rates between the four states of a node, we plot Fig.4.1.

The IBMFA equations Equ.4.1 for node i has the following physical interpretation. In the differential equation Equ.4.1a for the aware probability $u_i(t)$ of node i, we explain the three terms one by one:

1. **The $-\gamma\delta_1 u_i(t)$ term.** When the node i is aware with the probability $u_i(t)$, node i could recover from awareness with the awareness recovering rate $\gamma\delta_1$.
2. **The $(1 - u_i(t)) \left(\sum_{j=1}^N a_{ji} \gamma \beta_1 u_j(t) \right)$ term.** When the node i is unaware with the probability $(1 - u_i(t))$, it could get alertness of the epidemic from its aware neighbors in the social network layer. $a_{ji} = 1$ means node j is a neighbor of node i in the social network. If node j is aware with the probability $u_j(t)$, node j would contribute to the total infection rate of node i in the social network by $\gamma\beta_1 u_j(t)$. These explain the term $(1 - u_i(t)) \left(\sum_{j=1}^N a_{ji} \gamma \beta_1 u_j(t) \right)$.
3. **The $(1 - u_i(t)) \left((1 - v_i(t)) \sum_{j=1}^N b_{ij} \beta_2 v_j(t) \right)$ term.** For an unaware node i $(1 - u_i(t))$, if it is susceptible at time t with the probability $(1 - v_i(t))$, each infected neighbor of node i in the physical layer tries to infect node i with a rate β_2 . In total the infection rate for node i in the physical network at time t is $\beta_2 \sum_{j=1}^N b_{ji} v_j(t)$. As we introduced above, in our EAIP model I, when a node is in the US state, and it gets infected in the physical network layer, the injection of information would happen immediately. As a consequence, an unaware node i could get aware from the injection of information with the rate $(1 - v_i(t)) \sum_{j=1}^N b_{ij} \beta_2 v_j(t)$.

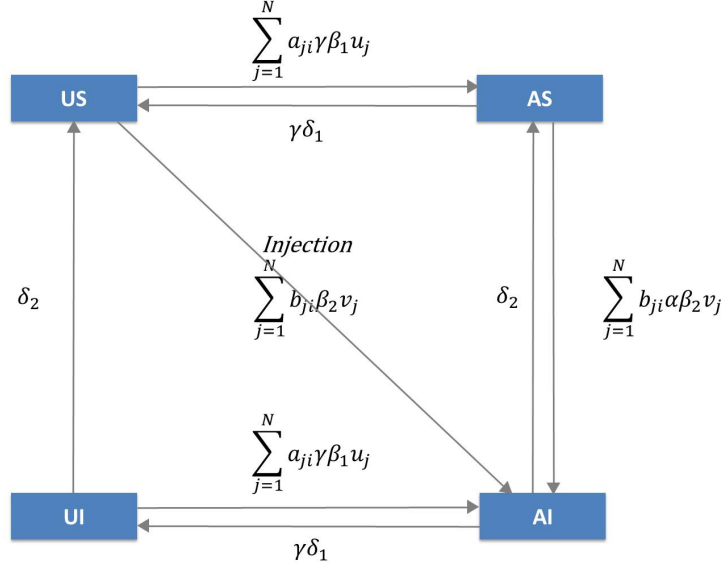


Figure 4.1: State transition processes between 4 possible states: Unaware and Susceptible (US), Unaware and Infected (UI), Aware and Susceptible (AS), and Aware and Infected (AI) in model 1. The infect and recover rates in the social network are β_1 and δ_1 respectively, and the infect and recover rates in the physical network are β_2 and δ_2 respectively. $a_{ij} = 1$ if node i and j are connected in the upper social network layer, otherwise $a_{ij} = 0$. In the physical contact layer, $b_{ij} = 1$ if there is a link between node i and j , otherwise $b_{ij} = 0$. At time t , node i has a probability $u_i(t)$ to be aware in the online social network, and a probability v_i to be infected in the physical contact network.

As for the differential equation Equ.4.1b for the infection probability $v_i(t)$, three terms are explained as followed:

1. **The term $-\delta_2 v_i(t)$.** When a node i is infected in the physical network with the probability $v_i(t)$, it could recover from the epidemic with the recovery rate δ_2 .
2. **The term $(1 - v_i(t))(1 - u_i(t))\left(\beta_2 \sum_{j=1}^N b_{ji} v_j(t)\right)$.** The rate that a susceptible node i ($1 - v_i(t)$) in the physical layer gets infected by its infected neighbors depends on the state of node i in the social network layer. If node i is unaware in the social network ($1 - u_i(t)$), each infected neighbor of node i $v_j(t)$ contributes to the total infection rate of node i by β_2 . Summing up the infection rate from all infected neighbors of node i , we get $\beta_2 \sum_{j=1}^N b_{ji} v_j(t)$. This explains the term $(1 - v_i(t))(1 - u_i(t))\left(\beta_2 \sum_{j=1}^N b_{ji} v_j(t)\right)$.
3. **The term $(1 - v_i(t)) u_i(t) \left(\alpha \beta_2 \sum_{j=1}^N b_{ji} v_j(t)\right)$.** When a susceptible node i ($1 - v_i(t)$) is aware in the social network with the probability $u_i(t)$, the rate that node i is infected by each infected neighbor in the physical network is reduced from β_2 to $\alpha \beta_2$. Summing up the reduced infection rate from all infected neighbors of node i at time t , we get $\alpha \beta_2 \sum_{j=1}^N b_{ji} v_j(t)$.

Note that in our IBMFA, we assume the independency between the infection states (infected or susceptible) of two neighboring nodes in the physical contact network as in NIMFA, the independency between the awareness states (aware or unaware) of two neighboring nodes in the social network, and the independency between the infection state and the awareness state of the same node though the injection has been taken into account.

In our EAIP model I, each node obeys two differential equations in Equ.4.1. By solving differential equations Equ.4.1 for each node in a two-layer network, we could get solutions representing the probabilities that each node stays in the aware state in the social network layer u_i , and the probabilities that each node stays in the infected state in the physical network layer v_i in the steady state. Denoting $U(t)$ as a column vector with

$N = 1000$ elements $U(t) = [u_1(t) \ u_2(t) \ \cdots \ u_{1000}(t)]^T$, and $V(t)$ as a column vector with $N = 1000$ elements $V(t) = [v_1(t) \ v_2(t) \ \cdots \ v_{1000}(t)]^T$, IBMFA equations for a two-layer network with $N = 1000$ nodes could be expressed in the matrix form as

$$\frac{dU(t)}{dt} = -\gamma\delta_1 U(t) + \text{diag}(u - U(t)) (\gamma\beta_1 AU(t) + \text{diag}(u - V(t)) \beta_2 BV(t)) \quad (4.2a)$$

$$\frac{dV(t)}{dt} = -\delta_2 V(t) + \text{diag}(u - V(t)) (\text{diag}(\alpha U(t) + (u - U(t))) \beta_2 BV(t)) \quad (4.2b)$$

where u is an all 1 column vector with $N = 1000$ elements. In the steady state, $\frac{du_i}{dt} = 0$ and $\frac{dv_i}{dt} = 0$ hold for all nodes in the network, so we have

$$0 = -\gamma\delta_1 U(t) + \text{diag}(u - U(t)) (\gamma\beta_1 AU(t) + \text{diag}(u - V(t)) \beta_2 BV(t)) \quad (4.3a)$$

$$0 = -\delta_2 V(t) + \text{diag}(u - V(t)) (\text{diag}(\alpha U(t) + (u - U(t))) \beta_2 BV(t)) \quad (4.3b)$$

The exact steady state is the susceptible and unaware state for all the nodes, which is the only absorbing state of the exact Markovian process. However, this absorbing state will be reached within an unrealistically long time for realistic sizes of networks when the effective infection rate is higher than the epidemic threshold $\tau > \tau_c$ [46]. We are interested in the meta-stable state in which the system stays for long and is reached fast. The meta-stable state better characterizes real epidemics. With $\frac{du_i}{dt} = 0$ and $\frac{dv_i}{dt} = 0$, we could obtain a trivial solution $u_{i\infty} = 0$, $v_{i\infty} = 0$ indicating the only absorbing state, and a possibly positive solution representing the meta-stable state, which is called the steady state in this thesis since now on and will be explored further.

4.3.2. METHOD OF SOLVING IBMFA EQUATIONS

In a two-layer network with $N = 1000$ nodes, we need to solve 2000 differential equations to get the steady state for this network. Due to the complexity of Equ. 4.1, we are unable to achieve analytical solutions. Nonetheless, numerical solutions could be obtained. The computational method that we use to get numerical solutions of differential equations in IBMFA is the ode45 function in matlab 2014b [47]. ode45 [48] is used to solve nonstiff ordinary differential equations. It is the preferred method to get numerical solutions in differential equations that has been widely applied in the complex network field.

In order to compare IBMFA solutions and Monte-Carlo simulation results to verify the accuracy of the IBMFA, we use the same sets of parameters in the IBMFA and simulations. Monte-Carlo simulations contain so many random events that for a certain two-layer network with a certain set of parameters, results of the steady state of the whole network in several realizations could fluctuate. However, for a settled two-layer network with a specific set of parameters, the solution of IBMFA equations is fixed. Due to the stability of solutions in the IBMFA equations, the only uncertainty in solutions of IBMFA equations comes from structures of randomly generated two-layer networks. 10 times realizations are implemented in IBMFA equations for each set of parameters, each realization with an independently generated two-layer network.

To solve differential equations Equ. 4.2 in IBMFA with the ode45 function, we set the initial values $u_i(0) = 1$, $v_i(0) = 1$ for all nodes. The steady state of a Markov chain does not depend on the initial condition [29, pp. 191]. Initial values $u_i(0) = 1$, $v_i(0) = 1$ has been widely applied to solve mean field differential equations, which could result in correct and stable numerical solutions. Given a two-layer network with $N = 1000$ nodes, we would get the steady state column vector $U(t)$ with 1000 elements, and the steady state column vector $V(t)$ with 1000 elements. The fraction of awareness ρ_1 in the steady state in the entire network is the average of $U(t)$, and the fraction of infection ρ_2 in the steady state is the average of $V(t)$.

$$\begin{aligned} \rho_1 &= \frac{\sum_{i=1}^N u_i}{N} \\ \rho_2 &= \frac{\sum_{i=1}^N v_i}{N} \end{aligned} \quad (4.4)$$

Comparison between IBMFA solutions and Monte-Carol simulation results is carried out in the following sections.

4.4. MICROSCOPIC MARKOV CHAIN APPROACH

The Microscopic Markov Chain Approach (MMCA) is the dynamical equations governing a two-layer network with the epidemic and awareness interacting processes. The Microscopic Markov Chain Approach was proposed in [49, 50] and has been shown to be an accurate approximation for the epidemic and awareness interacting processes in two-layer networks [2]. This is the second theoretical analysis tool in our EAIP model I. Based on our EAIP model I, we develop in this chapter the MMCA equations for our interacting processes. Later, we will compare the MMCA with the IBMFA, the two seemingly most advanced analytical approaches so far.

4.4.1. DERIVATION OF MMCA EQUATIONS

The Microscopic Markov Chain Approach examines the discrete time evolution of the probability that each node i is in each of the 4 possible states. In the MMCA, the dependency between states of nodes in the network is neglected.

Firstly we could establish a state transition tree of a standard SIS process in the discrete-time Markov chain, as shown in Fig.4.2:

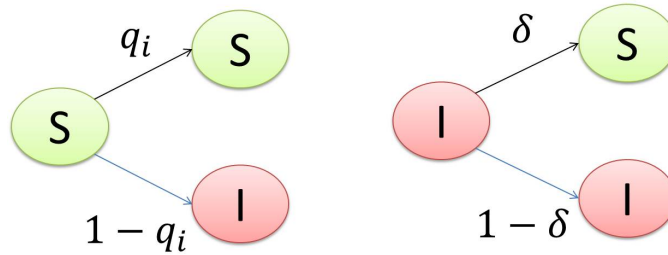


Figure 4.2: A standard SIS process state transition. q_i stands for the probability that node i does not get infected in this time step. δ is the probability that node i recovers from epidemic in this time step.

The root of a state transition tree is the state of node i at time t , and the two leaves of a state transition tree are two possible states of node i at time $(t+1)$. From state transition trees in Fig.4.2, we could derive equations for this discrete-time Markov process as:

$$\begin{aligned} p_i^S(t+1) &= p_i^S(t)q_i + p_i^I(t)\delta \\ p_i^I(t+1) &= p_i^S(t)(1 - q_i) + p_i^I(t)(1 - \delta) \end{aligned} \quad (4.5)$$

With the normalization condition

$$p_i^S(t) + p_i^I(t) = 1 \quad (4.6)$$

where $p_i^S(t)$ is the probability that node i is susceptible at time t , and $p_i^I(t)$ is the probability that node i is infected at time t .

In our two-layer network with four possible states: Unaware and Susceptible (US), Unaware and Infected (UI), Aware and Susceptible (AS), Aware and Infected (AI), we denote $r_i(t)$ as the probability that a node i is

not informed by neighbors at time t , $q_i^U(t)$ as the probability that unaware node i is **not** infected by neighbors at time t , and $q_i^A(t)$ as the probability that aware node i is **not** infected by neighbors at time t . $r_i(t)$, $q_i^U(t)$ and $q_i^A(t)$ could be written as

$$r_i(t) = \prod_j \left(1 - a_{ji} p_j^A(t) \beta_1^*\right) \quad (4.7a)$$

$$q_i^U(t) = \prod_j \left(1 - b_{ji} p_j^I(t) \beta_2^*\right) \quad (4.7b)$$

$$q_i^A(t) = \prod_j \left(1 - b_{ji} p_j^I(t) \alpha \beta_2^*\right) \quad (4.7c)$$

where the probability that a node gets informed by an aware neighbor within a time step of interval Δt follows $\beta_1^* = \gamma \beta_1 \cdot \Delta t$. Similarly, $\beta_2^* = \beta_2 \cdot \Delta t$, $\delta_1^* = \gamma \delta_1 \cdot \Delta t$ and $\delta_2^* = \delta_2 \cdot \Delta t$. The time interval Δt should be small so that this discrete time approach well approximates the continuous time processes. In consistent with Monte-Carol simulations, we use the sample time $\Delta t = 0.01$.

Equivalent to Equ.4.5, the MMCA equations describe the one time evolution of the probability that each node is in each of the 4 possible states:

$$p_i^{US}(t+1) = p_i^{UI}(t) r_i(t) \delta_2^* + p_i^{AI}(t) \delta_1^* \delta_2^* + p_i^{US}(t) r_i(t) q_i^U(t) + p_i^{AS}(t) \delta_1^* q_i^A(t) \quad (4.8a)$$

$$p_i^{UI}(t+1) = p_i^{UI}(t) r_i(t) (1 - \delta_2^*) + p_i^{AI}(t) \delta_1^* (1 - \delta_2^*) \quad (4.8b)$$

$$p_i^{AS}(t+1) = p_i^{UI}(t) (1 - r_i(t)) \delta_2^* + p_i^{AI}(t) (1 - \delta_1^*) \delta_2^* + \quad (4.8c)$$

$$p_i^{US}(t) (1 - r_i(t)) q_i^U(t) + p_i^{AS}(t) (1 - \delta_1^*) q_i^A(t)$$

$$p_i^{AI}(t+1) = p_i^{UI}(t) (1 - r_i(t)) (1 - \delta_2^*) + p_i^{AI}(t) (1 - \delta_1^*) (1 - \delta_2^*) + \quad (4.8d)$$

$$p_i^{US}(t) [(1 - r_i(t)) (1 - q_i^U(t)) + r_i(t) (1 - q_i^U(t))] +$$

$$p_i^{AS}(t) [\delta_1^* (1 - q_i^A(t)) + (1 - \delta_1^*) (1 - q_i^A(t))]$$

subject to the normalization condition

$$p_i^{US}(t) + p_i^{UI}(t) + p_i^{AS}(t) + p_i^{AI}(t) = 1 \quad (4.9)$$

The steady state of the MMCA is reached when $p_i(t+1) = p_i(t)$ is satisfied for all states and nodes. We could then get the fraction of awareness in the steady state ρ_1 and the fraction of infection in the steady state ρ_2 in the entire two-layer network from

$$\rho_1 = \frac{\sum_{i=1}^N (p_i^{AS}(\infty) + p_i^{AI}(\infty))}{N} \quad (4.10)$$

$$\rho_2 = \frac{\sum_{i=1}^N (p_i^{UI}(\infty) + p_i^{AI}(\infty))}{N}$$

In the MMCA, we could derive the epidemic threshold τ_c for the epidemic spreading. However, we are interested to discover the steady state fraction of infection ρ_2 and the steady state fraction of awareness ρ_1 in this thesis. The derivation of the epidemic threshold in the MMCA is shown in Appendix.A.2.

4.4.2. SOLVING MMCA EQUATIONS

We write MMCA equations Equ.4.8 for every nodes in matlab 2014b. The time steps should be large enough that the steady state is reached, i.e. $p_i(t+1) = p_i(t)$ holds for all states and nodes. In order to compare the accuracy of MMCA with the IBMFA, same sets of parameters are shared between Monte-Carol simulations, IBMFA and MMCA. 10 times realizations are implemented in MMCA equations for each set of parameters, each realization with an independently generated two-layer network. When steady states for all nodes are

reached, the fraction of awareness ρ_1 and the fraction of infection ρ_2 are calculated by

$$\begin{aligned}\rho_1 &= \frac{\sum_{i=1}^N (p_i^{AS}(\infty) + p_i^{AI}(\infty))}{N} \\ \rho_2 &= \frac{\sum_{i=1}^N (p_i^{UI}(\infty) + p_i^{AI}(\infty))}{N}\end{aligned}\quad (4.11)$$

Comparison between MMCA and IBMFA is shown in the following sections.

4.5. ACCURACY OF IBMFA AND MMCA

In this section we study the accuracy of our theoretical analysis methods, i.e. IBMFA and MMCA. In Monte-Carol simulations, the accurate steady state fraction of infection ρ_2 in our EAIP model I is achieved. Therefore, we compare the numerical solutions of IBMFA and MMCA with the simulation results to estimate the precision of these two analytical approaches. The approximation that approaches better to MC simulation results is the more accurate one. We use the time scale $\gamma = 1$ and the overlap extent $\phi = 1$ situation as an example, while the same phenomena are observed in other time scales and overlap extents.

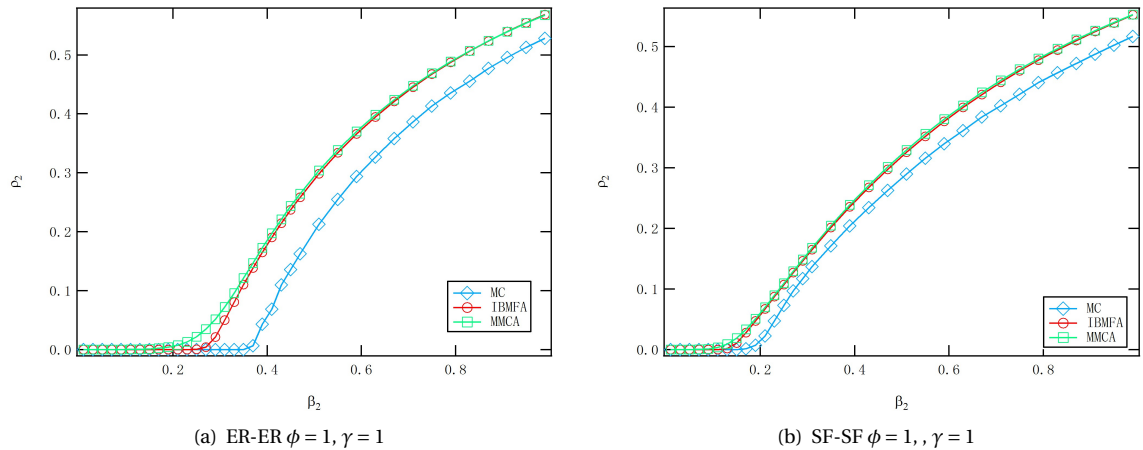


Figure 4.3: Compare the accuracy between Monte-Carol simulations, the IBMFA approximation and the MMCA approximation under the same set of parameters. Two-layer Erdős-Rényi random networks with overlap $\phi = 1$, and two-layer scale-free networks with overlap $\phi = 1$ are used. Parameters we choose here are as followed: $\beta_1 = 0.3, \delta_1 = 0.6, \delta_2 = 1.0, \alpha = 0.5, \gamma = 1$. The network size is $N = 1000$. For Erdős-Rényi random networks, the average degree $E[d] = 4$. For scale-free networks, the exponent in the power-law degree distribution is $\lambda = 2.5$.

From Fig.4.3, we could see that IBMFA outperforms MMCA in both ER-ER networks and SF-SF networks, especially around the epidemic threshold. The comparison between MC, IBMFA and MMCA in other sets of parameters are shown in Appendix.A.3. IBMFA is shown in these figures a better approximation for our EAIP model I.

4.6. THE INFLUENCE OF TIME SCALE γ ON EPIDEMIC MITIGATION

After introducing the three methods that we applied to tackle the steady state in our EAIP model I: Monte-Carol simulations, our original IBMFA, and the MMCA, we would like to explore two key factors that may influence the performance of such epidemic mitigation via awareness propagation: (i) the time scale of the awareness propagation in the (online) social network relative to that of the epidemic spreading in the physical contact network, or equivalently, the information update frequency in the online social network, and (ii) the

structure of the two-layer networks. In this section, we investigate the effect of the relative time scale γ in the social network layer on the epidemic mitigation.

Since Monte-Carol simulations simulate the actual stochastic processes in our EAIP model I with an adequate small sample time $\Delta t = 0.01$, the accurate steady state fraction of infection ρ_2 is achieved in simulation results. We only use the simulation results to investigate the influence of the time scale γ as well as the influence of the overlap extent ϕ in this chapter, while same phenomena are observed in the IBMFA solutions and the MMCA solutions (shown in Appendix.A.4).

We consider the following parameters with respect to the interacting SIS and UAU processes: $\beta_1 = 0.3, \delta_1 = 0.6, \delta_2 = 1.0, \alpha = 0.5$ and β_2 being the control parameter ranging over $\beta_2 \in [0, 1]$ with the step size $\Delta t = 0.01$. The effective awareness spreading rate $\tau_1 = \beta_1/\delta_1$ is chosen above the critical spreading threshold of the social network layer such that epidemic spreading can be possibly reduced via awareness. Each of the Monte-Carol simulation results, e.g. the fraction of infected nodes and the fraction of aware nodes, is averaged over 200 realizations.

First of all, we would show simulation results regarding different time scales γ in both two-layer ER-ER networks and two-layer SF-SF networks as followed:

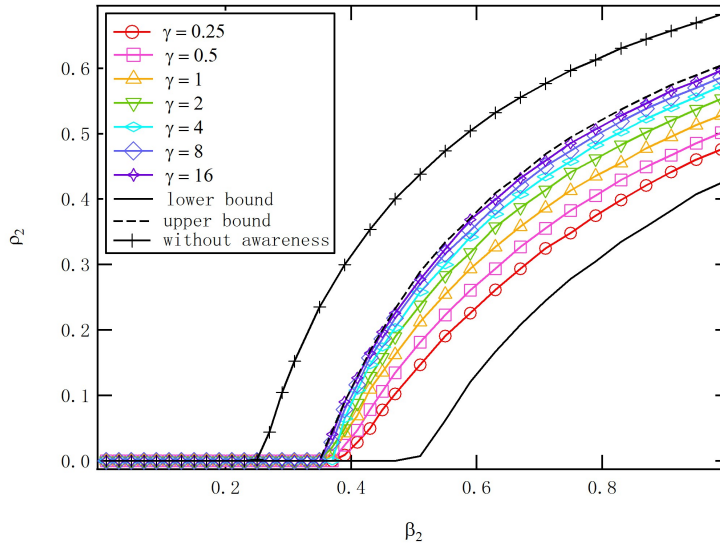


Figure 4.4: Effect of the time scale γ on the epidemic propagation in two-layer networks ER-ER. The x axis is the infection rate on each link in the physical network β_2 , and the y axis is the fraction of infection in the physical network in the steady state ρ_2 . Two-layer Erdős-Rényi random networks with the overlap extent $\phi = 1$ is used. Parameters we use here are as followed: $\beta_1 = 0.3, \delta_1 = 0.6, \delta_2 = 1.0, \alpha = 0.5$. The network size is $N = 1000$. For Erdős-Rényi random networks, the average degree $E[d] = 4$. Initially, 10% of randomly chosen nodes are aware and infected (AI). The rest of nodes in the network are unaware and susceptible (US). Results are averaged over 200 realizations.

As shown in Fig.4.4 and 4.5, the fraction of infection ρ_2 in the steady state can be indeed significantly reduced with the help of awareness information. We would discuss the effect of the time scale γ on the epidemic mitigation in more details.

4.6.1. THE RELATIVE TIME SCALE γ VS EPIDEMIC SPREADING

The relative time scale of awareness propagation with respect to epidemic spreading can be controlled by scaling both the spreading rate and the recovering rate of awareness as $\gamma\beta_1$ and $\gamma\delta_1$ respectively. The relative time scale of awareness propagation is, thus, characterized by the scaling parameter γ . The larger the time scale γ is, the faster the awareness propagation is, which represents the case when information is more

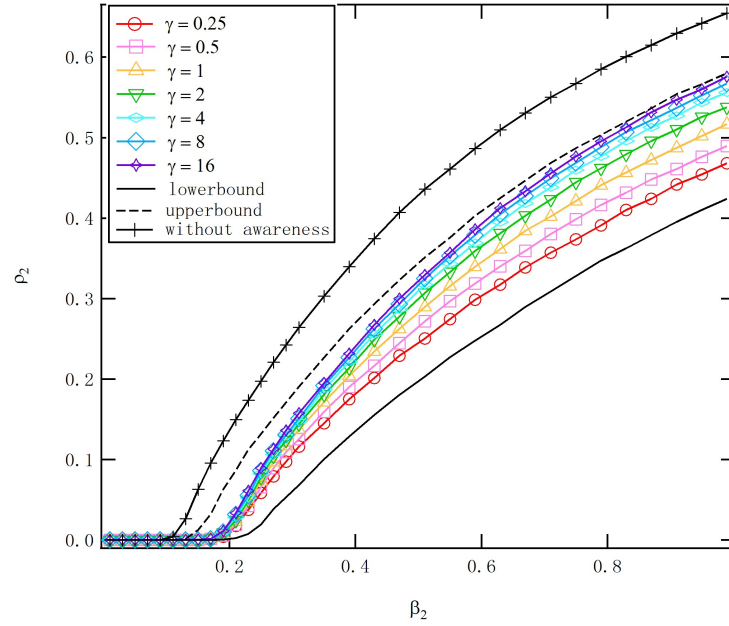


Figure 4.5: Effect of the time scale γ on the epidemic propagation in two-layer networks SF-SF. The x axis is the infection rate on each link in the physical network β_2 , and the y axis is the fraction of infection in the physical network in the steady state ρ_2 . Two-layer scale-free networks with the overlap extent $\phi = 1$ is used. Parameters we use here are as followed: $\beta_1 = 0.3, \delta_1 = 0.6, \delta_2 = 1.0, \alpha = 0.5$. The network size is $N = 1000$. For each scale-free network, the exponent in the power-law degree distribution is $\lambda = 2.5$. Initially, 10% of randomly chosen nodes are aware and infected (AI). The rest of nodes in the network are unaware and susceptible (US). Results are averaged over 200 realizations.

frequently updated in online social networks than their interaction in the physical contact network. γ influences the awareness spreading rate on each link: $\gamma\beta_1$, because when information in the social network is more frequently updated, individuals are more likely to post information in the social network. Meanwhile, γ also influences the awareness recovering rate on each node: $\gamma\delta_1$. The frequent information updates in the online social network could result in a large amount of information propagated in the social network, therefore the specific epidemic information is diluted by other important information that are also propagating in the social network.

Intuitively, when people update informations in the online social network more often, e.g. the value of γ is large, the awareness about the epidemic could spread out more easily and widely, therefore the epidemic could be better controlled. Nonetheless, as we observe in Fig.4.4 and 4.5, counterintuitively, the fraction of infection ρ_2 increases as we increase the time scale γ of the social network. The epidemic threshold τ_c , above which the epidemic breaks out, tends to decrease when the time scale is increased. These observations hold for both ER-ER networks and SF-SF networks. In general, a faster time scale in the social network degrades the mitigation effect, whereas a slower time scale better improves the robustness of the multi-layer network against viruses.

We explain the observations as follows. As shown in Equ. 4.1, the awareness in a node comes from two sources: (1) being informed by aware neighbors with a rate $\gamma\beta_1$ from each neighbor in the social network, and (2) the injection of information from the physical network layer, i.e. a node immediately gets aware once it is infected in the physical contact network. One SIS process in a single network would result in the same steady state fraction of infection when $\tau = \frac{\beta}{\delta}$ remains the same. This holds for both UAU and SIS spreading processes. As we tune the time scale γ , $\tau_1 = \frac{\beta_1}{\delta_1}$ remains the same, which would lead to the same fraction of awareness in the steady state if there were no injection. However, the amount of injection changes as we change the time scale γ . Review that the injection happens when an unaware and susceptible node gets infected in the physical network layer. As a consequence, the injection depends highly on the relative speed of the epidemic spreading. Fast epidemic spreading leads to the more frequently change between the suscep-

tible state and the infected state for nodes in the physical network layer, therefore more informations could be injected. When the time scale γ is small, the awareness propagation in the social network layer is slow compared to the spread of the epidemic in the physical network layer, thus is slow compared to injections. In this case, each injection of awareness would keep the node aware for a long time since the recover rate for awareness $\gamma\delta_1$ is small. Conversely, when the γ is large, the injection is slow compared to the awareness propagation. The injected awareness only last for a short time, being diluted by the fast dynamics in the social network layer. In this case the injection is not as effective as the small γ situation, therefore a lower fraction of awareness ρ_1 is achieved leading to a larger fraction of infection ρ_2 .

We verify our explanations by further simulations. In Monte-Carol simulations, to determine the source of awareness, we use two counters: an injection counter and an awareness spreading counter. The injection counter pluses one when the injection from the physical network to the social network happens once. The awareness spreading counter pluses one when an aware node informs an unaware neighbor in the social network. Then we could calculate the fraction of awareness that comes from injection.

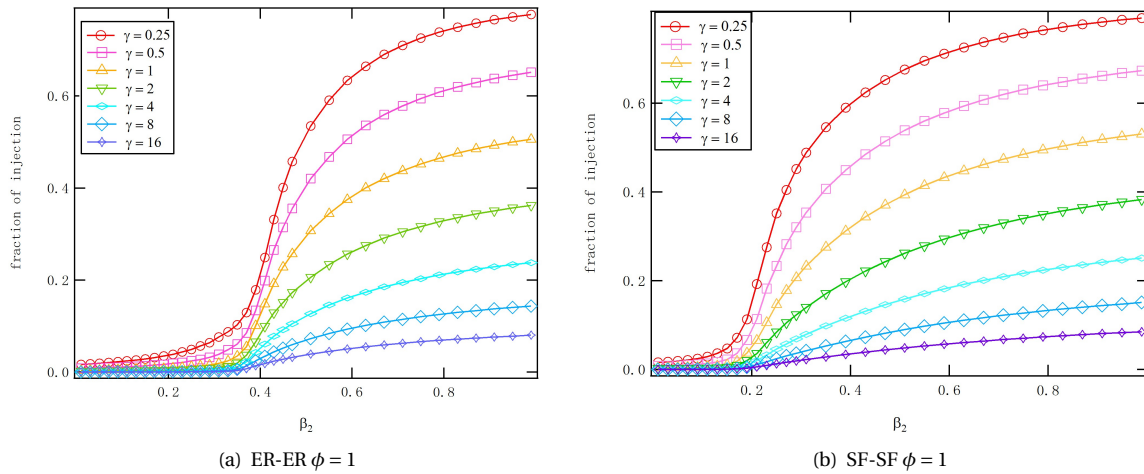


Figure 4.6: The amount of injection under different time scales γ . (a) shows the fraction of awareness that comes from injection in two layer Erdős-Rényi random networks ER-ER with overlap $\phi = 1$. (b) shows the fraction of awareness that comes from injection in two layer scale-free networks SF-SF with overlap $\phi = 1$.

As shown in figures Fig. 4.6(a) and Fig. 4.6(b), the percentage of nodes getting aware due to the injection in the steady state increases as the time scale γ decreases in both two-layer ER networks and two-layer SF networks. The overlap $\phi = 1$ case is shown as an example. Furthermore, the following three steady state quantities: the fraction of nodes getting aware due to injections, the fraction of aware nodes and the fraction of infected nodes, are averaged over all possibly values of $\beta_2 \in [0, 1]$. We call these averaged quantities as the integral fraction of injection, the integral fraction of awareness and the integral fraction of infection, respectively. Fig. 4.7(a) and Fig. 4.7(b) illustrate that a higher fraction of nodes getting aware due to the injection implies a higher fraction of awareness and a lower fraction of infection. Hence, a slow time scale in the social network better mitigates an epidemic.

Our findings and explanations point out an important fact that has been neglected: the frequent update of information in an online social network allows the sharing of timely information such as the alertness of an epidemic, however, may as well dilute a specific information due to the large amount of other information shared online. We may lose the alertness to an epidemic, thus become unaware, faster because of the frequent exposure to other information, which limits the mitigation effect of using the awareness information.

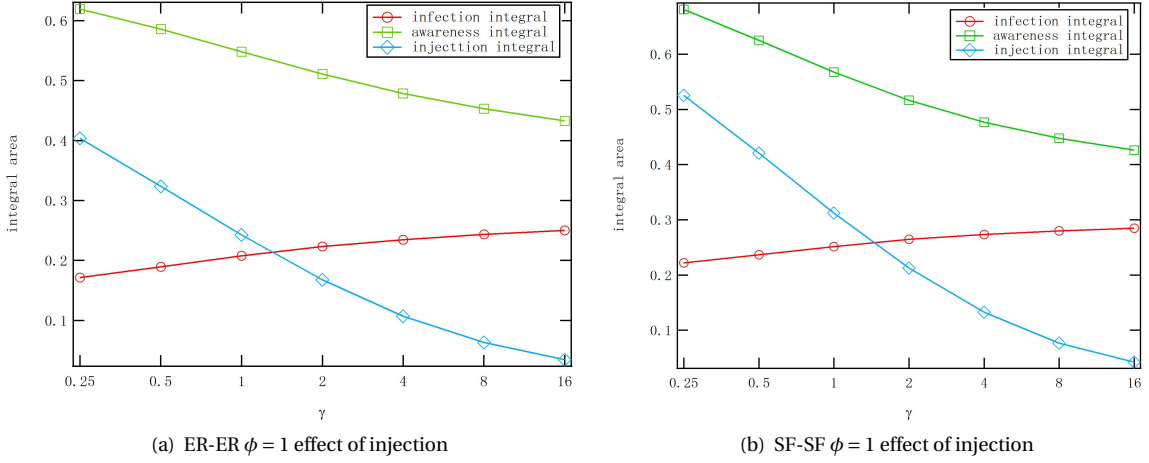


Figure 4.7: Effect of the injection on both ρ_1 and ρ_2 in different time scales. (a) shows the relationship between the injection, infection and awareness in two layer Erdős-Rényi random networks ER-ER with overlap $\phi = 1$. (b) shows the relationship between the injection, infection and awareness in two layer scale-free networks SF-SF with overlap $\phi = 1$.

4.6.2. ACCURACY OF SAMPLED-TIME MARKOV PROCESSES IN SIMULATIONS

In Section 4.6.1, we discussed the the relative time scale γ and its influence on the epidemic mitigation. However, information in Fig.4.4 and Fig.4.5 have not been thoroughly introduced. Before we go into more details of phenomena in those figures, we discuss in this section the accuracy of our Monte-Carlo simulations.

As we discussed in Section 4.2, in our simulations, we use the sample time $\Delta t = 0.01$ to sample the continuous-time Markov processes. The sample frequency must be large enough so that the sample-time Markov processes have exactly the same steady state as the continuous-time Markov process. In our simulations, the parameter γ functions in both awareness spreading rate and awareness recovering rate. We use γ that are in an exponent form of 2, i.e. $\gamma = \{0.25, 0.5, 1, 2, 4, 8, 16\}$, and $\gamma = \{32, 64\}$ if necessary. When the time scale γ is increased to a large number, e.g. $\gamma = 64$, the sample time $\Delta t = 0.01$ may not be large enough, which might lead to inaccurate steady states in simulations.

To verify the effectiveness of $\Delta t = 0.01$ in our simulations, we do some simple theoretical calculations here. Review that the steady state, or the long-run behavior of the sampled-time Markov chain is exactly the same as the steady-state of the continuous-time Markov chain for any sampling step $\Delta t \leq \frac{1}{\max_i q_i}$, as introduced in Section 4.2. Given a time scale $\gamma = 16$, we have the awareness spreading rate and the awareness recovering rate in the social network: $\gamma\beta_1 = 16 * 0.3 = 4.8$, $\gamma\delta_1 = 16 * 0.6 = 9.6$. For an aware node in the social network, the rate that it becomes unaware is $\gamma\delta_1 = 9.6$, which obviously satisfies the $\Delta t \leq \frac{1}{9.6}$ condition. On the other hand, the rate that an unaware node i becoming aware depends on the number of aware neighbors of node i at the moment. To satisfy the $\Delta t \leq \frac{1}{\max_i q_i}$ condition, the maximum number of aware neighbors n of node i is $n \cdot \gamma\beta_1 \leq 1/0.01$, therefore $n \leq 20.83$. From simulation results, when $\gamma = 16$, the steady state fraction of awareness in the entire network is less than 50%, which means the unaware node i could have in total $20.83/50\% = 41.66$ neighbors in the social network layer such that the sample time $\Delta t = 0.01$ is still small enough.

In a scale-free network with a power law degree distribution $Pr [d = k] \sim k^{-2.5}$, and the minimum degree and the maximum degree $K_{min} = 2$ and $K_{max} = 100$, we could calculate the probability distribution function (pdf) of this power-law degree distribution as

$$Pr [D = k] = \frac{k^{-2.5}}{\sum_{n=K_{min}}^{K_{max}} n^{-2.5}} \quad (4.12)$$

With the cumulative distribution function (cdf) derived from the pdf, the probability that node i has a degree

smaller than 41 in a scale-free network in our simulation is

$$\sum_{k=K_{min}}^{41} Pr [D = k] \approx 99.5\%$$

In the mean time, for our Erdős-Rényi random networks with the average degree $E[d] = 4$, the probability that there is a link between two randomly chosen node is

$$p = \frac{N \cdot E[d]}{\binom{N}{2}} = 0.004 \quad (4.13)$$

In a binomial distribution, the pdf of this Erdős-Rényi random network is indicated in Equ.2.5:

$$Pr[D = k] = \binom{N-1}{k} p^k (1-p)^{N-1-k}$$

Also with the cdf, we could derive the probability that node i has a degree larger than 41

$$1 - \left(\sum_{k=K_{min}}^{41} Pr [D = k] \right) < 1 \times 10^{-14}$$

As a conclusion, theoretically we could say that the sample time $\Delta t = 0.01$ is small enough for the $\gamma = 16$ case to reach the same steady state as its corresponding continuous-time Markov process. We also examine the accuracy of the sample time $\Delta t = 0.01$ when $\gamma = 16$ by simulations.

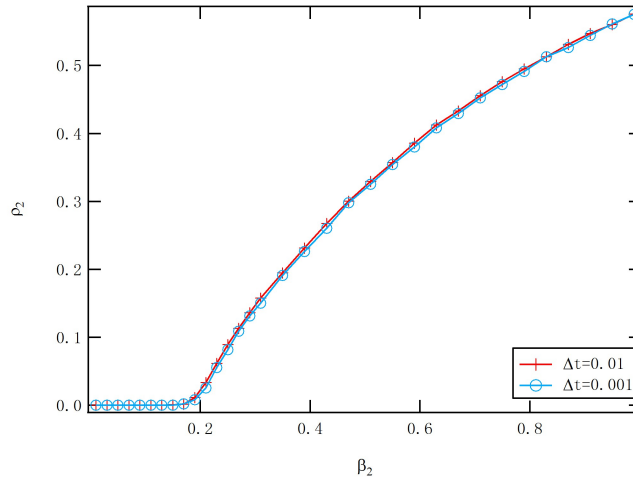


Figure 4.8: The accuracy of simulations in two-layer scale-free networks SF-SF with $\gamma = 16$. Other parameter we used here are: $\beta_1 = 0.3, \delta_1 = 0.6, \delta_2 = 1.0, \alpha = 0.5$. The network size is $N = 1000$. The overlap between two layers $\phi = 1$. For each scale-free network, the exponent in the power-law degree distribution is $\lambda = 2.5$. Initially, 10% of randomly chosen nodes are aware and infected (AI). The rest of nodes in the network are unaware and susceptible (US). Results are averaged over 200 realizations.

If the sample frequency with $\Delta t = 0.01$ is not large enough, when we reduce the sample time from $\Delta t = 0.01$ to $\Delta t = 0.001$ ($\Delta t = 0.001$ is definitely small enough for $\gamma = 16$ according to our simple calculations above), the steady state fraction of infection ρ_2 would change. Nevertheless, as shown in Fig.4.8, two curves with $\Delta t = 0.01$ and $\Delta t = 0.001$ almost overlap. Therefore, the sample time $\Delta t = 0.01$ is small enough for reaching the accurate steady state for the time scale $\gamma = 16$, and consequently small enough for $\gamma \leq 16$.

Normally, the time scale $\gamma = 16$ is large enough for observing changes in the mitigation effect along with time scale γ . Therefore, generally we use $\Delta t = 0.01$. When $\gamma > 16$ is necessary, we increase the sample frequency so that the sample step size is $\Delta t = 0.001$ to ensure the accuracy of steady states.

4.6.3. UPPER BOUND AND LOWER BOUND OF ρ_2

As explained in Section.4.6.1, when the time scale γ is small, the information spreading in the social network layer is slow compared to the epidemic spreading in the physical network layer, thus slow compared to the injection of information from the physical network layer to the social network layer. As a consequence, the fraction of infection ρ_2 in the physical network in the steady state is small, i.e. the effect of epidemic mitigation is good. Contrary, a large value of the time scale γ indicates fast information spreading compared to the injection of information, therefore the fraction of infection ρ_2 in the steady state in the physical network layer is large, i.e. the effect of epidemic mitigation is bad. We could inference from these findings that the best possible mitigation, i.e. the lower bound of the fraction of infection ρ_2 , could be achieved by the slowest time scale γ . The worst possible mitigation, i.e. the upper bound of the fraction of infection ρ_2 , could be obtained by the fastest time scale γ .

When the time scale γ is infinitely slow, i.e. $\gamma\beta_1 \approx 0$ and $\gamma\delta_1 \approx 0$, the injection from the physical layer is infinitely fast compared to the recover rate of the awareness. With fast injections of information from the physical network layer to the social network layer, and awareness recovering rate $\gamma\delta_1 \approx 0$, all the nodes tend to be aware in steady state. In this case, the interacting information propagation and epidemic spreading on the two-layer network is equivalent to the SIS model in a single physical contact network with the infection rate $\alpha * \beta_2$ and the recovery rate δ_2 . This best possible mitigation of an epidemic (or the lower bound) can be achieved both by simulations as shown in Fig. 4.4 and Fig. 4.5 with the solid black lines that are below the $\gamma = 0.25$ curve, and by our IBMFA, which in this case is equivalent to the NIMFA in a single network.

When the time scale γ is infinitely large, the very slow epidemic spreading makes the effect of injection negligible, since awareness that comes from the injection would be recovered instantly by the infinitely large awareness recovering rate $\gamma\delta_1$. The steady state fraction of aware nodes ρ_1 , as well as the probability of each node to be aware u_i are solely determined by the effective spreading rate in the social network layer $\tau_1 = \frac{\beta_1}{\delta_1}$, and the social network structure. Since γ is infinitely fast, the awareness propagation in the social network would reach the steady state instantly. At any time t , the rate that a node i gets infected by an infected neighbor is $\alpha * \beta_2$ with probability $u_i(t)$, and is β_2 with probability $1 - u_i(t)$. In this case, the upper bound, i.e. the worst possible mitigation, can be obtained via simulations (results are shown in Fig. 4.4 and Fig. 4.5, the dotted line that is just above $\gamma = 16$ curve) and via the following adapted IBMFA:

$$\begin{aligned} \frac{du_i}{dt} &= -\gamma\delta_1 u_i + (1 - u_i) \left(\sum_{j=1}^N a_{ji} \gamma \beta_1 u_j \right) \\ \frac{dv_i}{dt} &= -\delta_2 v_i + (1 - v_i) \left(\sum_{j=1}^N b_{ji} (u_i \alpha + (1 - u_i)) \beta_2 v_j \right) \end{aligned} \quad (4.14)$$

where the injection term $(1 - u_i(t))(1 - v_i(t)) \sum_{j=1}^N b_{ji} \beta_2 v_j(t)$ is neglected in $\frac{du_i}{dt}$ equation, since both $-\gamma\delta_1 u_i$ and $(1 - u_i) \left(\sum_{j=1}^N a_{ji} \gamma \beta_1 u_j \right)$ terms contain the infinitely large number γ , while the injection term only includes finite numbers. Therefore in the IBMFA equations Equ.4.14 for the upper bound, the epidemic spreading is influenced by the awareness propagation but not the other way around.

APPROXIMATE SIMULATIONS OF THE UPPER BOUND

While the lower bound is easy to achieve in simulations (for an infinitely slow time scale γ in the social network, we could use $\gamma = 0$ in simulations to get the lower bound), to achieve the upper bound in simulations, we cannot use an infinitely large γ due to the fact that the sample frequency $1/\Delta t = 100$ is not large enough for very large γ to get the accurate steady state as in the corresponding continuous-time Markov processes. Approximations need to be applied to achieve the upper bound in simulations.

APPROXIMATION METHOD 1

Enlightened by the analysis that the upper bound is reached when γ is infinitely large so that the injection from the physical network layer is negligible, we could simulate the upper bound approximately by canceling the injection mechanism in two-layer networks. However, even without injection, we cannot simulate this model with an arbitrary large γ in order to get the fraction of infection ρ_2 of the upper bound in the physical network layer.

The situation that injections are negligible when the relative time scale in the social network $\gamma \rightarrow +\infty$ is indeed equivalent to canceling the injection mechanism. However, when $\gamma \rightarrow +\infty$, the other phenomenon is, the infinitely large awareness spreading rate and awareness recovering rate $\gamma\beta_1$ and $\gamma\delta_1$ leads to the infinitely fast changes between aware and unaware states for each node in the social network. When we need to determine the infection rate on a node i in the physical network layer, we need to check the state of this node in the social network layer. Infinitely fast awareness propagation in the social network layer results in almost irrelevant observations between any two inspections of the state in the social network. If we approximate $\gamma \rightarrow +\infty$ by using a small γ without the injection mechanism, inspections of states in the social network could be strongly correlated. For example, for a node i , several times of checking its state in the social network could happen during a single aware period. A large γ is still required to get the accurate steady state fraction of infection ρ_2 of the upper bound. We believe that when γ is large enough that the state changes in the social network is sufficiently fast, the upper bound is reached such that further increases of γ could not improve the accuracy of the upper bound. Nonetheless, the adequately large γ is difficult to determine theoretically.

APPROXIMATION METHOD 2

The second approximation method of the upper bound is, in a specific two-layer network, we firstly run processes in a single social network with parameters $\gamma\beta_1$ and $\gamma\delta_1$ without being impacted by the physical network layer. With the steady state probability of awareness for each node u_i , we apply them to the physical network layer. For a node i in the physical network, each time the infection rate need to be determined, the infection rate would be β_2 with probability $1 - u_i$, and $\alpha\beta_2$ with probability u_i .

Our motivation of this approximation method is, when $\gamma \rightarrow +\infty$, awareness propagation in the social network is so fast that steady state could be reached immediately after the simulation starts. After that, infinitely fast changes between states for each node is performed according to the steady state probability of awareness u_i . In the physical layer, each time a node i checks its state in the social network, the state is likely random with a probability u_i to be aware, and $1 - u_i$ to be unaware. Note that in this method, processes in the social network and the physical network are performed independently since injections are negligible. As we discussed before, the spread of an epidemic in a single network has the same steady state fraction of infection as long as the effective infection rate $\tau = \frac{\beta}{\delta}$ remains the same. By the same token, awareness propagation in a single social network have the same fraction of awareness ρ_1 as long as $\tau_1 = \frac{\beta_1}{\delta_1}$ remains the same. In this method, arbitrary γ could lead to the same τ_1 . Therefore, large γ is not required for this method to approximate the upper bound. The upper bounds in Fig.4.4 and Fig.4.5 are achieved by this second method.

In order to verify the effectiveness of the upper bound that we achieved in approximate simulations as we introduced above, we plot the changing trend of the fraction of infection ρ_2 along with the relatively time scale in the social network γ in Fig.4.9.

We could observe clearly in Fig.4.9 that fast information updates in the social network could in fact reduce the effectiveness of epidemic mitigation (the red curve is the fraction of infection in the physical network layer ρ_2). Meanwhile, the increase of ρ_2 , or the slope of the rising curve is getting smaller with increasing γ . The ascension of ρ_2 is almost negligible when γ increases from $\gamma = 32$ to $\gamma = 64$, where ρ_2 is very close

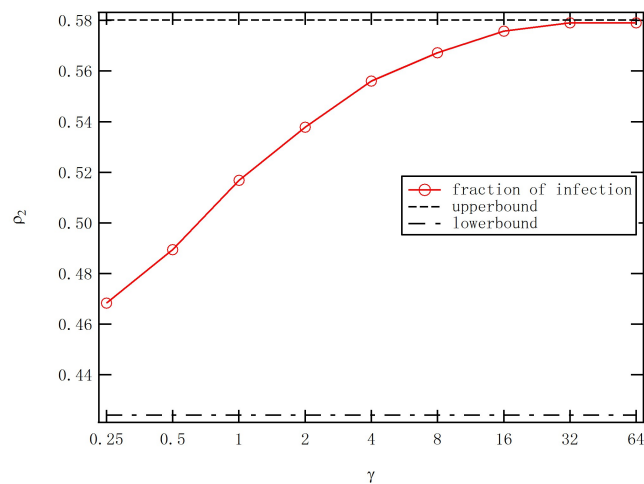


Figure 4.9: The rising trend of the fraction of infection ρ_2 along with the relatively time scale γ in two-layer networks SF-SF. The x axis is the time scale γ , and the y axis is the fraction of infection in the physical network in the steady state ρ_2 . Two-layer scale-free networks with the overlap extent $\phi = 1$ is used. Parameters we use here are as followed: $\beta_1 = 0.3, \delta_1 = 0.6, \beta_2 = 1.0, \delta_2 = 1.0, \alpha = 0.5$. The network size is $N = 1000$. For each scale-free network, the exponent in the power-law degree distribution is $\lambda = 2.5$. Initially, 10% of randomly chosen nodes are aware and infected (AI). The rest of nodes in the network are unaware and susceptible (US). Results are averaged over 200 realizations.

to, while still lower than the upper bound we achieved from our approximation. The explanation for this trend is, when the speed of awareness propagation in the social network layer is comparable with epidemic spreading in the physical network layer, a small change of the time scale could lead to a significant rise in ρ_2 . However, when γ reaches 16 or 32, the awareness propagation in the social network is much faster than the epidemic spreading in the physical layer. Therefore, slow injections of information from the physical network compared to the awareness propagation in the social network and the fast recovery of awareness result in the not remarkable effect of injections (which is close to "no injection" phenomenon when $\gamma \rightarrow \infty$), and consequently the change of ρ_2 is insignificant when γ is very large. We could therefore verify that the upper bound we achieved in approximate simulations is effective.

4.7. INFLUENCE OF OVERLAP ϕ

After exploring the effect of time scales γ , in this section we further investigate the influence of the structure of two-layer networks on the epidemic mitigation in our EAIP model I. In reality, some people would prefer to keep in touch with real life friends, like their families, classmates and coworkers, in online social networks, while other people are keen to socialize with new friends in online social networks. Inspired by this phenomenon, we investigate here how the link overlap extent between two layers of a multi-layer network affects the spread of an epidemic.

In both two-layer ER-ER networks and two-layer SF-SF networks, we compare two extreme situations: the overlap extent $\phi = 1$, and the overlap extent $\phi = 0$. In the overlap $\phi = 1$ case, everyone in a two-layer network have exactly the same sets of friends in the social network and in the physical network. Under such circumstance people only share information with their acquaintance in real life. When the overlap between layers is $\phi = 0$, people would completely separate their real life with their social intercourse online. They may find it interesting to share their insights with strangers. We use Monte-Carlo simulations to investigate these two extreme cases.

As shown in Fig.4.10 and Fig.4.11, the effect of overlap is more evident around the epidemic threshold and when the time scale γ is relatively large. These observations can be explained by the following physical in-

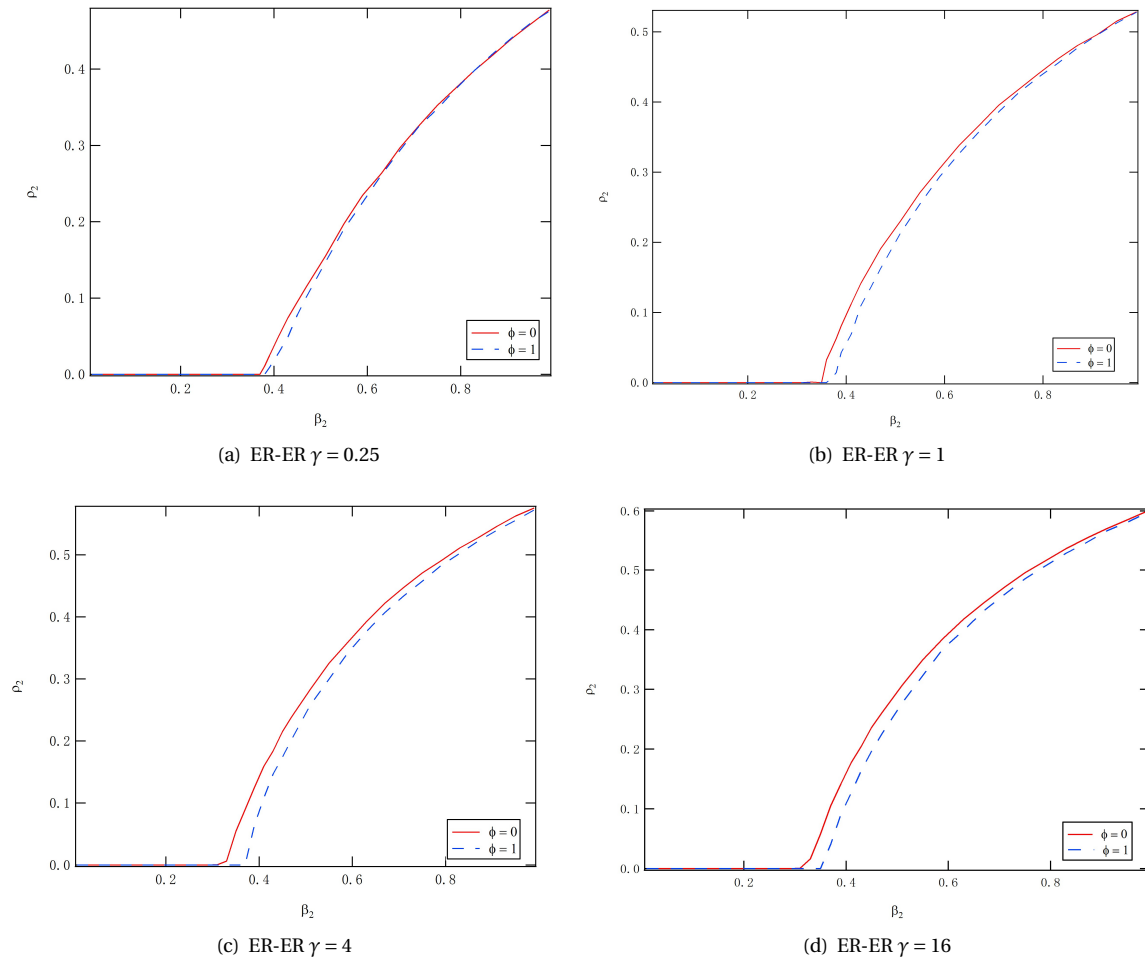


Figure 4.10: The influence of overlap in two layer Erdős-Rényi random networks ER-ER. Time scales γ we used in figures are: (a) $\gamma = 0.25$. (b) $\gamma = 1$. (c) $\gamma = 4$. (d) $\gamma = 16$. Parameters we choose here are as followed: $\beta_1 = 0.3, \delta_1 = 0.6, \delta_2 = 1.0, \alpha = 0.5$. The network size is $N = 1000$. For each Erdős-Rényi random network, the average degree $E[d] = 4$. Initially, 10% of randomly chosen nodes are infected and aware. Results are averaged over 200 realizations.

terpretations. When the time scale γ is infinitely small, all nodes stay in the aware state. This is actually the lower bound situation as we mentioned in Section 4.6.3 where the interacting awareness propagation and epidemic spreading are equivalent to the SIS model for epidemic spreading in a single network with a infection rate $\alpha\beta_2$ and a recovery rate δ_2 . The overlap extent ϕ , in this case, has no influence on the epidemic spreading. Hence, the difference between fractions of infection ρ_2 in different overlap extents is noticeable only when the time scale is not small. When the time scale is large such that the injections from the physical contact network to the social network is negligible, $\phi = 1$ or equivalently, the same topology for both layers, enables the more efficient usage of the awareness information than the case when $\phi = 0$: a node with a high (low) risk of infection tends to have as well a high (low) chance to get aware. When the time scale γ is neither too large nor too small, the complete overlap $\phi = 1$ also allows a newly infected node to inform its neighbors before they get infected, effectively reducing the infection rate of the neighbors. However, the effect of overlap extents would be diminished when β_2 is large where most nodes are aware due to large amount of injections from the large fraction of infection ρ_2 .

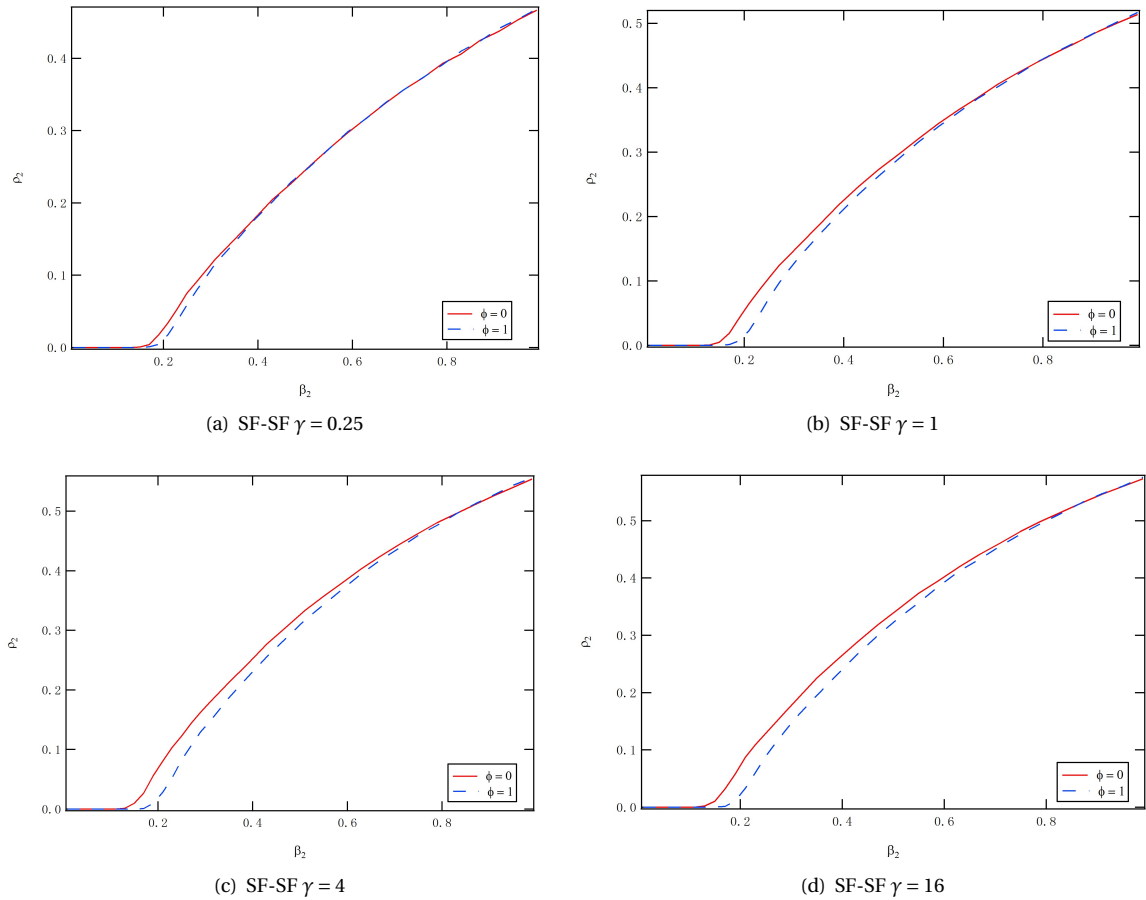


Figure 4.11: The influence of overlap in two layer scale-free networks SF-SF. Time scales γ we used in figures are: (a) $\gamma = 0.25$. (b) $\gamma = 1$. (c) $\gamma = 4$. (d) $\gamma = 16$. Parameters we choose here are as followed: $\beta_1 = 0.3, \delta_1 = 0.6, \delta_2 = 1.0, \alpha = 0.5$. The network size is $N = 1000$. The exponent for scale-free networks is $\lambda = 2.5$. Initially, 10% of randomly chosen nodes are infected and aware. Results are averaged over 200 realizations.

As a conclusion, in general a large extent of overlap between the two layers facilitates the mitigation. This finding encourages individuals to keep in touch with their physical contacts as well online, since it is beneficial for the epidemic mitigation. Interacting with strangers in the online social network is good, but it does not help the epidemic mitigation as much as interacting with physical contacts.

5

EPIDEMIC AND AWARENESS INTERACTION PROCESSES MODEL II

In Chapter.4, our first epidemic and awareness interaction processes (EAIP) model is introduced and analyzed by Monte-Carol simulations, theoretical analysis and physical interpretations. The influence of relative time scales γ and the overlap between layers ϕ are studied in detail. The processes in EAIP model I (as shown in Fig.4.1) assume that when an individual is infected by the epidemic, he or she immediately gets aware of the epidemic and starts sharing alertness to friends in the online social network. However, if the online social network is not used very frequently, people may not update their information about the epidemic immediately when they get infected. According to this situation, we propose our epidemic and awareness Interaction processes (EAIP) model II.

In this chapter, we study the EAIP model II that describes the scenario where infected individuals get aware of the epidemic with a certain rate. Monte-Carol simulations, the IBMFA and the MMCA approximations are also applied in this chapter, but in different forms compared to the EAIP model I. We still study the effect of the time scales γ and the overlap extent between two layers ϕ on epidemic mitigation. Compared to our model I, the steady state fraction of infection ρ_2 does not increase monotonously with the relative time scale γ of awareness propagation anymore. Instead, a clear lowest ρ_2 is observed where the spread of an epidemic is most efficiently hindered by using the information propagated in the social network.

5.1. DEFINITION OF PROCESSES IN THE EAIP MODEL II

The rapid development of online social networks helps the information propagation, which provides a possibility to mitigate the spread of an epidemic by using information propagated in the social networks. Our EAIP model II is consisted of a bottom layer of physical contact network where an epidemic spreads, and a top layer of online social network where information about the epidemic, or awareness about the epidemic, propagates. The awareness of an epidemic could drive people taking precaution measures to protect themselves from getting infected by the epidemic.

In consistent with the EAIP model I, in the EAIP model II we model epidemic spreading in the physical contact network with the Susceptible-Infected-Susceptible(SIS) model. The infection rate on each link and the recover rate for each node in the physical network are represented by β_2 and δ_2 , respectively. The awareness

propagation in the social network layer is modeled by the Unaware-Aware-Unaware(UAU) model as defined in Section.4.1. An aware node informs each of its unaware neighbors with an awareness spreading rate β_1 , whereas an aware node recovers from the awareness to become unaware with an awareness recovering rate δ_1 . Taking the time scale γ into consideration, the awareness spreading rate and the awareness recovering rate in the social network becomes $\gamma\beta_1$ and $\gamma\delta_1$, respectively.

In this model, epidemic spreading and awareness propagation also interacts with each other. The mechanism that awareness propagation impacts epidemic spreading in this model is the same as in EAIP model I. If an individual gets aware in the social network layer, he or she would take precautions which reduces the infection rate of this individual by a factor of α . Recovery of the epidemic is independent with awareness propagation.

The main difference between our EAIP model II and the EAIP model I which has been introduced in Chapter 4 is the injection of information mechanism. In the EAIP model I, we assume that everyone is enthusiastic to inform his neighbors in the online social network about the epidemic at the moment he gets infected. In other words, the injection happens immediately when an unaware and susceptible (US) node gets infected. However, in this model we consider the situation that people may not be so crazy about online socializing. If an individual only logs in to his or her social network account once a week, the update of awareness about the epidemic in the social network could be delayed instead of immediately update. Therefore, the injection of information is related to the frequency that people use the online social network. If everyone are keen on online socializing, the injection might happen immediately. If people are indifferent about online socializing, then injections take some time. Taking this into consideration, in this EAIP model II injections of information happen with an injection rate that is related to the relative time scale γ .

Without losing generality, we assume the injection rate in the EAIP model II is γ^ϵ . The polynomial relationship is general and flexible mathematically. Here a new parameter ϵ , the exponent of injection rate, is introduced in the EAIP model II. When the exponent of the injection rate is $\epsilon = 1$, the injection rate is linearly related to the time scale γ . Under this injection rate γ^ϵ , frequent information updates in the online social network (γ is large) leads to not only fast information updates in the social network, but also fast injections of information. Contrary, rare information updates in the online social network (γ is small) results in slow injections.

After introducing the injection rate, we could see that when an unaware and susceptible (US) node i is infected, it does not directly go to the aware and infected (AI) state. Instead, node i would become unaware and infected (UI), and has a rate γ^ϵ to inject the information and becomes AI. Meanwhile, we define that during the period from a node i gets infected in the physical layer, until node i is recovered from the epidemic, injection of information could happen at most once. Our consideration here is, in real life after an individual gets aware because he or she is infected by an epidemic, this individual might stay aware for a while until he or she gets tired of the awareness and forgets about the awareness. After that, this individual might get aware again because he or she sees some new information about the epidemic in the social network, but it is unlikely that this individual would be aware again because of the epidemic, since this individual is not recovered and gets used to the long-time infection. For a newly infected node i , injection could happen under two constraints:

1. When the node i gets infected, on the social network layer it is unaware. In other words, only if the node i was US before getting infected instead of aware and susceptible (AS) could injection happen. If node i was already aware of the epidemic right before it gets infected, then getting infected cannot make node i become aware again. One may argue that if an aware individual gets infected, his information of the epidemic is "refreshed", and might take longer time for this individual to lose awareness. For example, if normally awareness in node i would recover after 20 hours, meanwhile 10 hours after the node i gets aware, injection of information happens in node i , then the awareness is refreshed and would take another 20 hours to get recovered. However, in our case, the recovery of awareness is a Poisson process, and the interarrival time of a Poisson process follows an independent exponential distribution. A characteristic of an exponential distribution is the memoryless property: $Pr(T > s + t | T > t) = Pr(T > s)$.

Therefore, even if awareness is "refreshed", the distribution of its recovery time of awareness still remains the same. We define in the EAIP model II that if a node i was AS right before it gets infected, before this node is recovered from the epidemic, injection would not happen for this node.

2. After the node i gets infected, if node i gets aware from aware neighbors in the social network layer, injection would not happen for this node before it is recovered in the physical layer. The reason is, if an individual gets alertness from friends after he or she is infected, we could say the mission of injection is completed, since this individual already gets aware.

Due to the complexity of the injection process in this model, we have to add one more state to clearly illustrate the state transitions compared to the EAIP model I. State transitions between in total 5 states for a node in the EAIP model II are described in detail as followed:

Unaware and Susceptible (US) state. A node could leave the US state with two possibilities. One is that the node i gets informed by its aware neighbors in the social network to become aware and susceptible (AS). The other is that node i gets infected by its infected neighbors in the physical network. After getting infected, node i becomes unaware and infected, meanwhile it has an injection rate γ^e to inject awareness from the physical network layer to the social network layer. We define this state as Unaware, Infected and able to Inject (UII).

Unaware, Infected and able to Inject (UII) state. In the EAIP model II, we divide the Unaware and Infected (UI) state into two states. One of them is UII. A node i could leave UII state with three possibilities. The first possibility is that the epidemic in the physical network is recovered, and becomes US. The Second possibility is that injection of awareness happens in this node. After the injection, node i becomes Aware and Infected (AI). The Last possibility is that node i is informed by aware neighbors in the social network and also becomes AI.

Unaware, Infected and canNot inject (UIN) state. The other division of the UI state is the UIN state. In the UIN state node i is unaware and infected, but injection cannot happen for this node. Node i could leave the UIN state either by recovering from the epidemic in the physical network and becomes US, or by getting aware from aware neighbors in the social network and becomes AI.

Aware and Susceptible (AS) state. Node i who is aware of the epidemic could lose alertness to the epidemic and become US. Furthermore, an aware individual might get infected and become Aware and Infected (AI).

Aware and Infected (AI) state. An AI node could either lose alertness and become UIN, or recover from the epidemic in the physical layer and become Aware and Susceptible (AS).

5.2. MONTE-CAROL SIMULATIONS

Similar Monte-Carol simulations as in the EAIP model I, which are written in C++ language, are used to simulate dynamic processes in the EAIP model II. In consistent with EAIP model I, we use similar parameters as used in model 1. Each layer of a two-layer network has $N = 1000$ nodes, and all nodes have one-one inter-layer links representing the same set of nodes in different network layers. Both layers have the same degree distribution, either ER-ER, or SF-SF. For an Erdős-Rényi (ER) random network, we set the average degree $E[D] = 4$. For a scale-free network, the exponent of the power law degree distribution $Pr[D = k] = ck^{-\lambda}$ is $\lambda = 2.5$. We set the minimum degree $K_{min} = 2$, and the maximum degree $K_{max} = 100$ for scale-free networks. The overlap extent ϕ between two network layers is a controllable parameter. We use a sample time $\Delta t = 0.01$ to sample the continuous-time Markov processes in the EAIP model II. Some constant parameters that we chose for all simulations are: the basic awareness spreading rate on each link $\beta_1 = 0.3$, the basic awareness

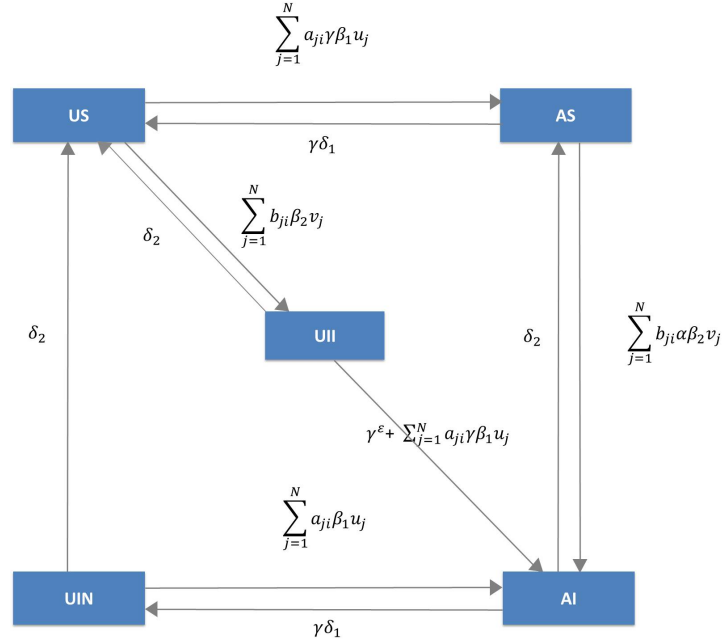


Figure 5.1: State transition processes between 5 possible states: Unaware and Susceptible (US), Unaware and Infected and could Inject (UII), Unaware and Infected and canNot inject (UIN), Aware and Susceptible (AS), and Aware and Infected (AI) in model 5. Infect and recover rates on social network are β_1 and δ_1 respectively, and infect and recover rates on physical network are β_2 and δ_2 respectively. $a_{ij} = 1$ if node i and j are connected in the upper social network layer, otherwise $a_{ij} = 0$. In the physical contact layer, $b_{ij} = 1$ if there is a link between node i and j , otherwise $b_{ij} = 0$. At time t , node i has a probability u_i to be aware in online social network, and probability v_i to be infected in physical contact network.

recovery rate on each node $\delta_1 = 0.6$, the epidemic recovery rate on each node $\delta_2 = 1.0$. When a susceptible node is aware of epidemic, the infection rate for this node is reduced by a factor of α . The epidemic spreading rate on each link β_2 and the time scale γ are controllable, and manipulated in our simulations to understand the influence of these parameters. Initially 10% of randomly chosen nodes are set to be unaware and infected (UII). The rest of nodes in the network are unaware and susceptible (US). 200 realizations are implemented for each set of parameters. The most important result we get from simulations is the steady state fraction of infection ρ_2 . In the meantime, a lot of other results are obtained for us to better understand what happened in the EAIP model II, such as the steady state fraction of awareness ρ_1 and the time evolution of the epidemic in the physical network layer.

5.3. INDIVIDUAL-BASED MEAN FIELD APPROXIMATION I

We develop our original Individual-Based Mean Field Approximation (IBMFA) as a theoretical analysis of the EAIP model II. In the IBMFA, we could calculate the steady state fraction of infection ρ_2 and the steady state fraction of awareness ρ_1 in the EAIP model II where interactions between epidemic spreading and awareness propagation happen.

5.3.1. INDIVIDUAL-BASED MEAN FIELD APPROXIMATION EQUATIONS

The derivation of IBMFA equations for the EAIP model II is similar to that for the EAIP model I. We denote state $Y_i(t) = 1$ as node i is aware at time t in the social network layer, and $Y_i(t) = 0$ as node i is unaware at time t . In the physical network layer, we denote $X_i^S(t) = 1$ as node i is susceptible at time t , and $X_i^S(t) = 0$ as node i

is infected at time t . As described in Section 5.1, since the injection of information from the physical network to the social network does not happen at the moment an US node gets infected in the physical network, we divide the UI state into an UIN state and an UII state. Similarly, in the IBMFA we divide the infected state in the physical network into two states, where $X_i^{II}(t) = 1$ means node i is infected in the physical network and injection is possible at time t , and $X_i^{IN}(t) = 1$ means node i is infected but cannot inject. The normalization condition is that at any time t , for a node i one and only one of $X_i^S(t)$, $X_i^{II}(t)$ and $X_i^{IN}(t)$ is 1, meanwhile the other two are 0.

Furthermore, we denote $u_i(t) = Pr[Y_i(t) = 1]$ as the probability that node i is aware at time t in the social network, and $Pr[Y_i(t) = 0] = 1 - u_i(t)$ as the probability that node i is unaware at time t . According to the three states S, II and IN in the physical network, we denote $v_i^S(t) = Pr[X_i^S(t) = 1]$ as the probability that node i is susceptible at time t in the physical network, $v_i^{II}(t) = Pr[X_i^{II}(t) = 1]$ as the probability that node i is infected and could inject information to the social network at time t , and $v_i^{IN}(t) = Pr[X_i^{IN}(t) = 1]$ as the probability that node i is infected and cannot inject information at time t . The normalization condition here is $v_i^S(t) + v_i^{II}(t) + v_i^{IN}(t) = 1$ for all nodes at any time t . The IBMFA equations are

$$\frac{du_i(t)}{dt} = -\gamma\delta_1 u_i(t) + (1 - u_i(t))\gamma\beta_1 \sum_{j=1}^N a_{ji} u_j(t) + \gamma^\epsilon v_i^{II}(t) \quad (5.1a)$$

$$\frac{dv_i^S(t)}{dt} = -v_i^S(t) \left([u_i(t)\alpha + (1 - u_i(t))]\beta_2 \sum_{j=1}^N b_{ji} (v_j^{II}(t) + v_j^{IN}(t)) \right) + \delta_2 (v_i^{II}(t) + v_i^{IN}(t)) \quad (5.1b)$$

$$\frac{dv_i^{II}(t)}{dt} = -v_i^{II}(t) \left(\delta_2 + \gamma^\epsilon + \gamma\beta_1 \sum_{j=1}^N a_{ji} u_j(t) \right) + v_i^S(t) (1 - u_i(t)) \left(\beta_2 \sum_{j=1}^N b_{ji} (v_j^{II}(t) + v_j^{IN}(t)) \right) \quad (5.1c)$$

$$\frac{dv_i^{IN}(t)}{dt} = -\delta_2 v_i^{IN}(t) + v_i^S(t) u_i(t) \left(\alpha\beta_2 \sum_{j=1}^N b_{ji} (v_j^{II}(t) + v_j^{IN}(t)) \right) + v_i^{II}(t) \left(\gamma^\epsilon + \gamma\beta_1 \sum_{j=1}^N a_{ji} u_j(t) \right) \quad (5.1d)$$

Here we interpret the physical meanings for each term in the Equ.5.1. In the aware probability $u_i(t)$ equation Equ.5.1a, there are three terms:

1. **The $-\gamma\delta_1 u_i(t)$ term.** When the node i is aware in the social network with a probability $u_i(t)$, node i could recover from the awareness with a rate $-\gamma\delta_1$.
2. **The $(1 - u_i(t))\gamma\beta_1 \sum_{j=1}^N a_{ji} u_j(t)$ term.** When the node i is unaware with a probability $(1 - u_i(t))$, node i could get aware from aware neighbors in the social network layer. Each aware neighbor contributes to the total infection rate of node i in the social network by a rate $\gamma\beta_1$. The total infection rate of node i in the social network is therefore $\gamma\beta_1 \sum_{j=1}^N a_{ji} u_j(t)$.
3. **The $\gamma^\epsilon v_i^{II}(t)$ term.** When a node i is in the II state in the physical network, node i is definitely unaware according to our definition of the EAIP model II. In this case, injection of information could happen with an injection rate γ^ϵ .

In the differential equation Equ.5.1b for the susceptible state in the physical network, the three terms are explained as followed:

1. **The $\delta_2 (v_i^{II}(t) + v_i^{IN}(t))$ term.** If node i is infected in the physical network with a probability $1 - v_i^S(t)$, due to the normalization condition $1 - v_i^S(t) = v_i^{II}(t) + v_i^{IN}(t)$. In this case node i could recover from the epidemic with a rate δ_2 and become susceptible.
2. **The $-v_i^S(t) u_i(t) \alpha\beta_2 \sum_{j=1}^N b_{ji} (v_j^{II}(t) + v_j^{IN}(t))$ term.** When a node i is susceptible with the probability $v_i^S(t)$, and meanwhile this node i is aware with the probability $u_i(t)$, this node could get infected from infected neighbors $(v_j^{II}(t) + v_j^{IN}(t))$ of node i with a reduced infection rate $\alpha\beta_2$ from each infected neighbor. After infected, node i becomes the IN state in the physical network.

3. The $-v_i^S(t)(1-u_i(t))\beta_2\sum_{j=1}^N b_{ji}(v_j^{II}(t)+v_j^{IN}(t))$ term. When the node i is susceptible $v_i^S(t)$ and unaware $(1-u_i(t))$, it could get infected from each infected neighbor $(v_j^{II}(t)+v_j^{IN}(t))$ with an infection rate β_2 . This explains the $-v_i^S(t)(1-u_i(t))\beta_2\sum_{j=1}^N b_{ji}(v_j^{II}(t)+v_j^{IN}(t))$ term. After infected, node i becomes the II state in the physical network.

In the differential equation Equ.5.1c, we explain the two terms as followed:

1. The $-v_i^{II}(t)(\delta_2+\gamma^\epsilon+\gamma\beta_1\sum_{j=1}^N a_{ji}u_j(t))$ term. If the node i is infected and could inject in the physical network with a probability $v_i^{II}(t)$, node i could recover from the epidemic with a rate δ_2 and become susceptible. In addition, the II state indicates that node i is unaware. If the injection of information happens in the node i with the injection rate γ^ϵ , node i becomes the IN state after the injection. On top of that, the unaware node i could get aware from aware neighbors with a total infection rate in the social network layer $(\gamma\beta_1\sum_{j=1}^N a_{ji}u_j(t))$. As described in the definition of the EAIP model II, the injection of information cannot happen if this node gets aware from aware neighbors. Therefore node i goes to the IN state after getting aware.

2. The $v_i^S(t)u_i(t)\alpha\beta_2\sum_{j=1}^N b_{ji}(v_j^{II}(t)+v_j^{IN}(t))$ term. This is the same term as the second explained term in the differential equation for the susceptible state Equ.5.1b in the physical network.

In the differential equation Equ.5.1d, all terms have been explained in the former explanation. Therefore, the physical meaning of all terms in the IBMFA equations Equ.5.1 are explained.

In the IBMFA for this model, we assume the independency between the infection states (infected or susceptible) of two neighboring nodes in the physical contact network as in NIMFA, the independency between the awareness states (aware or unaware) of two neighboring nodes in the social network, and the independency between the infection state and the awareness state of the same node though the injection has been taken into account.

In Equ.5.1, we need to solve four differential equations for each node in our EAIP model II. In a two-layer network with in total $N = 1000$ nodes, we denote $U(t)$ as a column vector with $N = 1000$ elements $U(t) = [u_1(t), u_2(t) \cdots u_{1000}(t)]^T$, and similarly column vectors with $N = 1000$ elements $V^S(t)$, $V^{II}(t)$ and $V^{IN}(t)$. Writing the differential equations Equ.5.1 in the matrix format, we get

$$\frac{dU(t)}{dt} = -\gamma\delta_1 U(t) + \text{diag}(u - U(t))\gamma\beta_1 AU(t) + \gamma^\epsilon V^{II}(t) \quad (5.2a)$$

$$\frac{dV^S(t)}{dt} = -\text{diag}(V^S(t))(\text{diag}[U(t)\alpha + (u - U(t))]\beta_2 B(V^{II}(t) + V^{IN}(t))) + \delta_2(V^{II}(t) + V^{IN}(t)) \quad (5.2b)$$

$$\begin{aligned} \frac{dV^{II}(t)}{dt} = & -\text{diag}(V^{II}(t))(\delta_2 u + \gamma^\epsilon u + \gamma\beta_1 AU(t)) \\ & + \text{diag}(V^S(t))\text{diag}((u - U(t)))(\beta_2 B(V^{II}(t) + V^{IN}(t))) \end{aligned} \quad (5.2c)$$

$$\begin{aligned} \frac{dV^{IN}(t)}{dt} = & -\delta_2 V^{IN}(t) + \text{diag}(V^S(t))\text{diag}(U(t))(\alpha\beta_2 B(V^{II}(t) + V^{IN}(t))) \\ & + \text{diag}(V^{II}(t))(\gamma^\epsilon u + \gamma\beta_1 AU(t)) \end{aligned} \quad (5.2d)$$

where u is all 1 column vector with $N = 1000$ elements. Still, we are interested in the meta-stable state of the system in the IBMFA solutions.

5.3.2. METHOD OF SOLVING IBMFA EQUATIONS

In a two-layer network with $N = 1000$ nodes, we need to solve in total 4000 differential equations to get the steady state for this network. Analytical solutions cannot be solved due to complexity of Equ.5.2. However, numerical solutions of differential equations in Equ.5.2 could be obtained with the ode45 function in matlab. With a set of parameters (we use same sets of parameters in the IBMFA and the Monte-Carol simulations in order to verify the accuracy of the IBMFA) and a two-layer network (shown in the adjacency matrix A and B), we solve Equ.5.2 with ode45. 10 realizations were implemented in IBMFA equations for each set of parameters, each realization with an independently generated two-layer network. Initially, $u_i(0) = 1$ and $v_i^{IN}(0) = 1$ for all nodes. With sufficiently long spanning time, we could achieve the steady state fraction of aware nodes ρ_1 and the steady state fraction of infected nodes ρ_2 with

$$\begin{aligned}\rho_1 &= \frac{\sum_{i=1}^N u_i(\infty)}{N} \\ \rho_2 &= \frac{\sum_{i=1}^N v_i^{II}(\infty) + v_i^{IN}(\infty)}{N}\end{aligned}\quad (5.3)$$

5.4. INDIVIDUAL-BASED MEAN FIELD APPROXIMATION II

In addition to the IBMFA that we describe in Section.5.3, we find a second form of IBMFA equations for our EAIP model II. In this IBMFA equations II, we reduce the number of equations for each node in the EAIP model II from four as in Section.5.3 to three.

We still denote $Y_i(t) = 1$ as node i is aware at time t in the social network layer, and $Y_i(t) = 0$ as node i is unaware at time t . $X_i(t) = 1$ as node i is infected in the physical network layer, and $X_i(t) = 0$ as node i is healthy and susceptible. On top of that, we add the third state $T_i(t)$. $T_i(t)$ indicates the status of injection for node i . $T_i(t) = 1$ represents that it is possible for node i inject the information to the social network layer at time t , and $T_i(t) = 0$ as node i cannot inject. From the description of the EAIP model II in Section.5.1, we could see that $T_i(t) = 1$ represents the UII state, since the only state that injection the information could occur is the UII state. $T_i(t)$ makes the description of injection easy in this IBMFA.

Due to the similar derivation method with the IBMFA equations Equ.4.1 and 5.1, we omit the derivation of this IBMFA equations II and directly give the result. With expressions

$$\begin{aligned}u_i(t) &= Pr [Y_i(t) = 1] \\ v_i(t) &= Pr [X_i(t) = 1] \\ z_i(t) &= Pr [T_i(t) = 1]\end{aligned}\quad (5.4)$$

We achieve the IBMFA equations II as

$$\frac{du_i(t)}{dt} = -\gamma\delta_1 u_i(t) + (1 - u_i(t)) \left(\sum_{j=1}^N a_{ji} \gamma \beta_1 u_j(t) \right) + \gamma^\epsilon z_i(t) \quad (5.5a)$$

$$\frac{dv_i(t)}{dt} = -\delta_2 v_i(t) + (1 - v_i(t)) \left(\sum_{j=1}^N b_{ji} (u_i(t) \alpha + (1 - u_i(t))) \beta_2 v_j(t) \right) \quad (5.5b)$$

$$\frac{dz_i(t)}{dt} = -z_i(t) \left(\sum_{j=1}^N a_{ji} \gamma \beta_1 u_j(t) + \gamma^\epsilon + \delta_2 \right) + (1 - v_i(t)) (1 - u_i(t)) \left(\sum_{j=1}^N b_{ji} \beta_2 v_j(t) \right) \quad (5.5c)$$

The physical interpretations of Equ.5.5 are as followed.

1. The $\frac{du_i(t)}{dt}$ equation. An aware node i $u_i(t)$ could lose alertness of the epidemic with a rate $\gamma\delta_1$. If node i is unaware ($1 - u_i(t)$), it could get aware in two ways. The unaware node i could be informed by

aware neighbors, or get aware by injection from the physical network layer. According to our definition of $T_i(t)$, only when $T_i(t) = 1$ could injection occurs with the injection rate γ^e . In addition, $T_i(t) = 1$ indicates the UII states as we discussed in Section.5.1, therefore $z_i(t)$ includes the condition that node i is unaware ($1 - u_i(t)$). Hence the term describing injection is $\gamma^e z_i(t)$.

2. **The $\frac{dv_i(t)}{dt}$ equation.** This equation is the same as Equ.4.1b. Therefore we omit the explanation for this equation and focus on the $z_i(t)$ equation Equ.5.5c.
3. **The $\frac{dz_i(t)}{dt}$ equation.** An UII node i with the probability $z_i(t)$ could leave the UII state with three possibilities: recovers in the physical network with rate δ_2 , gets aware via injection of information with the injection rate γ^e , and gets aware from aware neighbors with the total infection rate in the social network $\sum_{j=1}^N a_{ji} \beta_1 u_j(t)$. If node i is not in the UII state with the probability $(1 - z_i(t))$, only if node i is unaware and susceptible could it directly change to the UII state by getting infected from infected neighbors in the physical network layer. The unaware and susceptible term $(1 - v_i(t))(1 - u_i(t))$ is a subset of $(1 - z_i(t))$, hence we don't multiple $1 - z_i(t)$ after using $(1 - v_i(t))(1 - u_i(t))$.

Worthy to mention is, in this IBMFA equations Equ.5.5, besides assuming the independency between the infection states (infected or susceptible) of two neighboring nodes in the physical contact network as in NIMFA, the independency between the awareness states (aware or unaware) of two neighboring nodes in the social network, and the independency between the infection state and the awareness state of the same node though the injection has been taken into account, it seems like we make a further assumption of the independency between the injection state of a node and the state of its neighbors in the social network layer. However, this new assumption is self-satisfied after assuming the independency between the infection states and the awareness states of two neighboring nodes. As a conclusion, we reduce the number of equations from four in the IBMFA equations Equ.4.1 to three in the IBMFA equations Equ.5.5 without further assumption.

In Equ.5.5, we need to solve three equations for each node i in the EAIP model II. In a two-layer network with $N = 1000$ nodes, we denote $U(t)$ as a column vector with $N = 1000$ elements $U(t) = [u_1(t), u_2(t) \cdots u_{1000}(t)]^T$, and similarly for column vectors $V(t)$ and $Z(t)$. We write Equ.5.5 in the matrix format as

$$\frac{dU(t)}{dt} = -\gamma\delta_1 U(t) + \text{diag}(u - U(t)) (\gamma\beta_1 AU(t)) + \gamma^e Z(t) \quad (5.6a)$$

$$\frac{dV(t)}{dt} = -\delta_2 V(t) + \text{diag}(u - V(t)) (\text{diag}(U(t)\alpha + (u - U(t)))\beta_2 BV(t)) \quad (5.6b)$$

$$\frac{dZ(t)}{dt} = -\text{diag}(Z(t)) (\gamma^e + \delta_2) - \text{diag}(Z(t)) \gamma\beta_1 AU(t) \quad (5.6c)$$

$$+ \text{diag}(u - V(t)) \cdot \text{diag}(u - U(t)) \cdot \beta_2 BV(t) \quad (5.6d)$$

In the steady state, $\frac{dU(t)}{dt} = 0$, $\frac{dV(t)}{dt} = 0$, and $\frac{dZ(t)}{dt} = 0$. Numerical solutions could be obtained by ode45 function in matlab, and initial conditions are $u_i(0) = 1$, $v_i(0) = 1$ and $z_i(0) = 0$ for all nodes. The steady state fraction of aware nodes ρ_1 and the fraction of infected nodes ρ_2 are obtained by

$$\begin{aligned} \rho_1 &= \frac{\sum_{i=1}^N u_i(\infty)}{N} \\ \rho_2 &= \frac{\sum_{i=1}^N v_i(\infty)}{N} \end{aligned} \quad (5.7)$$

5.5. MICROSCOPIC MARKOV CHAIN APPROACH

Due to the complexity of our EAIP model II, we need one more equation compared to the Microscopic Markov Chain Approach (MMCA) equations Equ.4.8 in the EAIP model I. The MMCA equations in accordance with this model is shown as followed.

For our EAIP model II with five possible states: Unaware and Susceptible (US) state, Unaware, Infected and able to Inject (UII) state, Unaware, Infected and canNot inject (UIN) state, Aware and Susceptible (AS) state, Aware and Infected (AI) state, we denote $r_i(t)$ as the probability that a node i is **not** informed by neighbors at time t in the social network, $q_i^U(t)$ as probability that unaware node i is **not** infected by neighbors at time t in the physical network, and $q_i^A(t)$ as the probability that aware node i is **not** infected by neighbors at time t in the physical network. Expressions of $r_i(t)$, $q_i^U(t)$ and $q_i^A(t)$ are the same as Equ.4.7:

$$r_i(t) = \prod_j \left(1 - a_{ji} p_j^A(t) \beta_1^*\right) \quad (5.8a)$$

$$q_i^U(t) = \prod_j \left(1 - b_{ji} p_j^I(t) \beta_2^*\right) \quad (5.8b)$$

$$q_i^A(t) = \prod_j \left(1 - b_{ji} p_j^I(t) \alpha \beta_2^*\right) \quad (5.8c)$$

where $p_j^A(t) = p_j^{AS}(t) + p_j^{AI}(t)$ is the probability that node j is aware at time t , and $p_j^I(t) = p_j^{UII}(t) + p_j^{UIN}(t) + p_j^{AI}(t)$ is the probability that node j is infected at time t . The probability that a node gets informed by an aware neighbor within a time step of interval Δt follows $\beta_1^* = \gamma \beta_1 \cdot \Delta t$. Similarly we have $\delta_1^* = \gamma \delta_1 \cdot \Delta t$, $\beta_2^* = \beta_2 \cdot \Delta t$, $\delta_2^* = \delta_2 \cdot \Delta t$. The time interval Δt should be small so that this discrete-time approach well approximates the continuous time processes. In consistent with Monte-Carol simulations, we use the sample time $\Delta t = 0.01$.

The MMCA equations describe the one time evolution of the probability that each node is in each of the five possible states:

$$p_i^{US}(t+1) = (p_i^{UII}(t) + p_i^{UIN}(t)) r_i(t) \delta_2^* + p_i^{AI}(t) \delta_1^* \delta_2^* + p_i^{US}(t) r_i(t) q_i^U(t) + p_i^{AS}(t) \delta_1^* q_i^A(t) \quad (5.9a)$$

$$p_i^{UIN}(t+1) = p_i^{UIN}(t) r_i(t) (1 - \delta_2^*) + p_i^{AI}(t) \delta_1^* (1 - \delta_2^*) + p_i^{AS}(t) \delta_1^* (1 - q_i^A(t)) \quad (5.9b)$$

$$p_i^{UII}(t+1) = p_i^{UII}(t) r_i(t) (1 - \delta_2^*) (1 - \gamma^{e*}) + p_i^{US}(t) r_i(t) (1 - q_i^U(t)) (1 - \gamma^{e*}) \quad (5.9c)$$

$$p_i^{AS}(t+1) = (p_i^{UII}(t) + p_i^{UIN}(t)) (1 - r_i(t)) \delta_2^* + p_i^{AI}(t) (1 - \delta_1^*) \delta_2^* + p_i^{US}(t) (1 - r_i(t)) q_i^U(t) + p_i^{AS}(t) (1 - \delta_1^*) q_i^A(t) \quad (5.9d)$$

$$p_i^{AI}(t+1) = p_i^{UII}(t) [(1 - r_i(t)) (1 - \delta_2^*) + r_i(t) (1 - \delta_2^*) \gamma^{e*}] + p_i^{UIN}(t) (1 - r_i(t)) (1 - \delta_2^*) + p_i^{AI}(t) (1 - \delta_1^*) (1 - \delta_2^*) + p_i^{US}(t) [(1 - r_i(t)) (1 - q_i^U(t)) + r_i(t) (1 - q_i^U(t)) \gamma^{e*}] + p_i^{AS}(t) (1 - \delta_1^*) (1 - q_i^A(t)) \quad (5.9e)$$

where γ^{e*} is the sampled injection rate from the physical network layer to the social network layer $\gamma^{e*} = \gamma^e \cdot \Delta t$. For each node i in the two-layer network, the normalization condition should be satisfied at any time t

$$p_i^{US}(t) + p_i^{UIN}(t) + p_i^{UII}(t) + p_i^{AS}(t) + p_i^{AI}(t) = 1 \quad (5.10)$$

In the steady state, $p_i(t+1) = p_i(t)$ is satisfied for all states and nodes. We could the derive the steady state fraction of awareness ρ_1 and the steady state fraction of infection ρ_2 by

$$\rho_1 = \frac{\sum_{i=1}^N (p_i^{AS}(\infty) + p_i^{AI}(\infty))}{N} \quad (5.11)$$

$$\rho_2 = \frac{\sum_{i=1}^N (p_i^{UIN}(\infty) + p_i^{UII}(\infty) + p_i^{AI}(\infty))}{N}$$

In this MMCA for the EAIP model II, we could still derive the epidemic threshold for epidemic spreading. The derivation of the epidemic threshold is shown in Appendix.B.2.

5.6. ACCURACY OF IBMFA AND MMCA

In this section we study the accuracy of our three theoretical analysis methods, i.e. IBMFA I, IBMFA II and MMCA for the EAIP model II. In Monte-Carol simulations, the accurate steady state fraction of infection ρ_2 is

achieved. Therefore, we compare the numerical solutions of IBMFA and MMCA with the simulation results to estimate the precision of these two analytical approaches. We plot Fig.5.2 and Fig.5.3 with results from four different methods in the same injection rate γ^e and the same time scale γ .

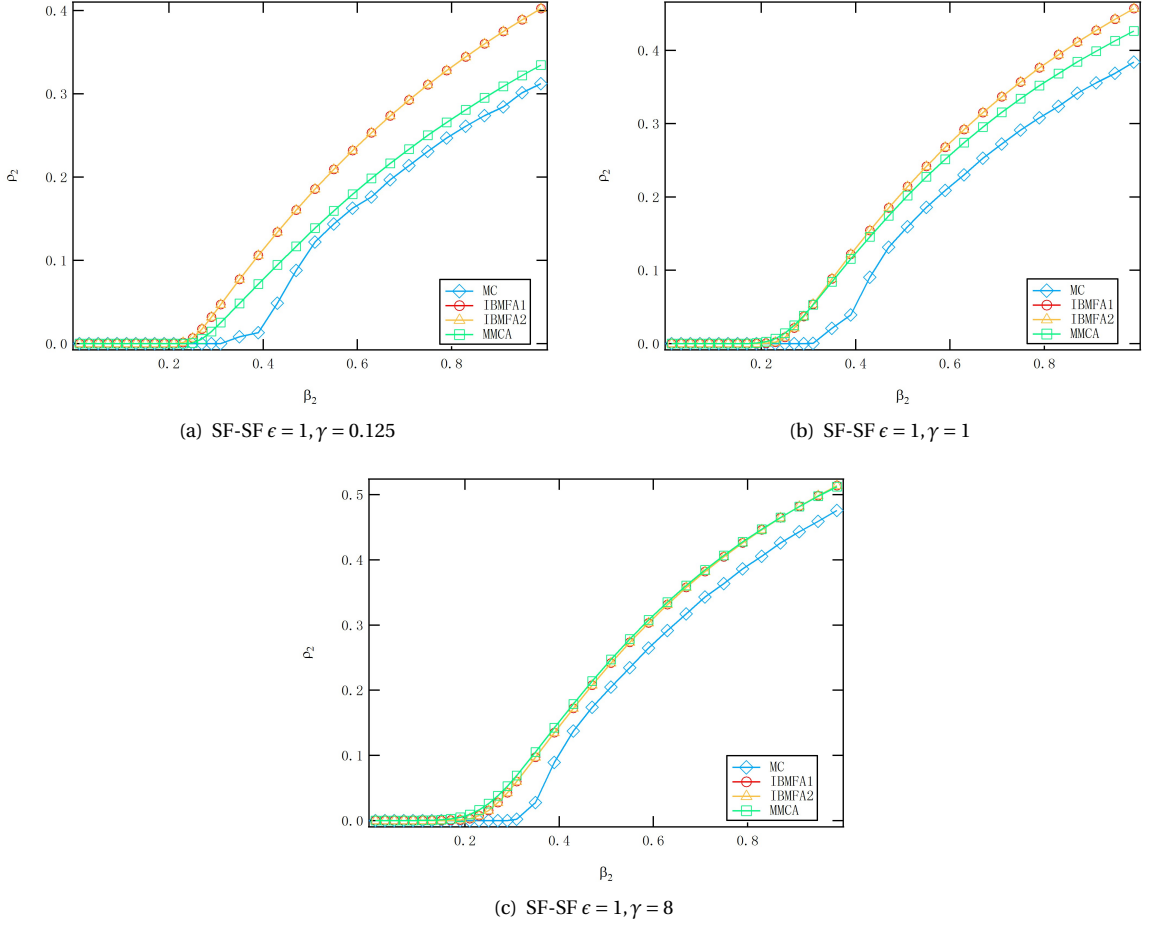


Figure 5.2: Compare results from Monte-Carlo simulations, IBMFA equations and MMCA equations. The injection rate is set to γ^e with $\epsilon = 1$. The relative time scale in the social network layer are: (a) $\gamma = 0.125$, (b) $\gamma = 1$, (c) $\gamma = 8$. Parameters we choose here are: $\beta_1 = 0.3$, $\delta_1 = 0.6$, $\delta_2 = 1.0$, $\alpha = 0.2$. Network size is $N = 1000$. In each scale-free network, exponent for the power-law degree distribution is $\lambda = 2.5$. The overlap between two network layers is $\phi = 1$. Results are averaged over 10 realizations.

In Fig.5.2 and Fig.5.3, we could observe that results of two types of IBMFA equations Equ.5.2 and Equ.5.6 are always the same. The comparison of performance between IBMFA equations and MMCA equations depends on the relative time scale γ in the social network layer. For a small γ , like $\gamma = 1/8$, MMCA solutions is closer to MC simulations results, while around the epidemic threshold the performance of MMCA and IBMFA are almost the same. When γ is increased to 1, the IBMFA shows a more accurate epidemic threshold τ_c than the MMCA, while at large β_2 the MMCA performs better. As γ continues increasing to $\gamma = 8$, the entire IBMFA curves are below the MMCA curve, in other words the IBMFA is more accurate than the MMCA. In conclusion, our IBMFA equations perform well at around the epidemic threshold τ_c for the physical network layer, and IBMFA equations totally outperform MMCA in the large γ .

Even though there are some difference between solutions from IBMFA and MMCA approximations and our numerical simulations, we develop IBMFA and MMCA as the theoretical analysis for our EAIP model II. We prove that our IBMFA is very accurate in some circumstance (when γ is large). Our original IBMFA methods outperform MMCA, which has been used in a lot of researches and papers, at the epidemic threshold in the physical network and at large γ . Another advantage of IBMFA is that solution for a certain two-layer network is definite. Therefore IBMFA is more stable than Monte-Carlo simulations, and the only randomness in solutions of IBMFA is in the generation of two-layer networks. Compared to Monte-Carlo simulations, IBMFA

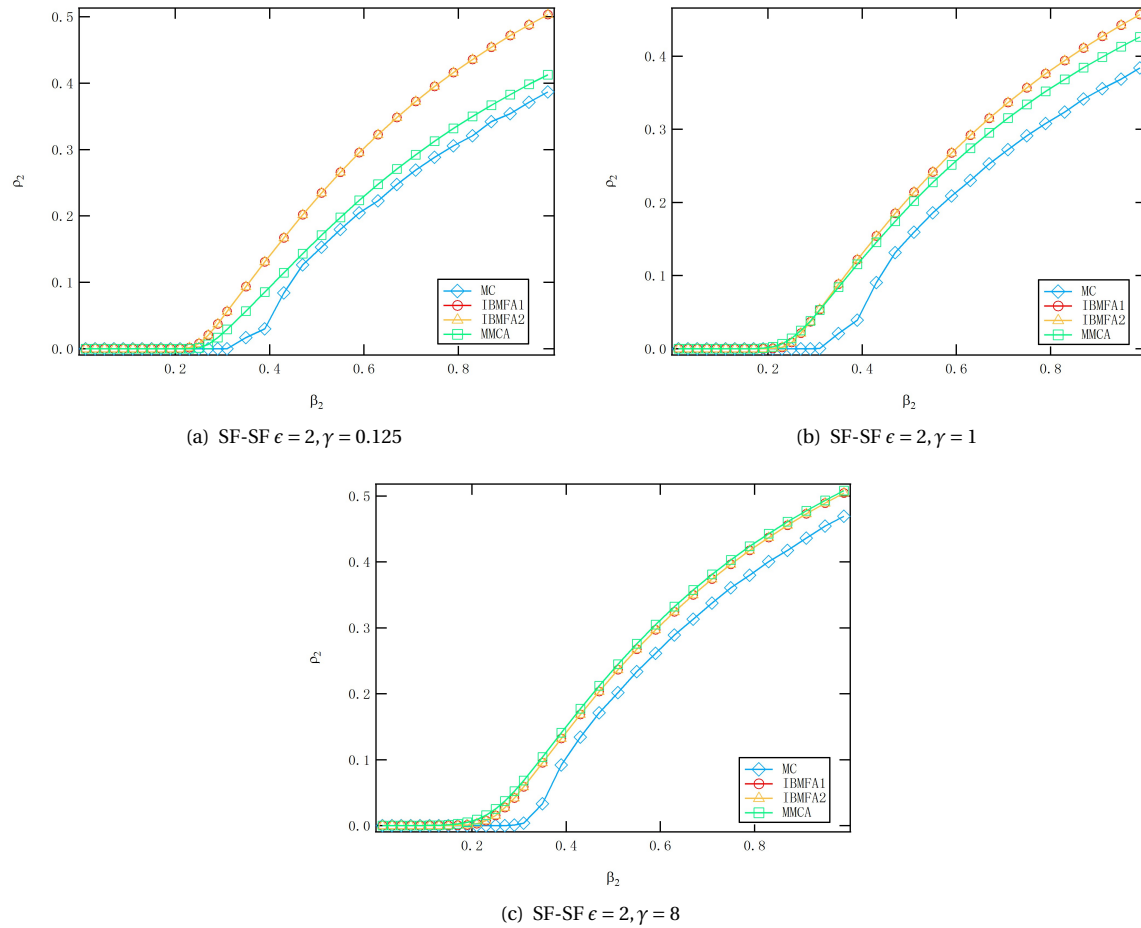


Figure 5.3: Compare results from Monte-Carlo simulations, IBMFA equations and MMCA equations. Injection rate is set to γ^ϵ with $\epsilon = 2$. Relative time scale in social network layer are: (a) $\gamma = 0.125$, (b) $\gamma = 1$, (c) $\gamma = 8$. Parameters we choose here are: $\beta_1 = 0.3$, $\delta_1 = 0.6$, $\delta_2 = 1.0$, $\alpha = 0.2$. Network size is $N = 1000$. In each scale-free network, exponent for the power-law degree distribution is $\lambda = 2.5$. The overlap between two network layers is $\phi = 1$. Results are averaged over 10 realizations.

takes much less time to get the steady state fraction of infection and the steady state fraction of awareness. On top of that, the time consumed in matlab to solve IBMFA equations is also much less than solving MMCA equations.

5.7. THE INFLUENCE OF TIME SCALE γ ON EPIDEMIC MITIGATION

After introducing in total four different tools (Monte-Carol simulation, two types of IBMFA, and MMCA) we develop to study the EAIP model II, we could explore the influence of two key factors on epidemic mitigation: (i) the relative time scale γ of information propagation in the social network layer to the spread of an epidemic in the physical contact network, and (ii) the structure of two-layer networks. We firstly discuss the relative time scale γ in this section. We only use Monte-Carol simulations in this section since the simulations are supposed to precisely simulate the continuous-time Markov processes. The results of investigating the influence of γ on epidemic mitigation with the IBMFA and the MMCA are shown in Appendix.B.3.

5.7.1. THE RELATIVE TIME SCALE γ VS EPIDEMIC SPREADING

As defined in Section.5.1, in the EAIP model II the injection of information from the physical network layer to the social network layer is positively related to the relative time scale γ . We assume the injection rate is γ^ϵ because of the generality of the polynomial relation in mathematical.

In addition, the injection rate γ^ϵ is also a practical value. In reality, when the time scale γ in the social network layer is small, awareness (or information about the epidemic) propagates slower than the epidemic spreading in the physical contact network. In this case, most people would get infected before they get the awareness information, hence propagation of information does not play well in the role of prevention of the epidemic. People don't have enough motivation to inform their friends about the epidemic when they are infected since information propagation is not very effective, which leads to a very small injection rate. Oppositely, when the time scale γ in the social network is large, awareness propagates faster than the epidemic, and people tend to get information before they get infected by the epidemic. Consequently the information could effectively remind people to take precautions, hence people are more motivated to share the information when they are infected. Additionally, the fast propagation of information would cause extensive discussions about the precautions of the epidemic, therefore practical information of precautions is more likely to be extracted. Individuals would be more willing to share these exact information with friends when they get infected, because the effective precaution methods could truly prevent their friends from getting infected. As a conclusion, a large time scale γ results in a very large injection rate. These interpretations reflect the realistic significance of the injection rate γ^ϵ .

To comprehensively consider different relationships between the injection rate and the time scale, we show simulations results of the injection rate γ^ϵ with $\epsilon = 1$, where the injection rate is linearly related to the time scale γ , and $\epsilon = 2$, where the injection rate is the square of the time scale γ . Two-layer scale-free networks SF-SF are used here to illustrate the phenomenon, while in ER-ER network the observation is similar (shown in Appendix.B.4).

As shown in Fig.5.4, when the injection rate is linearly related to the time scale γ , i.e. $\epsilon = 1$, the phenomenon is similar to Fig.4.4. With an increasing time scale γ , the fraction of infection ρ_2 in our EAIP model II seems to increase monotonously. However, when $\epsilon = 2$, the change of ρ_2 is no longer monotonous with the increase of γ . In Fig.5.5, $\gamma = 0.25$ and $\gamma = 0.5$ curves are actually below the $\gamma = 0.125$ curve.

In order to explain our observations, we would introduce the upper bound and the lower bound in our EAIP

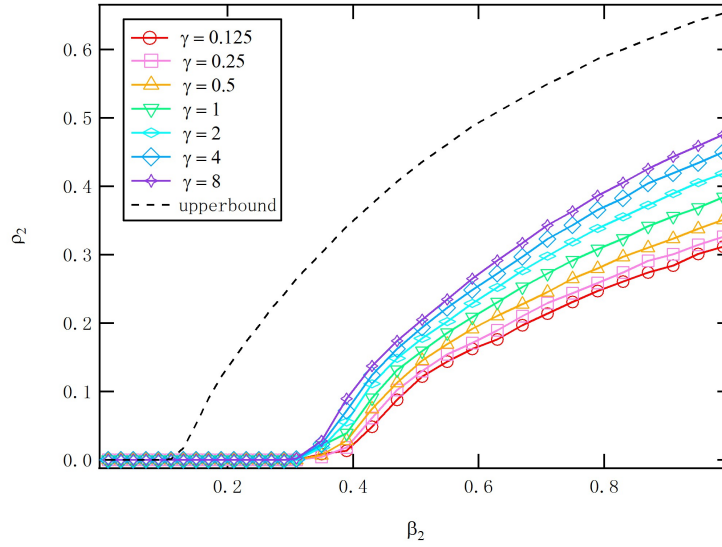


Figure 5.4: The Effect of time scales γ on epidemic spreading in two-layer networks SF-SF with the overlap $\phi = 1$. The x axis is the infection spreading rate β_2 , and the y axis is the steady state fraction of infection in the physical network ρ_2 . The injection rate is γ^c , and here we set the value $c = 1$, i.e. the injection rate is linearly related to the time scale γ . Other parameters used in this figure are: $\beta_1 = 0.3$, $\delta_1 = 0.6$, $\delta_2 = 1.0$, $\alpha = 0.2$. The network size is $N = 1000$. For a scale-free network, the exponent in the power-law degree distribution is $\lambda = 2.5$. Initially, 10% of randomly chosen nodes are unaware and infected (UII). The rest of nodes are unaware and susceptible (US). Results are averaged over 200 realizations.

model II. Since the observations in Fig.5.5 are not very clear (some curves are overlapped together), we would use one β_2 value: $\beta_2 = 1.0$, where the difference between curves is evident, to further explore the influence of changing γ on the steady state fraction of infection ρ_2 in the following.

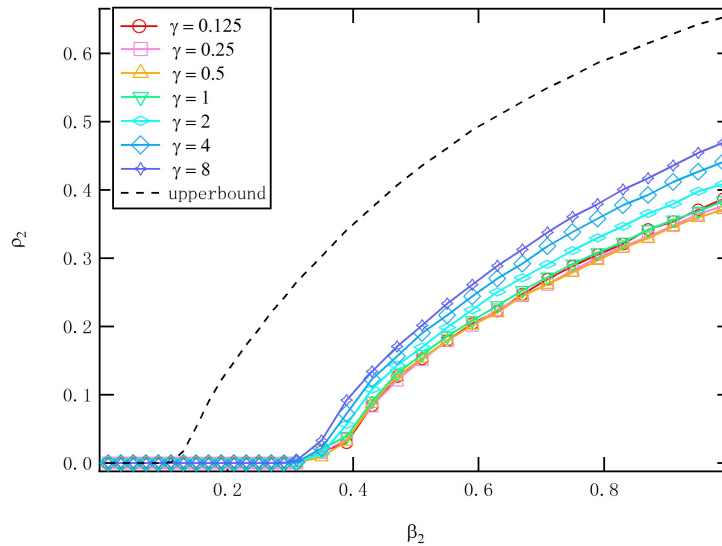


Figure 5.5: The effect of time scales γ on epidemic spreading in two-layer networks SF-SF with the overlap $\phi = 1$. The x axis is the infection spreading rate β_2 , and the y axis is the steady state fraction of infection in the physical network ρ_2 . The injection rate is γ^c , and here we set the value $c = 2$, i.e. the injection rate has square relationship with the time scale γ . Other parameters used in this figure are: $\beta_1 = 0.3$, $\delta_1 = 0.6$, $\delta_2 = 1.0$, $\alpha = 0.2$. The network size is $N = 1000$. For a scale-free network, the exponent in the power-law degree distribution is $\lambda = 2.5$. Initially, 10% of randomly chosen nodes are unaware and infected (UII). The rest of nodes are unaware and susceptible (US). Results are averaged over 200 realizations.

5.7.2. UPPER BOUND AND LOWER BOUND OF ρ_2

In the EAIP model II, the injection rate is positively related to the time scale γ . When $\gamma \rightarrow 0$, even though epidemic spreading is much faster compared to awareness propagation, injection hardly happens due to the very small injection rate. As we explained in the EAIP model I, two factors that affect the steady state fraction of awareness ρ_1 in the social network are the effective infection rate $\tau_1 = \beta_1/\delta_1$, and the amount of injection. If the online social network is a single network that is independent with the physical contact network, the change of time scale γ does not influence the steady state fraction of awareness ρ_1 because γ does not change the effective infection rate $\tau_1 = \gamma\beta_1/\gamma\delta_1$ in the social network. Therefore, the change of ρ_1 in the EAIP model II depends on the amount of injection. When $\gamma \rightarrow 0$, the very small injection rate γ^ϵ is so small that injection hardly occurs, consequently ρ_1 is almost not influenced by injections. Since injections would increase the fraction of awareness ρ_1 (with injection, awareness comes from both awareness propagation in the social network, and injection of information from the physical network, but without injection, awareness only comes from awareness propagation in the social network), the $\gamma \rightarrow 0$ results in a low ρ_1 , and therefore a high fraction of infection in the physical contact network ρ_2 .

Furthermore, we consider the extreme situation $\gamma = 0$. Both the awareness spreading rate $\gamma\beta_1$ and the awareness recovering rate $\gamma\delta_1$ are 0, and also the injection rate $\gamma^\epsilon = 0$. In other words, people do not use social network at all, as a consequence information about the epidemic cannot propagate. This is actually the worst situation for epidemic mitigation because no one takes precautions against the epidemic, hence the epidemic would spread in the physical network without obstruction. In this case the two-layer network is equivalent to a single physical network. In conclusion, with $\gamma = 0$ we could achieve the upper bound in our EAIP model II. Notice that this upper bound holds for all ϵ values.

In order to achieve the lower bound in this model, we need to find a situation that injection of information has a maximum effect on the social network layer. However, we are unable to achieve a uniform case that makes the effect of injection maximum for all ϵ values due to the complexity of the EAIP model II. There is indeed a γ where the best epidemic mitigation effect occurs for a certain value of ϵ . We could find this γ in simulations, but not with theoretical analysis. This optimum epidemic mitigation phenomenon will be further studied in the following sections.

While the exact lower bound cannot be simply indicated, we could derive theoretically a loose lower bound in this model. The best situation for epidemic mitigation is, all nodes stay aware in the steady state, i.e. $\rho_1 = 1$. In this case, everyone in the network knows about the epidemic and takes precautions. This is equivalent to the a single physical contact network with the infection spreading rate $\alpha\beta_2$ and the infection recovering rate δ_2 . However, this lower bound is unreachable in our EAIP model II, since it requires a large injection rate in a small γ situation (which is achievable in the EAIP model I).

By the theoretical analysis in this section, we show how the upper bound and the lower bound in the EAIP model II are achieved. In Monte-Carol simulations, the upper bound is reached with a time scale $\gamma = 0$, and the lower bound is reached in a single physical network with the infection rate $\alpha\beta_2$ and the recovery rate δ_2 . In the meantime, IBMFA equation for a single physical network with the infection rate β and the recovery rate δ is

$$\frac{dv_i(t)}{dt} = -\delta v_i(t) + (1 - v_i(t)) \beta \sum_{j=1}^N b_{ji} v_j(t) \quad (5.12)$$

We could replace the β by β_2 , and replace the δ by δ_2 in Equ.5.12 to obtain the upper bound of the steady state fraction of infection ρ_2 . The lower bound of ρ_2 is achieved by replacing β by $\alpha\beta_2$, and replacing δ by δ_2 .

5.7.3. OPTIMUM EPIDEMIC MITIGATION

Under a certain value of ϵ for the injection rate γ^ϵ , we would like to further explore the best relative time scale γ at which the best epidemic mitigation effect is reached.

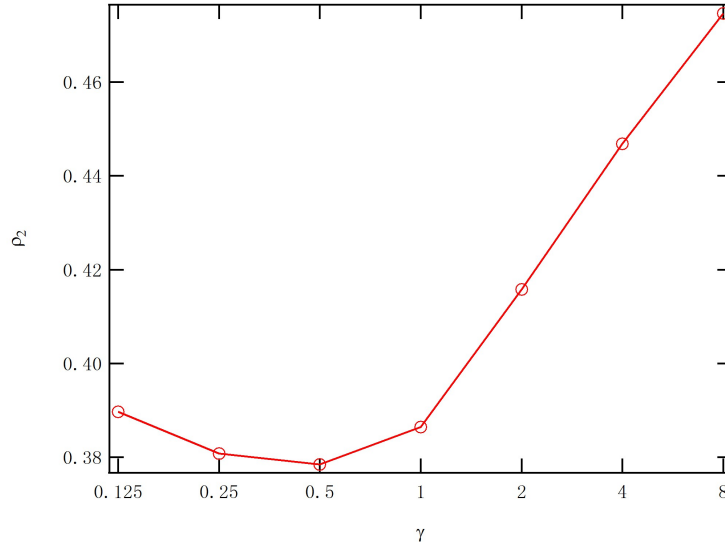


Figure 5.6: Effect of time scale γ on epidemic spreading in two-layer networks SF-SF with the overlap $\phi = 1$. The x axis is the time scale γ , and the y axis is the steady state fraction of infection in the physical network ρ_2 . The injection rate is γ^ϵ , and here we set the value $\epsilon = 2$. Other parameters used here are: $\beta_1 = 0.3$, $\delta_1 = 0.6$, $\beta_2 = 1.0$, $\delta_2 = 1.0$, $\alpha = 0.2$. The network size is $N = 1000$. For a scale-free network, the exponent in the power-law degree distribution is $\lambda = 2.5$. Initially, 10% of randomly chosen nodes are unaware and infected (UII). The rest of nodes are unaware and susceptible (US). Results are averaged over 200 realizations.

As shown in Fig.5.6, for the injection rate γ^ϵ with $\epsilon = 2$, there is a clear minimum steady state fraction of infection ρ_2 at $\gamma = 0.5$. It indicates that in reality, given the epidemic spreading rate β_2 and the epidemic recovering rate δ_2 , we could achieve the best epidemic mitigation effect by adjusting the relative time scale γ in the social network to a value that is close to the speed of epidemic spreading.

We could explain the optimum ρ_2 as followed. As discussed in the upper bound of the steady state fraction of infection ρ_2 , the highest ρ_2 is reached when the time scale $\gamma = 0$. When γ is slightly larger than 0, the awareness starts propagating in a slow speed. For $\epsilon = 2$, in small γ the injection rate is very small, which results in a very small amount of injection. In this case the steady state fraction of awareness ρ_1 is dominated by awareness propagation in the social network, consequently ρ_1 is low. Small amount of awareness cannot efficiently protect people from the epidemic, therefore ρ_2 is high.

As the time scale γ increases, information propagating in the social network layer become faster, meanwhile the injection rate γ^ϵ also increases. Larger amount of injections efficiently causes a high fraction of awareness ρ_1 , and therefore the epidemic is better controlled than the $\gamma \rightarrow 0$ situation. However, the increasingly fast processes in the social network layer results in faster recovery of awareness, which means the information that was injected from the physical network layer to the social network layer cannot stay for a long time (in $\gamma \rightarrow 0$ case, one awareness information that was injected could last for long because of the small recovery rate $\gamma\delta_1$ in the social network layer). In other words, the effect of each injection becomes weaker in faster time scale γ .

According to these two factors (the injection rate γ^ϵ , and the effect of each injection) that influence the effect of injections in the EAIP model II, we further analyze Fig.5.6. In $\gamma \ll 1$, where awareness propagation in the social network layer is much slower than epidemic spreading in the physical network layer, the augment of the injection rate γ^ϵ would significantly facilitate the amount of injected information from the physical network layer to the social network layer. When $\epsilon = 2$, the slope (or equally the increase of the injection rate

γ^ϵ) is small when γ is small. It means that in small γ the rising amount of injection is small, which leads to slow decreasing of ρ_2 in small γ . Therefore, before $\gamma = 0.5$ the fraction of infection ρ_2 in the physical network layer declines monotonously.

When time scale γ in the social network layer is increased to $\gamma = 0.5$, the speed of awareness propagation in the social network layer is already comparable with the spread of the epidemic in the physical network layer. In this case not only the rising injection rate γ^ϵ needs to be considered, but we also have to take the effect of each injection into account. When the time scale γ in the social network layer is close to the time scale in the physical network layer, the augment of γ in the social network layer leads to a larger injection rate γ^ϵ as well as a smaller effect of each injection. After $\gamma = 0.5$, the influence of the increasing injection rate γ^ϵ cannot exceed the influence of the smaller effect for each injection, therefore with the rising γ , the ascension of ρ_2 starts. Note that when the relative time scale γ is large enough, no matter how fast the injection rate γ^ϵ increases, in other words, no matter how large the ϵ is, ρ_2 would ascend with γ anyway, which could be derived from our EAIP model I where the injection rate could be regarded as $+\infty$.

After analyzing Fig.5.6, we could also discuss about the $\epsilon = 1$ situation which is shown in Fig.5.7.

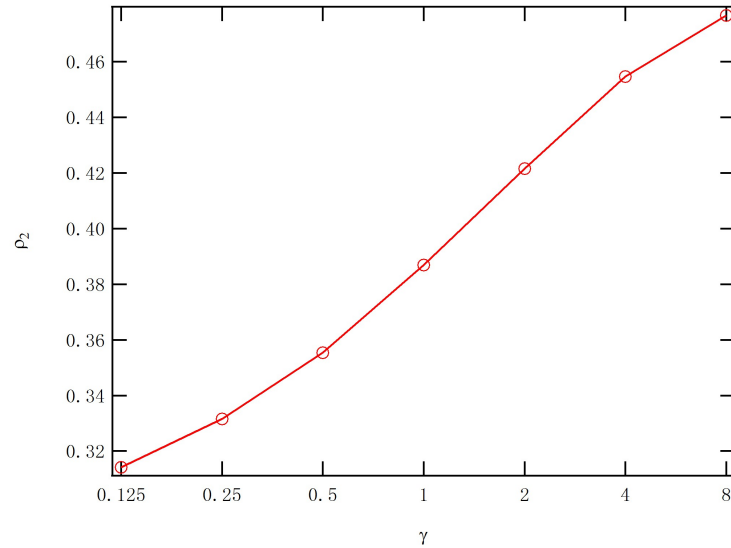


Figure 5.7: Effect of time scale γ on epidemic spreading in two-layer networks SF-SF with the overlap $\phi = 1$. The x axis is the time scale γ , and the y axis is the steady state fraction of infection in the physical network ρ_2 . The injection rate is γ^ϵ , and here we set the value $\epsilon = 1$. Other parameters we use here are: $\beta_1 = 0.3$, $\delta_1 = 0.6$, $\beta_2 = 1.0$, $\delta_2 = 1.0$, $\alpha = 0.2$. The network size is $N = 1000$. For a scale-free network, the exponent in the power-law degree distribution is $\lambda = 2.5$. Initially, 10% of randomly chosen nodes are unaware and infected (UII). The rest of nodes are unaware and susceptible (US). Results are averaged over 200 realizations.

In the $\epsilon = 1$ case, the upper bound of the steady state fraction of infection ρ_2 still occurs at $\gamma = 0$. As the relative time scale γ increases, the injection rate γ^ϵ increases linearly with γ , therefore even in small γ the augment of the amount of injection is significant. At a γ that is close to 0, the optimum point of epidemic mitigation is reached, and after that less effect of each injection caused by faster awareness propagation in the social network layer dominates the larger amount of injection from the injection rate γ^1 , consequently ρ_2 would increase with the rising γ .

The optimum point that the best epidemic mitigation effect is achieved in $\gamma = 1$ situation is not shown in Fig.5.7 because of limitations of Monte-Carol simulations. For a very small γ , awareness propagation in the social network layer are too slow that very long time is required to reach the steady state for both layers in two-layer networks. It means that we need more steps in the sampled-time Markov processes to reach the steady state. Normally for γ values that are shown in Fig.5.7, 5×10^4 steps are enough to get the steady state for both layers. However, for a very small γ , even 10^6 steps where Monte-Carol simulations take a long time are not long enough to reach the steady state. Therefore, we did not run simulations for such small γ . Instead

we focus on γ that makes the time scale of awareness propagation in the social network layer comparable to epidemic spreading in the physical network layer, where the simulation time is acceptable. We use the time scales from $\gamma = 1/8$ to $\gamma = 8$. In this range of γ the monotonously rising ρ_2 is observed when $\epsilon = 1$, however the bottom of ρ_2 curve does exist in a very small γ .

To further understand the influence of ϵ on the optimum epidemic mitigation effect, we show bottom points of ρ_2 under different exponents ϵ in the injection rate γ^ϵ .

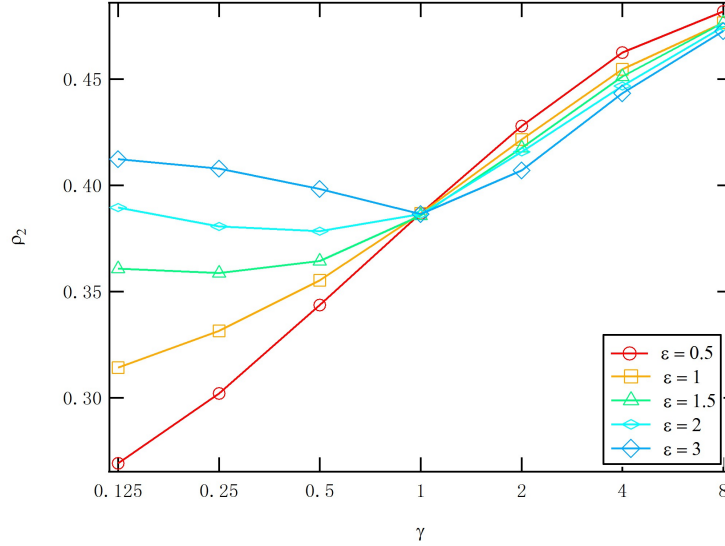


Figure 5.8: Influence of the exponent in injection rate γ^ϵ on the optimum point of steady state fraction of infection ρ_2 in two-layer networks SF-SF with the overlap $\phi = 1$. The x axis is the time scale γ , and the y axis is the steady state fraction of infection in the physical network ρ_2 . Other parameters we use are: $\beta_1 = 0.3$, $\delta_1 = 0.6$, $\beta_2 = 1.0$, $\delta_2 = 1.0$, $\alpha = 0.2$. The network size is $N = 1000$. For a scale-free network, the exponent in the power-law degree distribution is $\lambda = 2.5$. Initially, 10% of randomly chosen nodes are unaware and infected (UII). The rest of nodes are unaware and susceptible (US). Results are averaged over 200 realizations.

From Fig.5.8, we could see that in the range $\gamma \in [1/8, 8]$, the bottom of the $\epsilon = 0.5$ and the $\epsilon = 1$ curves cannot be observed. The lowest ρ_2 occurs at $\gamma = 0.25$ for the $\epsilon = 1.5$ curve, at $\gamma = 0.5$ for the $\epsilon = 2$ curve, and at $\gamma = 1$ for the $\gamma = 3$ curve. We could conclude from our observations in Fig.5.8 that the relative time scale γ where the optimum effect of epidemic mitigation occurs increases with the exponent ϵ in the injection rate γ^ϵ .

We would like to further explain the optimum epidemic mitigation effect here. For all values of ϵ in Fig.5.8, the curves overlap in three γ : $\gamma = 0$ where the injection rate is 0, $\gamma = 1$ where the injection rate is 1, and $\gamma = +\infty$ where infinite fast awareness propagation invalidates injections. For $\gamma > 1$, a larger value of ϵ leads to a larger amount of injections, consequently a larger steady state fraction of awareness ρ_1 and a smaller steady state fraction of infection ρ_2 . For $\gamma < 1$, on the other hand, a larger value of ϵ leads to a smaller amount of injection, consequently a smaller ρ_1 and a larger ρ_2 .

Mathematically, for the $\epsilon = 0.5$ curve, since when $\gamma < 1$ the injection rate for $\gamma^{0.5}$ is even larger than γ^1 situation, the optimum point might occur at an γ even closer to 0 than $\epsilon = 1$ situation. For $\epsilon > 1$, small changes in the injection rate is observed in $\gamma < 1$. At $\gamma = 1$ all curves overlap due to the fact that any power of 1 is 1 for the injection rate. A larger ϵ leads to a smaller injection rate γ^ϵ for $\gamma < 1$, which in turn results in higher fraction of infection in the physical network layer ρ_2 . For the $\epsilon = 3$ curve, when $\gamma < 1$, injection rate is reduced so significantly that the fraction of infection ρ_2 immediately starts increasing. Therefore the optimum point for the effect of epidemic mitigation occurs at $\gamma = 1$ when $\epsilon = 3$. For the $\epsilon = 2$ curve, the injection rate γ^ϵ is reduced slower than $\epsilon = 3$ case, therefore at $\gamma = 0.5$ the bottom of curve is reached. For $\epsilon = 1.5$ curve the bottom is similarly reached at a smaller γ . As the value of ϵ decreases, the optimum value of γ for the epidemic mitigation effect also decreases.

In conclusion, with the knowledge of the exponent in the injection rate γ^ϵ , we could find a γ that makes the epidemic mitigation effect by using awareness the best. In reality, this result could help us discovering the best time scale γ in the social network layer that facilitates the control of an epidemic. When an epidemic starts spreading in an area, the government or medias could adjust the intensity of news in order to control the relative time scale γ to a certain extent so that the epidemic is better controlled.

5.8. INFLUENCE OF OVERLAP ϕ

In addition to the relative time scale γ in the social network layer, in this section we explore the other fundamental factor that influences the effect of epidemic mitigation, the overlap ϕ between two layers in a two-layer network. We use two-layer scale-free networks as example here, while same phenomena are observed in two-layer ER-ER networks which is shown in Appendix.B.5.

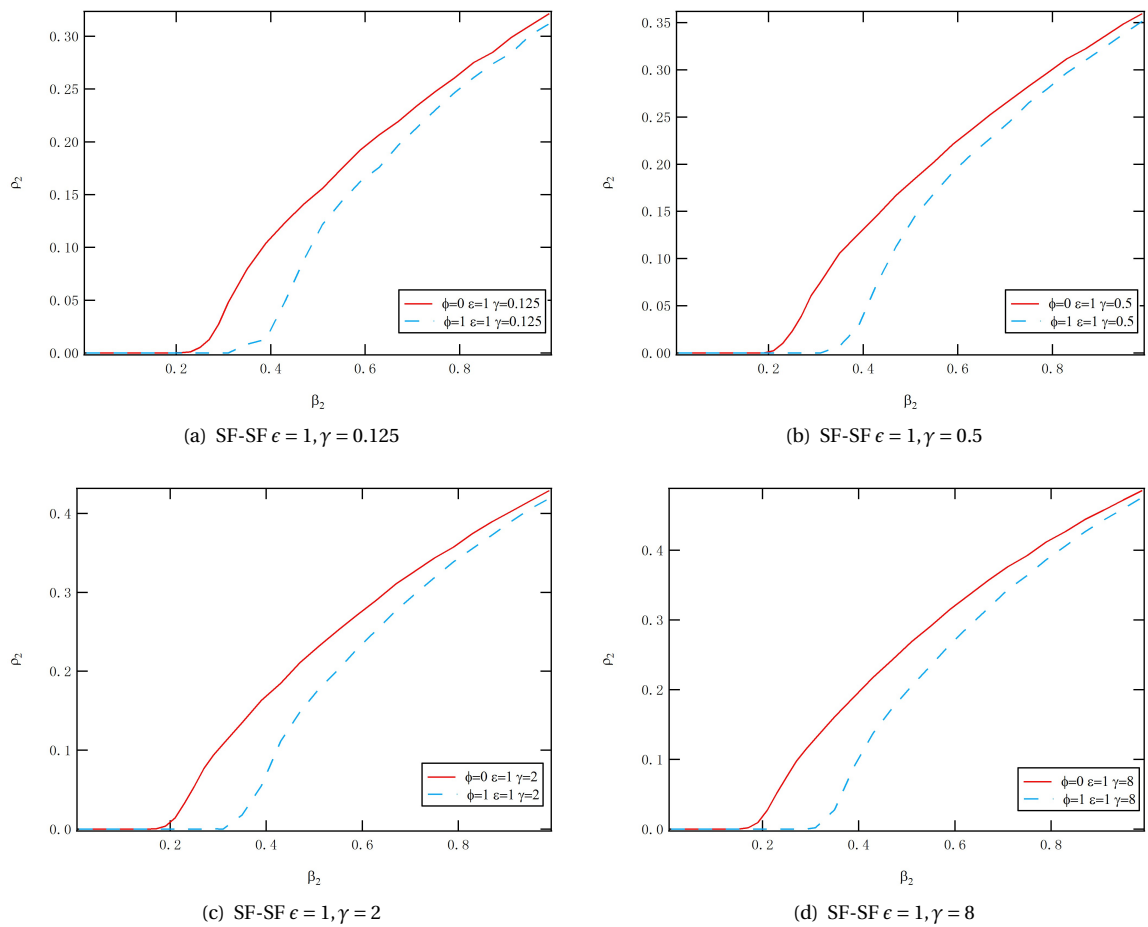


Figure 5.9: Influence of overlap ϕ between two layers in two-layer scale-free networks on the fraction of infection in the physical network ρ_2 . The injection rate is set to γ^ϵ with $\epsilon = 1$. The relative time scale in the social network layer are: (a) $\gamma = 0.125$, (b) $\gamma = 0.5$, (c) $\gamma = 2$, (d) $\gamma = 8$. Parameters we choose here are: $\beta_1 = 0.3$, $\delta_1 = 0.6$, $\delta_2 = 1.0$, $\alpha = 0.2$. The network size is $N = 1000$. In each scale-free network, the exponent for the power-law degree distribution is $\lambda = 2.5$. Initially 10% randomly chosen nodes are infected. Results are averaged over 200 realizations.

As shown in Fig.5.9, the overlap $\phi = 1$ situation always has a better epidemic mitigation effect compared to the $\phi = 0$ situation. Keeping in touch with real life friends is beneficial for hindering the epidemic spreading, since an infected individual could effectively propagate the information about the epidemic to his or her friends in the physical contact network who indeed need the information to prevent from getting infected by the infected individual. In different time scales γ , the difference between $\phi = 1$ and $\phi = 0$ is similar. It

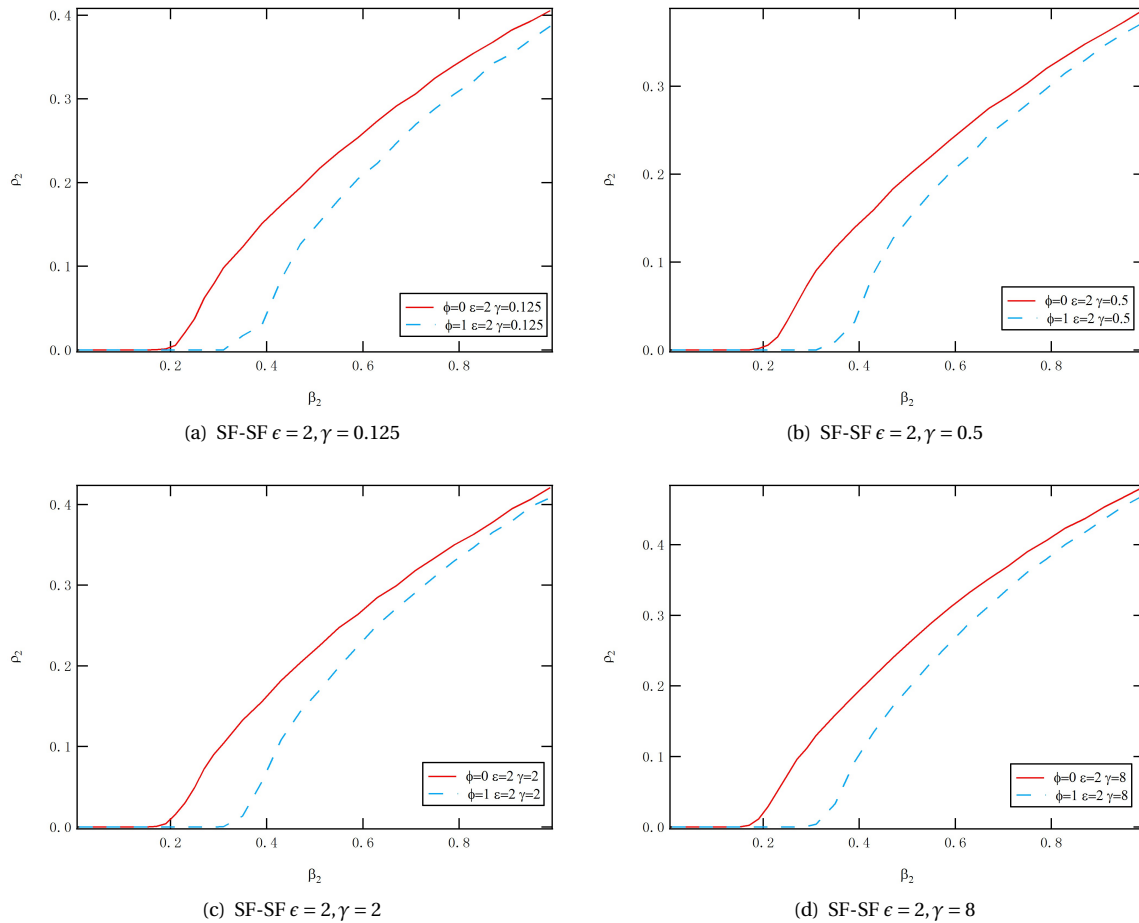


Figure 5.10: Influence of overlap ϕ between two layers in two-layer scale-free networks on the fraction of infection in the physical network ρ_2 . The injection rate is set to γ^ϵ with $\epsilon = 2$. The relative time scale in the social network layer are: (a) $\gamma = 0.125$, (b) $\gamma = 0.5$, (c) $\gamma = 2$, (d) $\gamma = 8$. Parameters we choose here are: $\beta_1 = 0.3$, $\delta_1 = 0.6$, $\delta_2 = 1.0$, $\alpha = 0.2$. The network size is $N = 1000$. In each scale-free network, the exponent for the power-law degree distribution is $\lambda = 2.5$. Initially 10% randomly chosen nodes are infected. Results are averaged over 200 realizations.

indicates that the effect of protections against epidemic by using $\phi = 1$ two-layer networks is almost the same under different time scales γ when the injection rate is γ^ϵ with $\epsilon = 1$.

From Fig.5.10, we could see that $\phi = 1$ is still beneficial for impeding epidemic spreading when the injection rate is γ^ϵ with $\epsilon = 2$. Around the epidemic threshold, the $\phi = 1$ is very effective because the few infected nodes in the physical contact network could inform neighbors in the physical network to take precautions. However, in the large β_2 situation most nodes are infected, therefore the advantage of $\phi = 1$ structure is not as evident as in small β_2 .

In conclusion, the structure of two-layer networks is essential for epidemic mitigation. The more overlapped two-layer networks structure should be suggested to defend a population from an epidemic.

6

CONCLUSION AND FUTURE WORK

6.1. CONCLUSION OF OUR WORKS

In this thesis, we mainly propose and investigate two models for dynamic interacting processes of epidemic spreading and awareness propagation in two-layer networks to study epidemic mitigation via awareness propagation. In our models, epidemic spreading in the physical network and awareness propagation in the social network interacts with each other. Aware individuals have a lower rate to get infected by an epidemic. The Epidemic and Awareness Interaction Processes (EAIP) model I describes the scenario where individuals get immediately aware when they get infected by an epidemic. The Epidemic and Awareness Interaction Processes (EAIP) model II describes the scenario where infected individuals get aware after some time instead of immediately get aware. Although the interactions between epidemic spreading and awareness propagation in two-layer networks make the model much more complicated than the simple viruses spreading in a single network, they are more realistic and practical for studying real-life processes.

Our focus is to understand how the optimum epidemic mitigation effect could be achieved with awareness propagation. There are two factors that influence the epidemic mitigation effect: the relative time scale γ of awareness propagation in the social network layer compared to that in the physical network layer, and the structure of two-layer networks. We develop Monte-Carlo simulations to study the steady state fraction of infected nodes in different scenarios. In addition, we analytically derive the infected probability and the aware probability for each node in both models via our original Individual-Based Mean Field Approximation IBMFA. IBMFA is proved to be an accurate approximation, and outperforms the Microscopic Markov Chain Approach MMCA, especially around the epidemic threshold in our two-layer networks.

In our EAIP model I, when an individual is infected by an epidemic in the physical network, he or she immediately becomes aware in the social network. In other words, the injection of information from the physical network layer to the social network layer happens immediately at the moment a node in the physical network layer is infected. Counter-intuitively, the epidemic mitigation effect becomes worse with rising γ , i.e. the frequent update of information in the social network layer leads to a higher steady state fraction of infection in the physical network layer. The reason is, the faster information updates in the social network actually dilute the specific information about the epidemic by other important information when people always get aware and share the information in the social network layer immediately when they get infected by an epidemic. Therefore, people could reduce the frequency of information updates in the social network to achieve a better epidemic mitigation effect.

In our EAIP model II, we consider the situation that if an individual does not use the social network very frequently, it takes some time for this individual to get aware in the social network layer. If an individual is very enthusiastic about socializing online, the chance that he or she updates information in the social network immediately after getting infected is high. Taking these facts into consideration, we propose a general form of the injection rate γ^c which considers different relationships between the injection rate and the time scale γ . In this model, an optimum γ for epidemic mitigation is witnessed where the propagation speed of information is comparable with the spreading speed of the epidemic.

Besides the time scale γ , the structure of two-layer networks is also essential for epidemic mitigation. We have shown that in both two-layer Erdős-Rényi random networks ER-ER, and in two-layer scale-free networks SF-SF, a higher overlap extent between two network layers always helps the control of an epidemic. To better protect people from an epidemic, communication with real life friends in the online social network should be encouraged.

One challenge in studying two-layer networks where epidemic spreading and awareness propagation interacts with each other is the too many parameters in a model. Therefore we propose these two fundamental models which are still analytical traceable.

Since we are unable to find detailed data for such two-layer dynamic interacting processes as in the EAIP model I and the EAIP model II, we propose two models to describe different scenarios. In the future, if some real life data is found, we could apply our models for such data to analyze the best situation for epidemic mitigation.

6.2. FUTURE WORKS

In this thesis work, we propose two fundamental models that are analytical traceable to capture the two key scenarios. Based on our two models, some possible extensions could be carried out with respect to the following directions:

- It is possible that during a chronic illness like cancer, even though a person has experienced being aware of the illness and then forgetting about the illness, after some time he might again become aware due to a new round of treatment, or the illness re-check. Therefore, we could describe this scenario by allowing possible injections as soon as an individual is infected in the physical network.
- In order to consider the influence of self-conscious of each individual on the recovery of awareness, we could add a constant value in the awareness recovering rate $\gamma\delta_1$.
- Instead of reducing the infection rate from each infected neighbors when an individual is aware as in our models, we could use adaptive networks that cut off links connected to infected neighbors of an aware individual. By using adaptive networks, we could describe the scenario where an aware individual stops meeting with infected friends to prevent from getting infected.
- People would pay more attentions to an epidemic when their real-life friends are infected by the epidemic, compared to when strangers are infected by the epidemic. Consequently, we could set different awareness propagating rates for the "neighbors are infected" case and the "strangers are infected" case representing different importance of the information.

A

APPENDIX FOR THE EPIDEMIC AND AWARENESS INTERACTION PROCESSES MODEL I

A.1. DERIVATION OF INDIVIDUAL-BASED MEAN FIELD APPROXIMATION IN EPIDEMIC AND AWARENESS INTERACTION PROCESSES MODEL I

As introduced in the mean-field approximation, the two state Markov chain for the SIS process in one network layer is characterized by an infinitesimal generator $Q_i(t)$ as

$$Q_i(t) = \begin{bmatrix} -q_i(t) & q_i(t) \\ \delta & -\delta \end{bmatrix} \quad (\text{A.1})$$

where $q_i(t)$ is the actual random infection rate for a node i at time t ,

$$q_i(t) = \beta \sum_{j=1}^N a_{ji} 1_{\{X_j(t)=1\}} \quad (\text{A.2})$$

In our two-layer networks, we denote the state $Y_i(t) = 1$ as node i is aware at time t in the social network layer, and $Y_i(t) = 0$ as node i is unaware at time t . Similarly, $X_i(t) = 1$ as a node i is infected at time t in the physical network layer, and $X_i(t) = 0$ as the node i is susceptible at time t . Here we consider time-dependent random variables $R_i(t) = 1_{\{Y_i(t)=1\}}$ for the social network layer, and $S_i(t) = 1_{\{X_i(t)=1\}}$ for the physical network layer [24]. $R_i(t) = 1$ if $Y_i(t) = 1$, and $R_i(t) = 0$ otherwise. $S_i(t) = 1$ if $X_i(t) = 1$, and $S_i(t) = 0$ otherwise. The change of $R_i(t)$ in an infinitesimal interval Δt in the social network layer is expressed as

$$\frac{R_i(t + \Delta t) - R_i(t)}{\Delta t} = -\gamma\delta_1 R_i(t) + (1 - R_i(t)) \left(\gamma\beta_1 \sum_{j=1}^N a_{ji} 1_{\{Y_j(t)=1\}} + (1 - S_i(t)) \beta_2 \sum_{j=1}^N b_{ji} 1_{\{X_j(t)=1\}} \right) \quad (\text{A.3})$$

We explain the equation Equ.A.3 in detail here. $R_i(t)$ could change from 1 to 0 with the awareness recovering rate $\gamma\delta_1$, which leads to the term $-\gamma\delta_1 R_i(t)$. When $R_i(t) = 0$, i.e. node i is unaware at time t , $R_i(t)$ could change to 1 with the sum of two rates:

1. Informed by aware neighbors. For an unaware node i $R_i(t) = 0$, it could get alertness of the epidemic from its aware neighbors in the social network layer. $a_{ji} = 1$ means node j is a neighbor of node i in the social

network. If node j is aware, i.e. $Y_j(t) = 1$, node j would contribute to the actual random infection rate of node i in the social network by $\gamma\beta_1$. These explain the term $(1 - R_i(t)) \left(\gamma\beta_1 \sum_{j=1}^N a_{ji} \mathbf{1}_{\{Y_j(t)=1\}} \right)$.

2. Injection from the physical network. For an unaware node i $R_i(t) = 0$, if it is susceptible at time t $X_i(t) = 0$, in the physical layer node i could get infected by each of its infected neighbors $X_j(t) = 1$ with a rate β_2 . In total the actual rate that node i get infected in the physical network at time t is $\beta_2 \sum_{j=1}^N b_{ji} \mathbf{1}_{\{X_j(t)=1\}}$. As we introduced above, in our two-layer network model, when a node is in the US state, and it gets infected in the physical network layer, the injection of information would happen immediately. As a consequence, $R_i(t)$ could change from 0 to 1 with a rate $(1 - R_i(t)) \left((1 - S_i(t)) \beta_2 \sum_{j=1}^N b_{ji} \mathbf{1}_{\{X_j(t)=1\}} \right)$ because of the injection mechanism.

Similarly, we explain here the change of $S_i(t)$ in an infinitesimal interval Δt in the physical network layer as followed.

term $-\delta_2 S_i(t)$. $S_i(t)$ could change from 1 to 0 with an epidemic curing rate δ_2 in the physical network layer.

term $(1 - S_i(t)) (1 - R_i(t)) \beta_2 \sum_{j=1}^N b_{ji} \mathbf{1}_{\{X_j(t)=1\}}$. The rate that a susceptible node i $S_i(t) = 0$ in the physical layer gets infected by its infected neighbors depends on the state of node i in the social network layer. If node i is unaware in the social network $(1 - R_i(t))$, the infection rate that each infected neighbor $X_j(t) = 1$ contributes is β_2 . Summing up the infection rate from all infected neighbors of node i , we get $\beta_2 \sum_{j=1}^N b_{ji} \mathbf{1}_{\{X_j(t)=1\}}$.

term $(1 - S_i(t)) R_i(t) \alpha \beta_2 \sum_{j=1}^N b_{ji} \mathbf{1}_{\{X_j(t)=1\}}$. When a susceptible node i $S_i(t) = 0$ is aware in the social network $Y_i(t) = 1$, the rate that node i is infected by any infected neighbors in the physical network is reduced from β_2 to $\alpha \beta_2$. Summing up the reduced infection rate from all infected neighbors of node i at time t , we get $\alpha \beta_2 \sum_{j=1}^N b_{ji} \mathbf{1}_{\{X_j(t)=1\}}$.

Consequently, the change of $S_i(t)$ in an infinitesimal interval Δt in the physical network layer is expressed as

$$\frac{S_i(t + \Delta t) - S_i(t)}{\Delta t} = -\delta_2 S_i(t) + (1 - S_i(t)) \left((1 - R_i(t)) + R_i(t) \alpha \right) \beta_2 \sum_{j=1}^N b_{ji} \mathbf{1}_{\{X_j(t)=1\}} \quad (\text{A.4})$$

Taking the expectation on both sides of Equ.A.3 and Equ.A.4, and denoting $u_i(t) = E[R_i(t)] = Pr[Y_i(t)]$ and $v_i(t) = E[S_i(t)] = Pr[X_i(t)]$, we get

$$\begin{aligned} \frac{u_i(t + \Delta t) - u_i(t)}{\Delta t} &= -\gamma\delta_1 u_i(t) + \gamma\beta_1 \sum_{j=1}^N a_{ji} v_j(t) - E \left[\mathbf{1}_{\{Y_i(t)=1\}} \gamma\beta_1 \sum_{j=1}^N a_{ji} \mathbf{1}_{\{Y_j(t)=1\}} \right] + \beta_2 \sum_{j=1}^N b_{ji} v_j(t) \\ &\quad - E \left[\mathbf{1}_{\{X_i(t)=1\}} \beta_2 \sum_{j=1}^N b_{ji} \mathbf{1}_{\{X_j(t)=1\}} \right] - E \left[\mathbf{1}_{\{Y_i(t)=1\}} \beta_2 \sum_{j=1}^N b_{ji} \mathbf{1}_{\{X_j(t)=1\}} \right] \\ &\quad + E \left[\mathbf{1}_{\{Y_i(t)=1\}} \cdot \mathbf{1}_{\{X_i(t)=0\}} \cdot \beta_2 \sum_{j=1}^N b_{ji} \mathbf{1}_{\{X_j(t)=1\}} \right] \end{aligned} \quad (\text{A.5a})$$

$$\begin{aligned} \frac{v_i(t + \Delta t) - v_i(t)}{\Delta t} &= -\delta_2 v_i(t) + \beta_2 \sum_{j=1}^N b_{ji} v_j(t) - E \left[\mathbf{1}_{\{Y_i(t)=1\}} \beta_2 \sum_{j=1}^N b_{ji} \mathbf{1}_{\{X_j(t)=1\}} \right] \\ &\quad + E \left[\mathbf{1}_{\{Y_i(t)=1\}} \alpha \beta_2 \sum_{j=1}^N b_{ji} \mathbf{1}_{\{X_j(t)=1\}} \right] - E \left[\mathbf{1}_{\{X_i(t)=1\}} \beta_2 \sum_{j=1}^N b_{ji} \mathbf{1}_{\{X_j(t)=1\}} \right] \\ &\quad + E \left[\mathbf{1}_{\{X_i(t)=1\}} \cdot \mathbf{1}_{\{Y_i(t)=1\}} \beta_2 \sum_{j=1}^N b_{ji} \mathbf{1}_{\{X_j(t)=1\}} \right] \\ &\quad - E \left[\mathbf{1}_{\{X_i(t)=1\}} \cdot \mathbf{1}_{\{Y_i(t)=1\}} \alpha \beta_2 \sum_{j=1}^N b_{ji} \mathbf{1}_{\{X_j(t)=1\}} \right] \end{aligned} \quad (\text{A.5b})$$

Since there is no self-loop in our two-layer model, $a_{ii} = 0$ and $b_{ii} = 0$ are always satisfied. According to Bayes law, the first remaining expectation in Equ.A.5a, as an example of an expectation with two $1_{\{Y_i(t)=1\}}$ -like terms could be written as

$$\begin{aligned} E \left[1_{\{Y_i(t)=1\}} \cdot 1_{\{Y_j(t)=1\}} \right] &= Pr [Y_i(t) = 1, Y_j(t) = 1] \\ &= Pr [Y_j(t) = 1 | Y_i(t) = 1] Pr [Y_i(t) = 1] \end{aligned} \quad (\text{A.6})$$

where the conditional probability meets

$$Pr [Y_j(t) = 1 | Y_i(t) = 1] \geq Pr [Y_j(t) = 1] \quad (\text{A.7})$$

because adding a condition cannot negatively affect the probability. Similarly, a remaining expectation with three $1_{\{Y_i(t)=1\}}$ -like terms in Equ.A.5a could be written as

$$\begin{aligned} E \left[1_{\{Y_i(t)=1\}} \cdot 1_{\{X_i(t)=1\}} \cdot 1_{\{X_j(t)=1\}} \right] &= Pr [Y_i(t) = 1, X_i(t) = 1, X_j(t) = 1] \\ &= Pr [Y_i(t) = 1, X_i(t) = 1 | X_j(t) = 1] Pr [X_j(t) = 1] \end{aligned} \quad (\text{A.8})$$

In our IBMFA approximation, we assume the independency between the infection states (infected or susceptible) of two neighboring nodes in the physical contact network as in NIMFA, the independency between the awareness states (aware or unaware) of two neighboring nodes in the social network, and the independency between the infection state and the awareness state of the same node though the injection has been taken into account.

Applying our assumption to Equ.A.5, we rewrite Equ.A.7 as

$$Pr [Y_j(t) = 1 | Y_i(t) = 1] = Pr [Y_j(t) = 1] \quad (\text{A.9})$$

Equ.A.6 becomes

$$E \left[1_{\{Y_i(t)=1\}} \cdot 1_{\{Y_j(t)=1\}} \right] = Pr [Y_j(t) = 1] Pr [Y_i(t) = 1] = u_j(t) u_i(t) \quad (\text{A.10})$$

With the same principle, Equ.A.8 is rewritten as

$$\begin{aligned} E \left[1_{\{Y_i(t)=1\}} \cdot 1_{\{X_i(t)=1\}} \cdot 1_{\{X_j(t)=1\}} \right] &= Pr [Y_i(t) = 1, X_i(t) = 1] Pr [X_j(t) = 1] \\ &= Pr [Y_i(t) = 1 | X_i(t) = 1] Pr [X_j(t) = 1] \\ &= Pr [Y_i(t) = 1] Pr [X_i(t) = 1] Pr [X_j(t) = 1] \\ &= u_i(t) v_i(t) v_j(t) \end{aligned} \quad (\text{A.11})$$

Other remaining expectations in Equ.A.5 could be rewritten the same way as Equ.A.10 and Equ.A.11. After rewriting all remaining expectations, Equ.A.5 becomes

$$\frac{du_i(t)}{dt} = -\gamma \delta_1 u_i(t) + (1 - u_i(t)) \left(\sum_{j=1}^N a_{ji} \gamma \beta_1 u_j(t) + (1 - v_i(t)) \sum_{j=1}^N b_{ij} \beta_2 v_j(t) \right) \quad (\text{A.12a})$$

$$\frac{dv_i(t)}{dt} = -\delta_2 v_i(t) + (1 - v_i(t)) \left(\sum_{j=1}^N b_{ji} (u_i(t) \alpha + (1 - u_i(t))) \beta_2 v_j(t) \right) \quad (\text{A.12b})$$

This is the derivation of IBMFA equations in our EAIP model I.

A.2. DERIVATION OF THE EPIDEMIC THRESHOLD τ_c IN THE MMCA

In the MMCA, we could calculate the epidemic threshold τ_c in the physical network layer as a function of the rest of parameters in the system [1]. Probability that node i is infected in the steady state is

$$p_i^I = p_i^{UI} + p_i^{AI} \quad (\text{A.13})$$

Similar to Equ.4.5, p_i^I could be rewritten by adding Equ.4.8b and 4.8d as

$$p_i^I = p_i^I(1 - \delta_2) + p_i^{US}(1 - q_i^U) + p_i^{AS}(1 - q_i^A) \quad (\text{A.14})$$

Near the epidemic threshold τ_c , probability that nodes are infected is close to 0, i.e. $p_i^I = \epsilon_i \ll 1$. In this situation, Equ.4.7b and 4.7c are written as

$$\begin{aligned} q_i^U &\approx 1 - \beta_2 \sum_j b_{ji} \epsilon_j = 1 - \sigma_i \\ q_i^A &\approx 1 - \alpha \beta_2 \sum_j b_{ji} \epsilon_j = 1 - \alpha \sigma_i \end{aligned} \quad (\text{A.15})$$

where

$$\sigma_i = \beta_2^* \sum_j b_{ji} \epsilon_j \quad (\text{A.16})$$

Then Equ.A.14 becomes

$$\begin{aligned} \epsilon_i = p_i^{UI} + p_i^{AI} &= \epsilon_i(1 - \delta_2^*) + p_i^{US} \sigma_i + p_i^{AS} \alpha \sigma_i \\ &\approx \epsilon_i(1 - \delta_2^*) + p_i^U \sigma_i + p_i^A \alpha \sigma_i \end{aligned} \quad (\text{A.17})$$

The approximately equal is because $p_i^I \approx 0$, so $p_i^U \approx p_i^{US}$, and $p_i^A \approx p_i^{AS}$. Replacing σ_i in Equ.A.17, we have

$$\epsilon_i = \epsilon_i(1 - \delta_2^*) + (p_i^U + p_i^A \alpha) \beta_2^* \sum_j b_{ji} \epsilon_j \quad (\text{A.18})$$

which equals to

$$\sum_j [\beta_2^* (p_i^U + p_i^A \alpha) b_{ji} - \delta_2^* e_{ij}] \epsilon_j = 0 \quad (\text{A.19})$$

e_{ij} is an element of an identity matrix, i.e. $\{e_{ij} = 1, i = j\}$, and $\{e_{ij} = 0, i \neq j\}$. We define the matrix H with elements

$$h_{ij} = (p_i^U + p_i^A \alpha) b_{ji} \quad (\text{A.20})$$

Non-trivial solutions of Equ.A.19 are eigenvectors of H, whose largest real eigenvalues are equal to δ_2^*/β_2^* . Therefore, the epidemic threshold $\tau_c = \beta_2^*/\delta_2^*$ in the physical network layer is given by

$$\tau_c = \frac{\beta_2}{\delta_2} = \frac{\beta_2^*}{\delta_2^*} = \frac{1}{\Lambda_{\max}(H)} \quad (\text{A.21})$$

A.3. COMPARISON OF THE ACCURACY OF THE IBMFA AND THE MMCA

In this section, we plot figures Fig.A.1 to compare the accuracy between the IBMFA and the MMCA in the overlap $\phi = 0$ situation.

A.4. INVESTIGATE THE INFLUENCE OF TIME SCALE γ IN THE IBMFA AND THE MMCA

In this section we study the effectiveness of our theoretical analysis methods, i.e. the IBMFA and the MMCA. We plot figures that is comparable with our simulation results as in Fig.4.4 and Fig.4.5. For the IBMFA equations, we achieved the upper bound from Equ.4.14, and the lower bound from normal IBMFA equation Equ.4.2 with $\gamma = 0$.

As shown in Fig.A.2, all phenomena that we observed in Monte-Carol simulations could be observed in IBMFA results. As the time scale γ increases, the effect of epidemic mitigation through awareness propagation gets worse, and when $\gamma = 16$ the curve is very close to the upper bound.

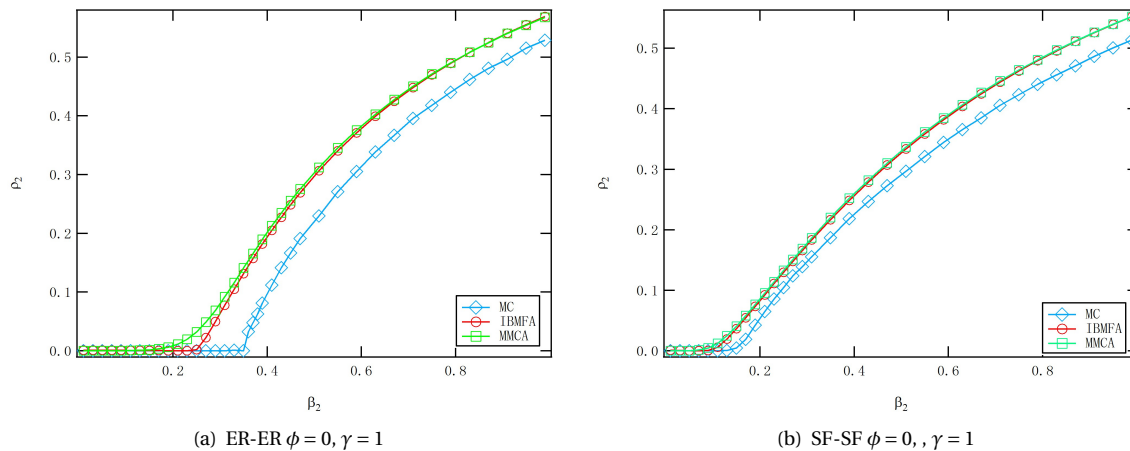


Figure A.1: Compare the accuracy between Monte-Carlo simulations, the IBMFA approximation and the MMCA approximation under the same set of parameters. Two-layer Erdős-Rényi random networks with overlap $\phi = 0$, and two-layer scale-free networks with overlap $\phi = 0$ are used. Parameters we choose here are as followed: $\beta_1 = 0.3, \delta_1 = 0.6, \delta_2 = 1.0, \alpha = 0.5, \gamma = 1$. The network size is $N = 1000$. For Erdős-Rényi random networks, the average degree $E[d] = 4$. For scale-free networks, the exponent in the power-law degree distribution is $\lambda = 2.5$.

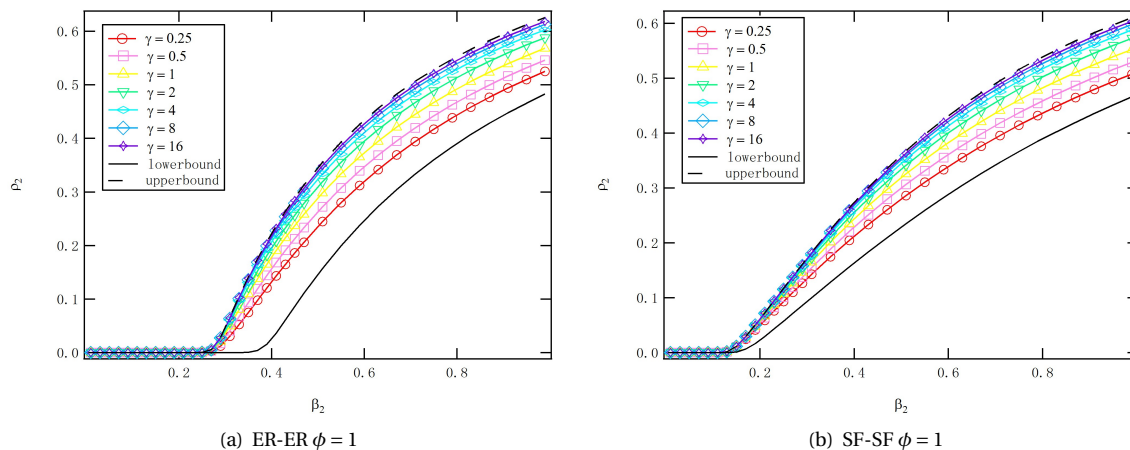


Figure A.2: Effect of time scales γ on the epidemic spreading in two-layer networks by IBMFA equations. X axis is the infection rate on each link in the physical network β_2 , and y axis is the fraction of infection in the physical network in the steady state ρ_2 . Two-layer Erdős-Rényi random network with an overlap extent $\phi = 1$, and two-layer scale-free network with the overlap extent $\phi = 1$ are used. Parameters we use here are as followed: $\beta_1 = 0.3, \delta_1 = 0.6, \delta_2 = 1.0, \alpha = 0.5$. The network size is $N = 1000$. For Erdős-Rényi random networks, the average degree $E[d] = 4$. For each scale-free network, the exponent in the power-law degree distribution is $\lambda = 2.5$. Initially, all nodes are aware and infected (AI). Results are averaged over 10 realizations.

For MMCA equations, we were unable to achieve the upper bound due to the fact that probabilities in Equ.4.7 cannot be larger than 1. We got the lower bound by setting $\gamma = 0$.

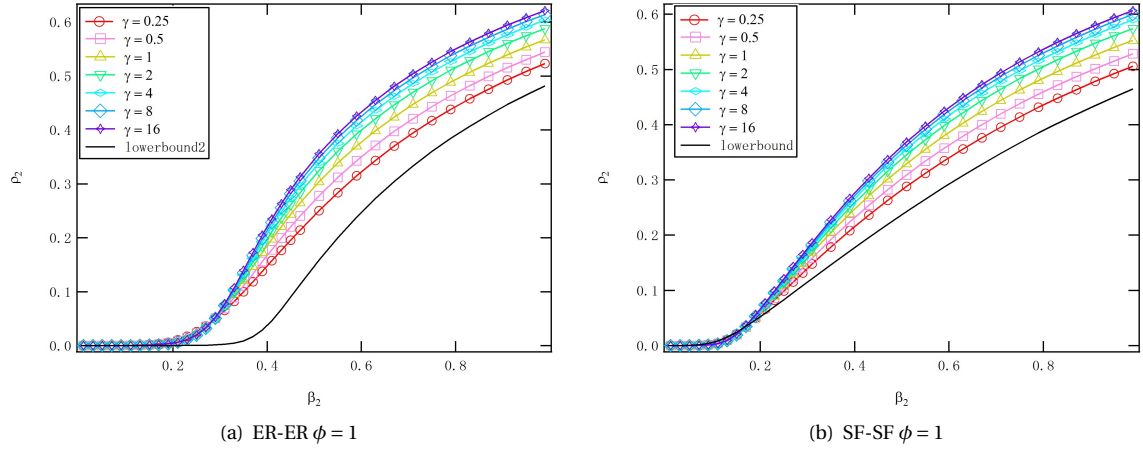


Figure A.3: Effect of time scales γ on the epidemic spreading in two-layer networks by **MMCA** equations. The x axis is the infection rate on each link in the physical network β_2 , and the y axis is the fraction of infection in the physical network in the steady state ρ_2 . Two-layer Erdős-Rényi random networks with the overlap extent $\phi = 1$, and two-layer scale-free networks with the overlap extent $\phi = 1$ are used. Parameters we use here are as followed: $\beta_1 = 0.3, \delta_1 = 0.6, \delta_2 = 1.0, \alpha = 0.5$. The network size is $N = 1000$. For Erdős-Rényi random networks, the average degree $E[d] = 4$. For scale-free networks, the exponent in the power-law degree distribution is $\lambda = 2.5$. Initially, all nodes are aware and infected (AI). Results are averaged over 10 realizations.

From Fig.A.3, we could see that the MMCA also works well for our model. Observations for the changes in the epidemic mitigation effect with γ from Monte-Carol simulations could also be observed in the MMCA.

B

APPENDIX FOR THE EPIDEMIC AND AWARENESS INTERACTION PROCESSES MODEL II

B.1. DERIVATION OF INDIVIDUAL-BASED MEAN FIELD APPROXIMATION I IN EPIDEMIC AND AWARENESS INTERACTION PROCESSES MODEL II

We consider time-dependent random variables $R_i(t) = 1_{\{Y_i(t)=1\}}$ for social network layer, and $S_i^S(t) = 1_{\{X_i^S(t)=1\}}$, $S_i^{II}(t) = 1_{\{X_i^{II}(t)=1\}}$ and $S_i^{IN}(t) = 1_{\{X_i^{IN}(t)=1\}}$ for physical network layer. The change of $R_i(t)$ in infinitesimal interval Δt in social network layer is expressed as

$$\frac{R_i(t + \Delta t) - R_i(t)}{\Delta t} = -\gamma\delta_1 R_i(t) + (1 - R_i(t)) \left(\gamma\beta_1 \sum_{j=1}^N a_{ji} 1_{\{Y_j(t)=1\}} \right) + \gamma^\epsilon S_i^{II}(t) \quad (\text{B.1})$$

$R_i(t) = 1$ indicates that node i is aware at time t , so $R_i(t)$ could change from 1 to 0 with awareness recovering rate $\gamma\delta_1$, which leads to the term $-\gamma\delta_1 R_i(t)$. When $R_i(t) = 0$, i.e. node i is unaware at time t , $R_i(t)$ could change to 1 in two ways.

1. First way is that node i gets aware from aware neighbors in the social network layer. If a neighbor of node i is node j , and node j is aware $Y_j(t) = 1$, node j contributes to infection rate of node i by $\gamma\beta_1$. Getting awareness from neighbors leads to the term $(1 - R_i(t)) \left(\gamma\beta_1 \sum_{j=1}^N a_{ji} 1_{\{Y_j(t)=1\}} \right)$.
2. Second way is, node i get aware by injection from physical network layer. Injection requires $S_i^{II}(t) = 1$ in physical network layer. When $S_i^{II}(t) = 1$, from dynamic processes we defined in two-layer network model 2, $R_i(t) = 0$ is certainly met, i.e. $Pr[R_i(t) = 0 | S_i^{II}(t) = 1] = 1$. Considering injection rate γ^ϵ , we reach the term $\gamma^\epsilon S_i^{II}(t)$.

Similarly for physical contact layer, there are three terms for change of $S_i^S(t)$ which are listed as followed.

term $\delta_2 (S_i^{II}(t) + S_i^{IN}(t))$. If node i is infected ($S_i^{II}(t) = 1$ or $S_i^{IN}(t) = 1$) at time t , node i has recovery rate δ_2 in physical network layer. In this case ($S_i^{II}(t) = 1$ or $S_i^{IN}(t) = 1$), $S_i^S(t) = 0$ is self satisfied.

term $-S_i^S(t)R_i(t)\alpha\beta_2\sum_{j=1}^N b_{ji}1_{\{X_j^{II}(t)=1\oplus X_j^{IN}(t)=1\}}$. An aware and susceptible (AS) node i $S_i^S(t) = 1$, $R_i(t) = 1$ could be infected by each of its infected neighbors $X_j^{II}(t) = 1$ or $X_j^{IN}(t) = 1$ with rate $\alpha\beta_2$.

term $-S_i^S(t)(1-R_i(t))\beta_2\sum_{j=1}^N b_{ji}1_{\{X_j^{II}(t)=1\oplus X_j^{IN}(t)=1\}}$. An unaware and susceptible node i $S_i^S(t) = 1$ and $R_i(t) = 0$ might get infection from each of its infected neighbors $X_j^{II}(t) = 1$ or $X_j^{IN}(t) = 1$ with rate β_2 .

In conclusion, change of $S_i^S(t)$ in infinitesimal interval Δt is expressed in equation

$$\begin{aligned} \frac{S_i^S(t+\Delta t) - S_i^S(t)}{\Delta t} = & \delta_2 (S_i^{II}(t) + S_i^{IN}(t)) - S_i^S(t)R_i(t)\alpha\beta_2 \sum_{j=1}^N b_{ji}1_{\{X_j^{II}(t)=1\oplus X_j^{IN}(t)=1\}} \\ & - S_i^S(t)(1-R_i(t))\beta_2 \sum_{j=1}^N b_{ji}1_{\{X_j^{II}(t)=1\oplus X_j^{IN}(t)=1\}} \end{aligned} \quad (\text{B.2})$$

Terms for the change of $S_i^{II}(t)$ are:

term $-S_i^{II}(t)\delta_2$. An II node i at time t $S_i^{II}(t) = 1$ could be recovered and become susceptible in physical network with rate δ_2 .

term $-S_i^{II}(t)\gamma^e$. An II node i at time t is certainly unaware. It could become aware via injection from physical network layer with injection rate γ^e . After injection, in physical layer II state goes to IN state.

term $-S_i^{II}(t)\gamma\beta_1\sum_{j=1}^N a_{ji}1_{\{Y_j(t)=1\}}$. Node i in II state $S_i^{II}(t) = 1$ could also get awareness from aware neighbors. After getting aware, node i goes to IN state.

term $S_i^S(t)(1-R_i(t))\beta_2\sum_{j=1}^N b_{ji}1_{\{X_j^{II}(t)=1\oplus X_j^{IN}(t)=1\}}$. When $S_i^{II}(t) = 0$, node i is either susceptible, or in IN state in physical network layer. IN state cannot directly go to II state, therefore we only consider susceptible state here, i.e. $S_i^S(t) = 1$. In this case, if in social network layer node i is unaware $R_i(t) = 0$, node i could get infected with infection rate β_2 from each of its infected neighbors in physical network, and becomes II state.

Thus change of $S_i^{II}(t)$ in infinitesimal interval Δt is expressed as

$$\begin{aligned} \frac{S_i^{II}(t+\Delta t) - S_i^{II}(t)}{\Delta t} = & -S_i^{II}(t)\delta_2 - S_i^{II}(t)\gamma^e - S_i^{II}(t)\gamma\beta_1 \sum_{j=1}^N a_{ji}1_{\{Y_j(t)=1\}} \\ & + S_i^S(t)(1-R_i(t))\beta_2 \sum_{j=1}^N b_{ji}1_{\{X_j^{II}(t)=1\oplus X_j^{IN}(t)=1\}} \end{aligned} \quad (\text{B.3})$$

Similarly, node i could leave IN state with rate δ_2 and become susceptible, meanwhile S state as well as II state could change to IN state. Change of $S_i^{IN}(t)$ in infinitesimal interval Δt is

$$\begin{aligned} \frac{S_i^{IN}(t+\Delta t) - S_i^{IN}(t)}{\Delta t} = & -S_i^{IN}(t)\delta_2 + S_i^{II}(t)\gamma^e + S_i^{II}(t)\gamma\beta_1 \sum_{j=1}^N a_{ji}1_{\{Y_j(t)=1\}} \\ & + S_i^S(t)R_i(t)\alpha\beta_2 \sum_{j=1}^N b_{ji}1_{\{X_j^{II}(t)=1\oplus X_j^{IN}(t)=1\}} \end{aligned} \quad (\text{B.4})$$

We take expectation on both sides of Equ.B.1, B.2, B.3 and B.4, and denote

$$\begin{aligned}
 u_i(t) &= E[R_i(t)] = Pr[Y_i(t) = 1] \\
 v_i^S(t) &= E[S_i^S(t)] = Pr[X_i^S(t) = 1] \\
 v_i^{II}(t) &= E[S_i^{II}(t)] = Pr[X_i^{II}(t) = 1] \\
 v_i^{IN}(t) &= E[S_i^{IN}(t)] = Pr[X_i^{IN}(t) = 1]
 \end{aligned} \tag{B.5}$$

We could take expectation on both sides and derive

$$\frac{u_i(t + \Delta t) - u_i(t)}{\Delta t} = -\gamma\delta_1 u_i(t) + \gamma\beta_1 \sum_{j=1}^N a_{ji} u_j - E \left[\mathbf{1}_{\{Y_i(t)=1\}} \gamma\beta_1 \sum_{j=1}^N a_{ji} \mathbf{1}_{\{Y_j(t)=1\}} \right] + \gamma^\epsilon v_i^{II}(t) \tag{B.6a}$$

$$\begin{aligned}
 \frac{v_i^S(t + \Delta t) - v_i^S(t)}{\Delta t} &= \delta_2 (v_i^{II}(t) + v_i^{IN}(t)) - E \left[\mathbf{1}_{\{X_i^S(t)=1\}} \cdot \mathbf{1}_{\{Y_i(t)=1\}} \cdot \alpha\beta_2 \sum_{j=1}^N b_{ji} \mathbf{1}_{\{X_j^{II}(t)=1 \oplus X_j^{IN}(t)=1\}} \right] \\
 &\quad - E \left[\mathbf{1}_{\{X_i^S(t)=1\}} \beta_2 \sum_{j=1}^N b_{ji} \mathbf{1}_{\{X_j^{II}(t)=1 \oplus X_j^{IN}(t)=1\}} \right] \\
 &\quad + E \left[\mathbf{1}_{\{X_i^S(t)=1\}} \cdot \mathbf{1}_{\{Y_i(t)=1\}} \cdot \beta_2 \sum_{j=1}^N b_{ji} \mathbf{1}_{\{X_j^{II}(t)=1 \oplus X_j^{IN}(t)=1\}} \right]
 \end{aligned} \tag{B.6b}$$

$$\begin{aligned}
 \frac{v_i^{II}(t + \Delta t) - v_i^{II}(t)}{\Delta t} &= -v_i^{II}(t) (\delta_2 + \gamma^\epsilon) - E \left[\mathbf{1}_{\{X_i^{II}(t)=1\}} \gamma\beta_1 \sum_{j=1}^N a_{ji} \mathbf{1}_{\{Y_j(t)=1\}} \right] \\
 &\quad + E \left[\mathbf{1}_{\{X_i^S(t)=1\}} \beta_2 \sum_{j=1}^N b_{ji} \mathbf{1}_{\{X_j^{II}(t)=1 \oplus X_j^{IN}(t)=1\}} \right] \\
 &\quad - E \left[\mathbf{1}_{\{X_i^S(t)=1\}} \cdot \mathbf{1}_{\{Y_i(t)=1\}} \cdot \beta_2 \sum_{j=1}^N b_{ji} \mathbf{1}_{\{X_j^{II}(t)=1 \oplus X_j^{IN}(t)=1\}} \right]
 \end{aligned} \tag{B.6c}$$

$$\begin{aligned}
 \frac{v_i^{IN}(t + \Delta t) - v_i^{IN}(t)}{\Delta t} &= -v_i^{IN}(t) (\delta_2) + v_i^{II}(t) (\gamma^\epsilon) + E \left[\mathbf{1}_{\{X_i^{II}(t)=1\}} \gamma\beta_1 \sum_{j=1}^N a_{ji} \mathbf{1}_{\{Y_j(t)=1\}} \right] \\
 &\quad + E \left[\mathbf{1}_{\{X_i^S(t)=1\}} \alpha\beta_2 \sum_{j=1}^N b_{ji} \mathbf{1}_{\{X_j^{II}(t)=1 \oplus X_j^{IN}(t)=1\}} \right]
 \end{aligned} \tag{B.6d}$$

Since II and IN states are exclusive states,

$$\begin{aligned}
 E \left[\mathbf{1}_{\{X_j^{II}(t)=1 \oplus X_j^{IN}(t)=1\}} \right] &= Pr \left[X_j^{II}(t) = 1 \cup X_j^{IN}(t) = 1 \right] \\
 &= Pr \left[X_j^{II}(t) = 1 \right] + Pr \left[X_j^{IN}(t) = 1 \right]
 \end{aligned} \tag{B.7}$$

By assuming independency between the infection states (infected or susceptible) of two neighboring nodes in the physical contact network as in NIMFA, the independency between the awareness states (aware or unaware) of two neighboring nodes in the social network, and the independency between the infection state and the awareness state of the same node though the injection has been taken into account, according to Bayes law we have

$$\begin{aligned}
 E \left[\mathbf{1}_{\{X_i^S(t)=1\}} \cdot \mathbf{1}_{\{Y_i(t)=1\}} \right] &= Pr \left[X_i^S(t) = 1, Y_i(t) = 1 \right] \\
 &= Pr \left[X_i^S(t) = 1 \right] Pr \left[Y_i(t) = 1 | X_i^S(t) = 1 \right] \\
 &= Pr \left[X_i^S(t) = 1 \right] Pr \left[Y_i(t) = 1 \right] \\
 &= v_i^S(t) u_i(t)
 \end{aligned} \tag{B.8}$$

With the same principle, we could rewrite all remaining expectations in Equ.B.6 as

$$\frac{du_i(t)}{dt} = -\gamma\delta_1 u_i(t) + (1 - u_i(t))\gamma\beta_1 \sum_{j=1}^N a_{ji} u_j(t) + \gamma^\epsilon v_i^{II}(t) \quad (\text{B.9a})$$

$$\frac{dv_i^S(t)}{dt} = -v_i^S(t) \left([u_i(t)\alpha + (1 - u_i(t))]\beta_2 \sum_{j=1}^N b_{ji} (v_j^{II}(t) + v_j^{IN}(t)) \right) + \delta_2 (v_i^{II}(t) + v_i^{IN}(t)) \quad (\text{B.9b})$$

$$\frac{dv_i^{II}(t)}{dt} = -v_i^{II}(t) \left(\delta_2 + \gamma^\epsilon + \gamma\beta_1 \sum_{j=1}^N a_{ji} u_j(t) \right) + v_i^S(t) (1 - u_i(t)) \left(\beta_2 \sum_{j=1}^N b_{ji} (v_j^{II}(t) + v_j^{IN}(t)) \right) \quad (\text{B.9c})$$

$$\frac{dv_i^{IN}(t)}{dt} = -\delta_2 v_i^{IN}(t) + v_i^S(t) u_i(t) \left(\alpha\beta_2 \sum_{j=1}^N b_{ji} (v_j^{II}(t) + v_j^{IN}(t)) \right) + v_i^{II}(t) \left(\gamma^\epsilon + \gamma\beta_1 \sum_{j=1}^N a_{ji} u_j(t) \right) \quad (\text{B.9d})$$

Equ.5.1 is the final IBMFA equation for our two-layer network model 2. Four differential equations need to be solved for each node i within totally $N = 1000$ nodes in a two-layer network. Write Equ.5.1 in matrix format, with $U(t)$ representing a column vector with $N = 1000$ elements $u_i(t)$, $i \in [1, 1000]$, and similarly $V^S(t)$, $V^{II}(t)$ and $V^{IN}(t)$, we get

$$\frac{dU(t)}{dt} = -\gamma\delta_1 U(t) + \text{diag}(u - U(t)) \gamma\beta_1 AU(t) + \gamma^\epsilon V^{II}(t) \quad (\text{B.10a})$$

$$\frac{dV^S(t)}{dt} = -\text{diag}(V^S(t)) (\text{diag}[U(t)\alpha + (u - U(t))]\beta_2 B(V^{II}(t) + V^{IN}(t))) + \delta_2 (V^{II}(t) + V^{IN}(t)) \quad (\text{B.10b})$$

$$\begin{aligned} \frac{dV^{II}(t)}{dt} = & -\text{diag}(V^{II}(t)) (\delta_2 u + \gamma^\epsilon u + \gamma\beta_1 AU(t)) \\ & + \text{diag}(V^S(t)) \text{diag}((u - U(t))) (\beta_2 B(V^{II}(t) + V^{IN}(t))) \end{aligned} \quad (\text{B.10c})$$

$$\begin{aligned} \frac{dV^{IN}(t)}{dt} = & -\delta_2 V^{IN}(t) + \text{diag}(V^S(t)) \text{diag}(U(t)) (\alpha\beta_2 B(V^{II}(t) + V^{IN}(t))) \\ & + \text{diag}(V^{II}(t)) (\gamma^\epsilon u + \gamma\beta_1 AU(t)) \end{aligned} \quad (\text{B.10d})$$

where u is all 1 column vector with $N = 1000$ elements. In steady state, $\frac{dU(t)}{dt} = 0$, $\frac{dV^S(t)}{dt} = 0$, $\frac{dV^{II}(t)}{dt} = 0$ and $\frac{dV^{IN}(t)}{dt} = 0$. Still, we are interested in meta-stable state of the system.

B.2. DERIVATION OF THE EPIDEMIC THRESHOLD τ_c IN THE MMCA

Similar to Equ.A.21, we derive epidemic threshold τ_c in the physical network layer as a function of the rest of parameters in the system in the steady state. The probability that node i is infected in the steady state is

$$p_i^I = p_i^{UIN} + p_i^{UII} + p_i^{AI} \quad (\text{B.11})$$

By adding Equ.5.9b, 5.9c and 5.9e, we get

$$p_i^I = p_i^I (1 - \delta_2) + p_i^{US} (1 - q_i^U) + p_i^{AS} (1 - q_i^A) \quad (\text{B.12})$$

Near the epidemic threshold τ_c , probability that nodes are infected is close to 0, i.e. $p_i^I = \epsilon_i \ll 1$. In this situation, Equ.5.8b and 5.8c are written as

$$\begin{aligned} q_i^U & \approx 1 - \beta_2 \sum_j b_{ji} \epsilon_j = 1 - \sigma_i \\ q_i^A & \approx 1 - \alpha\beta_2 \sum_j b_{ji} \epsilon_j = 1 - \alpha\sigma_i \end{aligned} \quad (\text{B.13})$$

where

$$\sigma_i = \beta_2^* \sum_j b_{ji} \epsilon_j \quad (\text{B.14})$$

Then Equ.B.12 becomes

$$\begin{aligned} \epsilon_i &= p_i^{UIN} + p_i^{UII} + p_i^{AI} = \epsilon_i(1 - \delta_2^*) + p_i^{US} \sigma_i + p_i^{AS} \alpha \sigma_i \\ &\approx \epsilon_i(1 - \delta_2^*) + p_i^U \sigma_i + p_i^A \alpha \sigma_i \end{aligned} \quad (\text{B.15})$$

The approximately equal is because $p_i^I \approx 0$, so $p_i^U \approx p_i^{US}$, and $p_i^A \approx p_i^{AS}$. Replace σ_i in Equ.A.17, we have

$$\epsilon_i = \epsilon_i(1 - \delta_2^*) + (p_i^U + p_i^A \alpha) \beta_2^* \sum_j b_{ji} \epsilon_j \quad (\text{B.16})$$

which equals to

$$\sum_j [\beta_2^* (p_i^U + p_i^A \alpha) b_{ji} - \delta_2^* e_{ij}] \epsilon_j = 0 \quad (\text{B.17})$$

e_{ij} is element of an identity matrix, i.e. $\{e_{ij} = 1, i = j\}$, and $\{e_{ij} = 0, i \neq j\}$. We define matrix H with elements

$$h_{ij} = (p_i^U + p_i^A \alpha) b_{ji} \quad (\text{B.18})$$

Non-trivial solutions of Equ.B.17 are eigenvectors of H, whose largest real eigenvalues are equal to δ_2^* / β_2^* . Therefore, epidemic threshold $\tau_c = \beta_2^* / \delta_2^*$ in physical network layer is given by

$$\tau_c = \frac{\beta_2}{\delta_2} = \frac{\beta_2^*}{\delta_2^*} = \frac{1}{\Lambda_{\max}(H)} \quad (\text{B.19})$$

B.3. INVESTIGATE THE INFLUENCE OF TIME SCALE γ WITH IBMFA AND MMCA

In Fig.B.1, we could see that for in Both IBMFA equations in Fig.B.1(a) and Fig.B.1(b), and MMCA equations in Fig.B.1(c) in the range $\gamma = 1/8$ to $\gamma = 8$, fraction of infection ρ_2 increases monotonously with time scale γ , which is the same as our result in Monte-Carol simulation as shown in Fig.5.4. Position of upper bound which we achieve from Equ.5.12 is also in the same position as in Fig.5.4. Difference between curves in MMCA is a little larger than IBMFA equations.

As shown in Fig.B.2, the difference between curves in IBMFA equations in Fig.B.2(a) and Fig.B.2(b) is not so evident as in Monte-Carol simulation. Optimum effect of epidemic mitigation via awareness propagation could be observed at around $\gamma = 1$ when injection rate is γ^ϵ with $\epsilon = 2$, instead of at $\gamma = 0.5$ as in Monte-Carol simulations. MMCA solutions in Fig.B.2(c) still shows larger difference between curves, while $\gamma = 0.125$, $\gamma = 0.25$ and $\gamma = 0.5$ curves are almost overlapped together. It seems that fraction of infection ρ_2 in MMCA Fig.B.2(c) is in monotonic relationship with time scale γ even though $\epsilon = 2$. We could say that the optimum γ is not very accurate in both IBMFA and MMCA equations.

B.4. INFLUENCE OF THE TIME SCALE γ IN TWO-LAYER ERDŐS-RÉNYI (ER) RANDOM NETWORKS

From figures Fig.B.3 and Fig.B.4, we could see that same observations for epidemic mitigation under different values of γ are achieved in ER-ER networks as in SF-SF networks.

B.5. INFLUENCE OF OVERLAP ϕ IN TWO-LAYER ERDŐS-RÉNYI (ER) RANDOM NETWORKS

Here we plot figures Fig.B.5 and Fig.B.6 to study the influence of overlap ϕ for two-layer ER-ER networks.

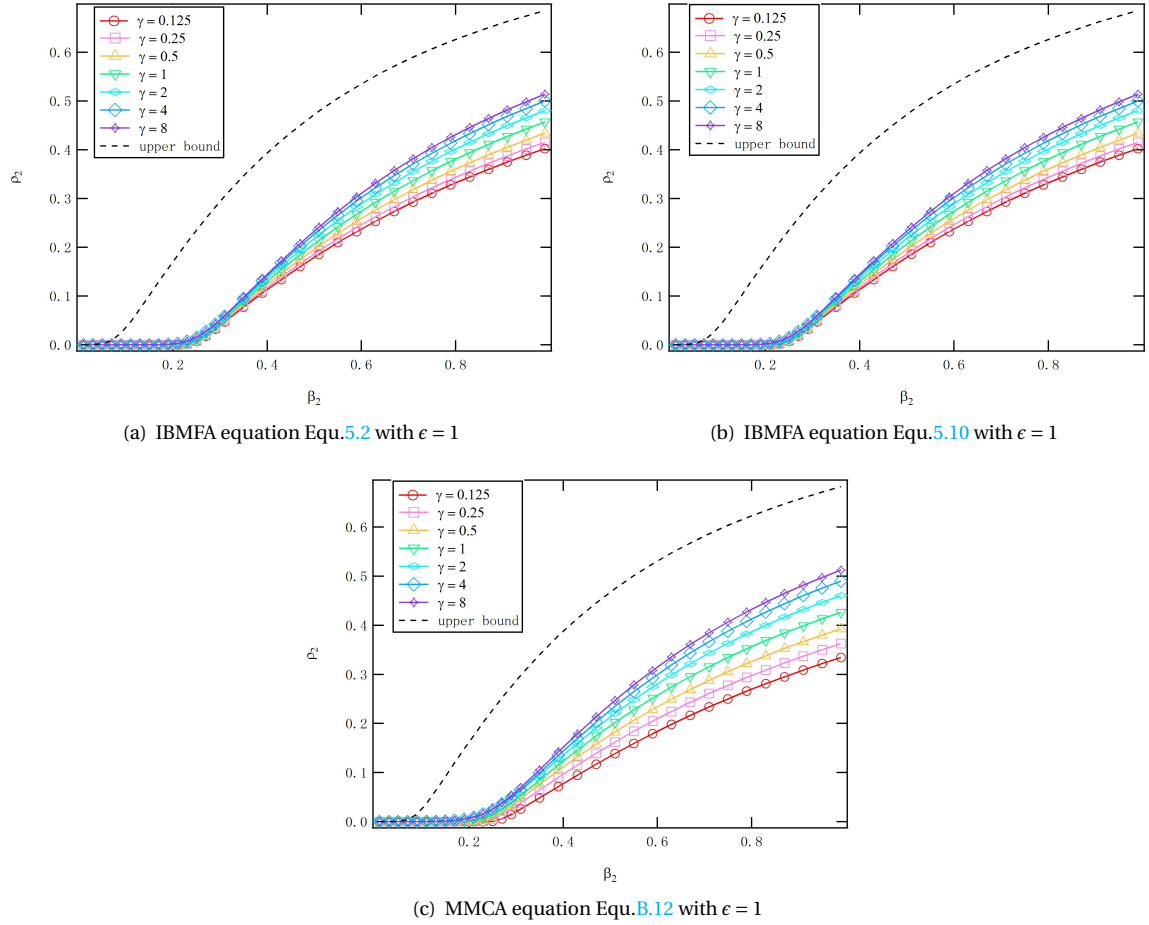


Figure B.1: Result of three theoretical approximations, (a) IBMFA equation Eq.5.2, (b) IBMFA equation 2 Eq.B.13 and (c) MMCA equations Eq.B.12. Injection rate is set to be γ^ϵ where $\epsilon = 1$. Two-layer scale-free networks SF-SF with overlap $\phi = 1$ is used here. Other parameters we chose here are: $\beta_1 = 0.3, \delta_1 = 0.6, \beta_2 = 1.0, \delta_2 = 1.0, \alpha = 0.2$. Network size is $N = 1000$. For each scale-free network, the exponent of power-law degree distribution is $\lambda = 2.5$. Solutions are averaged over 10 independently generated two-layer networks.

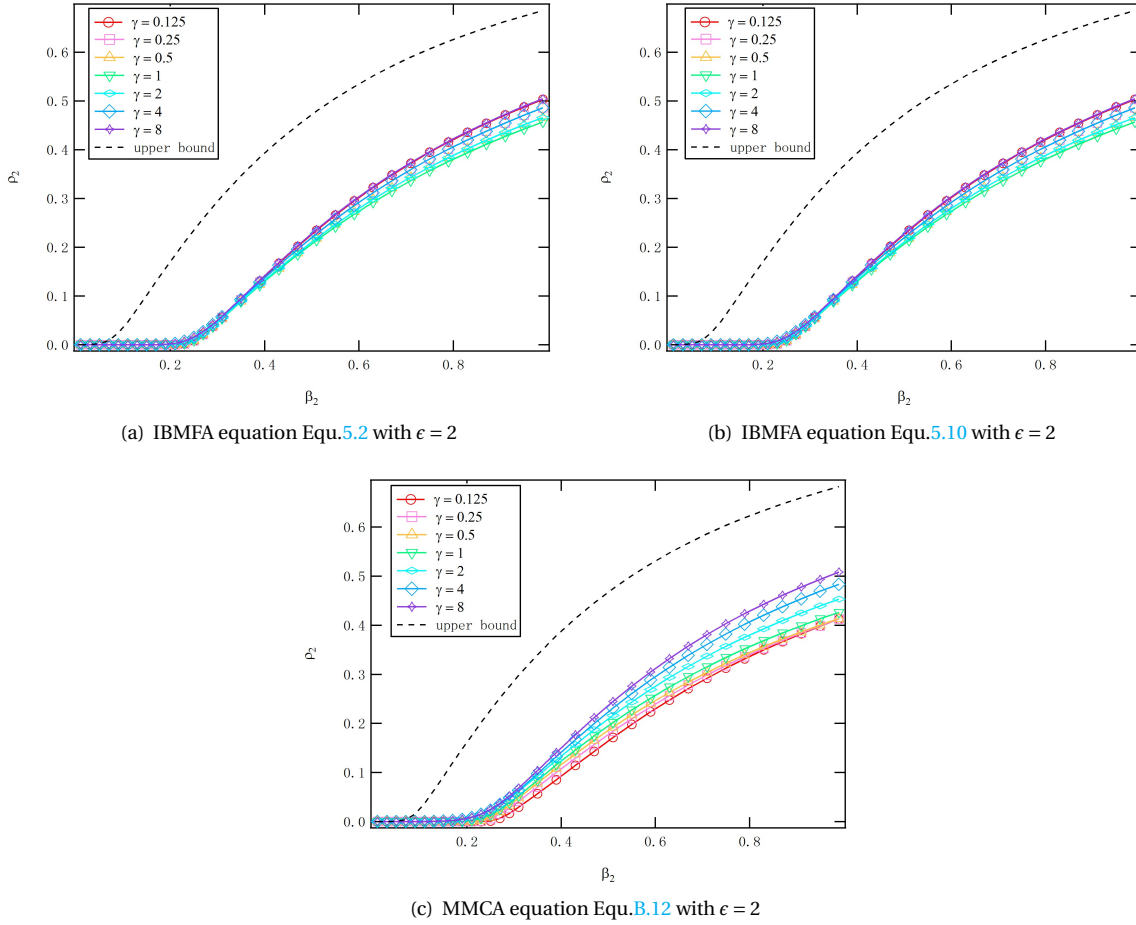


Figure B.2: Result of three theoretical approximations, (a) IBMFA equation Eq.5.2, (b) IBMFA equation 2 Eq.5.6 and (c) MMCA equations Eq.5.9. Injection rate is set to be γ^ϵ where $\epsilon = 2$. Two-layer scale-free networks SF-SF with overlap $\phi = 1$ is used here. Other parameters we chose here are: $\beta_1 = 0.3, \delta_1 = 0.6, \beta_2 = 1.0, \delta_2 = 1.0, \alpha = 0.2$. Network size is $N = 1000$. For each scale-free network, the exponent of power-law degree distribution is $\lambda = 2.5$. Solutions are averaged over 10 independently generated two-layer networks.

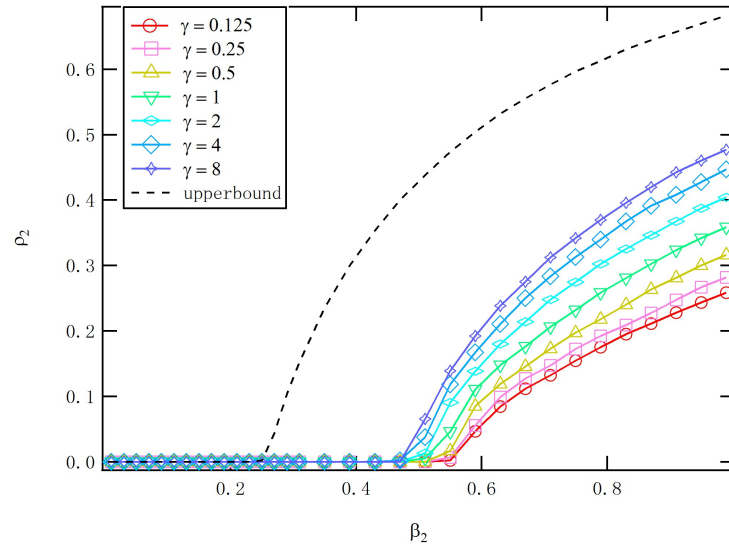


Figure B.3: The Effect of time scales γ on epidemic spreading in two-layer networks ER-ER with the overlap $\phi = 1$. The x axis is the infection spreading rate β_2 , and the y axis is the steady state fraction of infection in the physical network ρ_2 . The injection rate is γ^ϵ , and here we set the value $\epsilon = 1$, i.e. the injection rate is linearly related to the time scale γ . Other parameters used in this figure are: $\beta_1 = 0.3$, $\delta_1 = 0.6$, $\delta_2 = 1.0$, $\alpha = 0.2$. The network size is $N = 1000$. For an Erdős-Rényi (ER) random network, the average degree is $E[d] = 4$. Initially, 10% of randomly chosen nodes are unaware and infected (UII). The rest of nodes are unaware and susceptible (US). Results are averaged over 200 realizations.

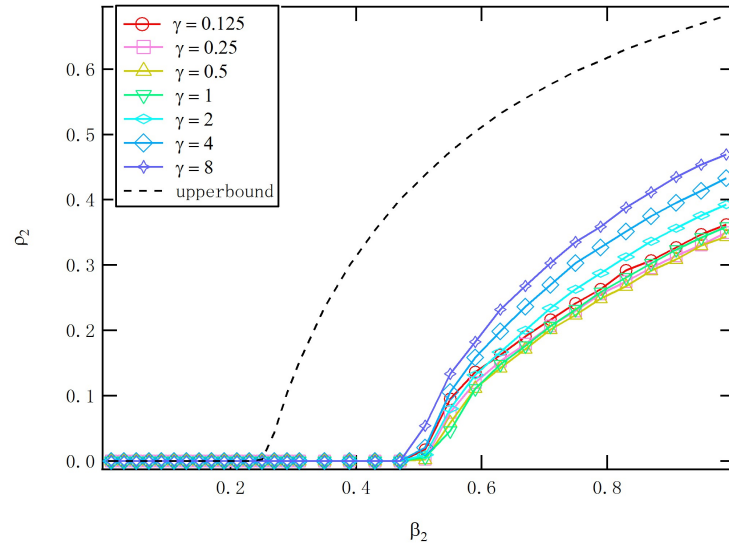


Figure B.4: The Effect of time scales γ on epidemic spreading in two-layer networks ER-ER with the overlap $\phi = 1$. The x axis is the infection spreading rate β_2 , and the y axis is the steady state fraction of infection in the physical network ρ_2 . The injection rate is γ^ϵ , and here we set the value $\epsilon = 2$. Other parameters used in this figure are: $\beta_1 = 0.3$, $\delta_1 = 0.6$, $\delta_2 = 1.0$, $\alpha = 0.2$. The network size is $N = 1000$. For an Erdős-Rényi (ER) random network, the average degree is $E[d] = 4$. Initially, 10% of randomly chosen nodes are unaware and infected (UII). The rest of nodes are unaware and susceptible (US). Results are averaged over 200 realizations.

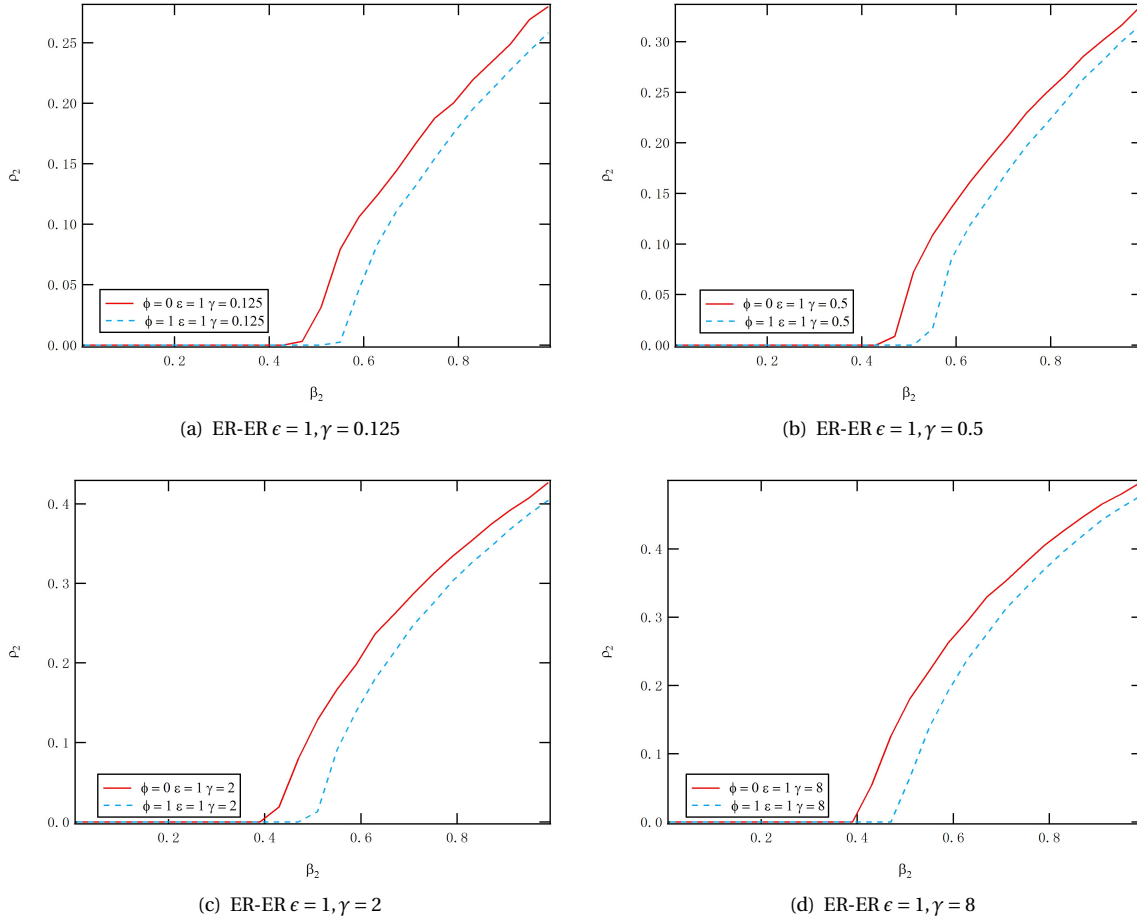


Figure B.5: Influence of overlap ϕ between two layers in two-layer Erdős-Rényi (ER) random networks on the fraction of infection in the physical network ρ_2 . The injection rate is set to γ^ϵ with $\epsilon = 1$. The relative time scale in the social network layer are: (a) $\gamma = 0.125$, (b) $\gamma = 0.5$, (c) $\gamma = 2$, (d) $\gamma = 8$. Parameters we choose here are: $\beta_1 = 0.3$, $\delta_1 = 0.6$, $\delta_2 = 1.0$, $\alpha = 0.2$. The network size is $N = 1000$. In each Erdős-Rényi (ER) random network, the average degree is $E[d] = 4$. Initially 10% randomly chosen nodes are infected. Results are averaged over 200 realizations.

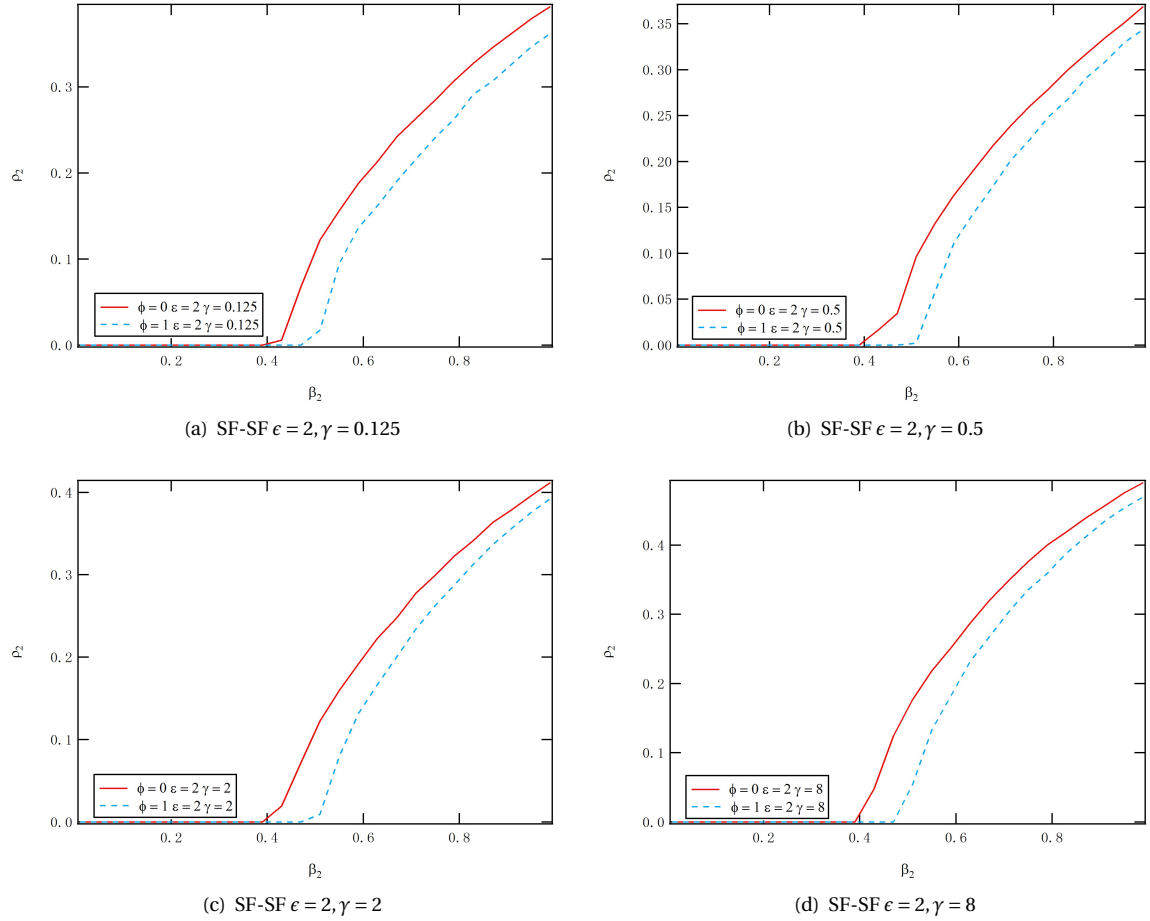


Figure B.6: Influence of overlap ϕ between two layers in two-layer Erdős-Rényi (ER) random networks on the fraction of infection in the physical network ρ_2 . The injection rate is set to γ^ϵ with $\epsilon = 2$. The relative time scale in the social network layer are: (a) $\gamma = 0.125$, (b) $\gamma = 0.5$, (c) $\gamma = 2$, (d) $\gamma = 8$. Parameters we choose here are: $\beta_1 = 0.3$, $\delta_1 = 0.6$, $\delta_2 = 1.0$, $\alpha = 0.2$. The network size is $N = 1000$. In each Erdős-Rényi (ER) random network, the average degree is $E[d] = 4$. Initially 10% randomly chosen nodes are infected. Results are averaged over 200 realizations.

ACKNOWLEDGEMENT

My master thesis is done in the Multimedia Computing Group, Faculty of Electrical Engineering, Mathematics, and Computer Science (EEMCS), Delft University of Technology.

First of all, I would like to give my wholehearted gratitude to Dr. Huijuan Wang. As my daily supervisor, she has been very supportive, and gave me so many valuable advices about the thesis and also about my live. During the thesis work, she spent much time and effort on helping my project and giving constructive comments. She is always very sharp in researches, and she guided me through some research bottlenecks. I learned so much from her academic research spirit. Besides, she encouraged me through some tough time in my live.

Then I would like to give my special thanks to Bo Qu, who is also my daily supervisor. He spent endless time discussing with me about my project. He gave me useful criticism on many details of my work. He helped me with great patience through troubles with his comprehensive knowledge in the research field. When I needed help, he was always there for me. I learned a lot from his personality, and from his manner of dealing with things.

I would like to thank my responsible professor Prof. Dr. A. Hanjalic for for taking time to be the committee member of my thesis defense and reading my thesis.

I would like to thank Dr. W. Ruszel from the Applied Probability Group for her interests in my thesis, and her willingness to be the committee member of my thesis defense.

I would like to thank Dr. D. Li from Beihang University for providing sharp insights for my work. And thank him for his interests to join in writing our paper.

I would like to thank Dr. S. Gomez and Ms. C. Granell from Universitat Rovira i Virgili. They nicely provided me with the settings and methods in their paper, which helped me verify my simulations in the first stage of my thesis work.

I would like to thank Dr. Z. Zhang from Hangzhou Normal University for the suggestions in some details of my work.

I would like to thank my family for supporting my study, caring about my life and selfless love. Thank my friends in TU Delft for accompanying me throughout these two years. Thank my girlfriend for her supportive and her encouragement during my thesis work.

Chuyi CHEN
Delft, September 2015

BIBLIOGRAPHY

- [1] C. Granell, S. Gómez, and A. Arenas, *Competing spreading processes on multiplex networks: awareness and epidemics*, Physical Review E **90**, 012808 (2014).
- [2] C. Granell, S. Gómez, and A. Arenas, *Dynamical interplay between awareness and epidemic spreading in multiplex networks*, Physical review letters **111**, 128701 (2013).
- [3] E. Quill, *When networks network: Once studied solo, systems display surprising behavior when they interact*, Science News **182**, 18 (2012).
- [4] J. Gao, S. V. Buldyrev, H. E. Stanley, and S. Havlin, *Networks formed from interdependent networks*, Nature physics **8**, 40 (2012).
- [5] M. Liu, D. Li, P. Qin, C. Liu, H. Wang, and F. Wang, *Epidemics in interconnected small-world networks*. PloS one **10**, e0120701 (2015).
- [6] H. Wang, Q. Li, G. D. Agostino, S. Havlin, H. E. Stanley, and P. Van Mieghem, *Effect of the interconnected network structure on the epidemic threshold*, Physical Review E **88**, 022801 (2013).
- [7] D. Li, P. Qin, H. Wang, C. Liu, and Y. Jiang, *Epidemics on interconnected lattices*, EPL (Europhysics Letters) **105**, 68004 (2014).
- [8] X. Huang, S. Shao, H. Wang, S. V. Buldyrev, H. E. Stanley, and S. Havlin, *The robustness of interdependent clustered networks*, EPL (Europhysics Letters) **101**, 18002 (2013).
- [9] W. de Haan, W. M. van der Flier, H. Wang, P. F. Van Mieghem, P. Scheltens, and C. J. Stam, *Disruption of functional brain networks in alzheimer's disease: what can we learn from graph spectral analysis of resting-state magnetoencephalography?* Brain connectivity **2**, 45 (2012).
- [10] J. Martín-Hernández, H. Wang, P. Van Mieghem, and G. D. Agostino, *Algebraic connectivity of interdependent networks*, Physica A: Statistical Mechanics and its Applications **404**, 92 (2014).
- [11] J. Martin-Hernandez, H. Wang, P. Van Mieghem, and G. D. Agostino, *On synchronization of interdependent networks*, arXiv preprint arXiv:1304.4731 (2013).
- [12] G. Baxter, S. Dorogovtsev, A. Goltsev, and J. Mendes, *Avalanche collapse of interdependent networks*, Physical review letters **109**, 248701 (2012).
- [13] M. Szell, R. Lambiotte, and S. Thurner, *Multirelational organization of large-scale social networks in an online world*, Proceedings of the National Academy of Sciences **107**, 13636 (2010).
- [14] G. Bianconi, *Statistical mechanics of multiplex networks: Entropy and overlap*, Physical Review E **87**, 062806 (2013).
- [15] F. Bagnoli and E. Massaro, *Epidemic spreading and risk perception in multiplex networks: a self-organized percolation method*, arXiv preprint arXiv:1405.5348 (2014).
- [16] W. Wang, M. Tang, H. Yang, Y. Do, Y.-C. Lai, and G. Lee, *Asymmetrically interacting spreading dynamics on complex layered networks*, Scientific reports **4** (2014).
- [17] D. H. Zanette, *Dynamics of rumor propagation on small-world networks*, Physical review E **65**, 041908 (2002).

- [18] B. Qu, Q. Li, S. Havlin, H. E. Stanley, and H. Wang, *Nonconsensus opinion model on directed networks*, *Physical Review E* **90**, 052811 (2014).
- [19] J. Zhou, Z. Liu, and B. Li, *Influence of network structure on rumor propagation*, *Physics Letters A* **368**, 458 (2007).
- [20] X.-X. Zhan, C. Liu, G. Zhou, Z.-K. Zhang, G.-Q. Sun, and J. J. Zhu, *Mutual feedback between epidemic spreading and information diffusion*, arXiv preprint arXiv:1506.03932 (2015).
- [21] Z. Ruan, M. Tang, and Z. Liu, *Epidemic spreading with information-driven vaccination*, *Physical Review E* **86**, 036117 (2012).
- [22] W. H. Organization *et al.*, *Consensus document on the epidemiology of severe acute respiratory syndrome (sars)*, (2003).
- [23] P. Van Mieghem, *The n-intertwined sis epidemic network model*, *Computing* **93**, 147 (2011).
- [24] P. Van Mieghem, J. Omic, and R. Kooij, *Virus spread in networks*, *Networking*, *IEEE/ACM Transactions on* **17**, 1 (2009).
- [25] E. Cator and P. Van Mieghem, *Susceptible-infected-susceptible epidemics on the complete graph and the star graph: Exact analysis*, *Physical Review E* **87**, 012811 (2013).
- [26] C. Li, R. van de Bovenkamp, and P. Van Mieghem, *Susceptible-infected-susceptible model: A comparison of n-intertwined and heterogeneous mean-field approximations*, *Physical Review E* **86**, 026116 (2012).
- [27] R. M. Anderson, R. M. May, and B. Anderson, *Infectious diseases of humans: dynamics and control*, Vol. 28 (Wiley Online Library, 1992).
- [28] N. T. Bailey *et al.*, *The mathematical theory of infectious diseases and its applications* (Charles Griffin & Company Ltd, 5a Crendon Street, High Wycombe, Bucks HP13 6LE., 1975).
- [29] P. Van Mieghem, *Performance analysis of complex networks and systems* (Cambridge University Press, 2014).
- [30] A. Barrat, M. Barthelemy, and A. Vespignani, *Dynamical processes on complex networks* (Cambridge University Press, 2008).
- [31] R. Pastor-Satorras and A. Vespignani, *Epidemic dynamics and endemic states in complex networks*, *Physical Review E* **63**, 066117 (2001).
- [32] C. Castellano and R. Pastor-Satorras, *Thresholds for epidemic spreading in networks*, *Physical review letters* **105**, 218701 (2010).
- [33] D. J. Daley, J. Gani, and J. M. Gani, *Epidemic modelling: an introduction*, Vol. 15 (Cambridge University Press, 2001).
- [34] Y. Zhu, D. Li, and F. Zhang, *Modeling the sis immunization epidemic on finite size of ba network*, in *Communications, Circuits and Systems (ICCCAS), 2013 International Conference on*, Vol. 2 (IEEE, 2013) pp. 98–102.
- [35] A.-L. Barabási and J. Frangos, *Linked: the new science of networks science of networks* (Basic Books, 2014).
- [36] P. ERDdS and A. R&WI, *On random graphs i*. *Publ. Math. Debrecen* **6**, 290 (1959).
- [37] B. Bollobás, *Random graphs* (Springer, 1998).
- [38] D. J. Watts and S. H. Strogatz, *Collective dynamics of small-world networks*, *nature* **393**, 440 (1998).
- [39] M. Catanzaro, M. Boguñá, and R. Pastor-Satorras, *Generation of uncorrelated random scale-free networks*, *Physical Review E* **71**, 027103 (2005).
- [40] R. Cohen and S. Havlin, *Scale-free networks are ultrasmall*, *Physical review letters* **90**, 058701 (2003).

- [41] A. A. Moreira, D. R. Paula, R. N. Costa Filho, and J. S. Andrade Jr, *Competitive cluster growth in complex networks*, Physical Review E **73**, 065101 (2006).
- [42] G. Fredrickson, *The equilibrium theory of inhomogeneous polymers (international series of monographs on physics)* (Oxford University Press, 2013).
- [43] T. Hotta, *Mean-field approximation*, in *Nanoscale Phase Separation and Colossal Magnetoresistance* (Springer, 2003) pp. 157–167.
- [44] P. Van Mieghem, *Performance analysis of communications networks and systems* (Cambridge University Press, 2006).
- [45] C. Li, *Characterization and Design of Complex Networks*, Ph.D. thesis, TU Delft, Delft University of Technology (2014).
- [46] A. Ganesh, L. Massoulié, and D. Towsley, *The effect of network topology on the spread of epidemics*, in *INFOCOM 2005. 24th Annual Joint Conference of the IEEE Computer and Communications Societies. Proceedings IEEE*, Vol. 2 (IEEE, 2005) pp. 1455–1466.
- [47] *matlab 2014b website*, http://nl.mathworks.com/videos/whats-new-in-matlab-and-simulink-r2014b-100228.html?s_tid=srchtitle.
- [48] *ode45 function in matlab*, <http://nl.mathworks.com/help/matlab/ref/ode45.html>.
- [49] D. Chakrabarti, Y. Wang, C. Wang, J. Leskovec, and C. Faloutsos, *Epidemic thresholds in real networks*, ACM Transactions on Information and System Security (TISSEC) **10**, 1 (2008).
- [50] S. Gómez, J. Gómez-Gardenes, Y. Moreno, and A. Arenas, *Nonperturbative heterogeneous mean-field approach to epidemic spreading in complex networks*, Physical Review E **84**, 036105 (2011).